CONSTRUCTION MATERIALS CONSULTANTS, INC.

Laboratory Investigation of Epoxy Terrazzo Failure From Concrete Slab-on-Grade

Knott Hall
Loyola Blakefield
Towson, Maryland

April 03, 2019
CMC 0219107

TABLE OF CONTENTS

EXECUTIVE SUMMARY

Located in Towson, Maryland, Loyola Blakefield, formerly Loyola High School, is an American Catholic, college preparatory school for boys established by the Society of Jesus. Building on a distinguished historic tradition, the new Knott Hall at Loyola Blakefield serves as a striking first impression for visitors. Situated atop a hill along Charles Street, the facility—which houses an Alumni Hall, dining facility, gymnasium and Student Commons—has become the heart of the school on this picturesque campus imbued with tradition.

Samples - Terrazzo floor across the hall has reportedly shown blistering and other bonding issues from the underlying concrete slab-on-grade. As a result, four terrazzo-concrete composite cores drilled through entire slab, and, a yellow liquid reportedly collected from underneath a blister were provided to investigate all possible reasons for terrazzo failure.

a. Core 1 was retrieved from a 7 mm thick white terrazzo floor, above two perpendicular control joints in concrete slab with associated through-depth cracks, where terrazzo was bonded to concrete with a 2.5-3 mm thick fibermesh reinforced green bond coat. The concrete slab is $5^1/_2$ in. thick and placed directly on a plastic vapor retarder.

b. Core 2 was reportedly retrieved from a blistered location, though the terrazzo itself does not show any blister but clean and complete debonding from concrete. The core was drilled over a dark blue band on terrazzo floor, where terrazzo is nominal 12 mm thick and completely debonded from concrete with no intermediate bond coat. The concrete slab is $4^3/_8$ in. thick and placed directly on a plastic vapor retarder.

c. Core 3 was retrieved from a 10 mm thick white terrazzo floor, where terrazzo was bonded to concrete with a 2.5-3 mm thick fibermesh reinforced green bond coat. The concrete slab is 5 in. thick and placed directly on a plastic vapor retarder.

d. Core 4 was retrieved from a 10 mm thick white terrazzo floor, where terrazzo was directly bonded to concrete without any bond coat, except perhaps a thin film of an organic primer on the concrete surface. The concrete slab is thickest, $8^3/_4$ in. and like the others placed directly on a plastic vapor retarder.

Methodologies - All four cores were examined by detailed petrographic examinations *a la* ASTM C 856, including optical and scanning electron microscopy and X-ray microanalyses, profiles of water-soluble ions through top, mid-depth and bottom locations of cores to determine moisture-induced migration of water-soluble ions towards the surface. Pulverized concrete samples sectioned from three depths in each core and digested in deionized water for 24 hours were filtered and filtrates containing water-soluble ions were analyzed for chloride by potentiometric titration (*a la* ASTM C 1218), chloride and sulfate by ion chromatography (*a la* ASTM D 4327), and water-soluble alkalis by X-ray fluorescence. Chemical fingerprints of increasing water-soluble ions towards the surface, if present, would confirm moisture upwelling and moisture-related issues for failures. Organic components in terrazzo, bonding coat, concrete surface, and blister liquid were done by FTIR.

Concrete Surface - In all four cores, the concrete surface is lightly ground/scarified where only fine aggregate particles are exposed but the near-surface dense, dark gray low *w/c* paste at the top 5 to 6 mm which is typical in many trowel-finished surfaces is still present as well as a thin film of carbonation at the very top, both of which could potentially prevent migration of essential bonding component(s) for a floor covering to develop a good chemical and/or mechanical bond to concrete. The bonded terrazzo-concrete composite in Core 4 shows some near-surface fine, hairline microcracks formed as a result of surface preparation, which, however, did not prevent a good bond between terrazzo and a thick concrete slab. By contrast, despite having a green fibermesh reinforced bond coat it showed a good bond to the underside of terrazzo but no bond to the concrete beneath. Debonding occurred between this bond coat and concrete in Core 3. In Core 2 the dark blue terrazzo was directly placed on a lightly scarified concrete surface where the surface wasn't rough enough to develop a good mechanical bond, nor was any bonding agent applied to develop a chemical bond between the epoxy terrazzo and dense trowel-finished surface of concrete slab.

Terrazzo - Two types of polymer terrazzo are present in four cores: (a) a white terrazzo in Cores 1, 3, and 4 consisting of crushed marble and crushed limestone chips mixed with finer sized marble dust and all crystalline components are mixed in a titanium oxide-based pigmented white epoxy resin binder, and (b) a dark blue terrazzo in Core 2 consisting of crushed marble, limestone, crushed glass in a pigmented blue polymer binder (different from the white epoxy resin binder in white terrazzo). These two types correspond to the dark blue color bands of terrazzo on the overwhelming white terrazzo flooring across the core locations. Nominal thicknesses of terrazzo varied from 7 mm, 12 mm , 10 mm, and 10 mm in Cores 1, 2, 3, and 4, respectively. Coarse marble and limestone chips are nominal 2 to 3 mm in white terrazzo and as coarse as 5 mm in blue variety. Except a fine, hairline long visible crack in white terrazzo in Core 3 which has extended through the 10 mm thickness of terrazzo but did not extend beyond, in three other cores terrazzo flooring is present in visually crack-free and sound conditions. There is no evidence of any chemical or physical deterioration of terrazzo or its components found in the cores examined to indicate its potential role for the reported failure.

Bond Coat - Cores 1 and 3 show the presence of a thin (2.5 to 3 mm thickness) green polymer bond coat well-adhered to the underside of terrazzo but completely de-bonded from the concrete beneath. This bond coat contained a fibermesh reinforcement mostly at the base of the coat, which did not provide any benefit to bond the coat to the concrete.

Concrete Slab - The concrete slab beneath the terrazzo flooring is found to be compositionally similar non-air-entrained Portland cement concrete consisting of crushed marble coarse aggregate having a nominal maximum size of 1 in. (25 mm), natural siliceous (quartz-quartzite-feldspar) sand fine aggregate having a nominal maximum size of $^{3}/_{8}$ in. (9.5 mm), a dense Portland cement paste, which is denser, harder, and darker gray at the top 5 to 6 mm due to trowel-finishing operations having water-cement ratio estimated at the trowel densified surface to be 0.35 to 0.40, and a relatively normal dense paste in the interior body where cement content is estimated to be $6^{1}/_{2}$ to 7 bags per cubic yard and water-cement ratio estimated to be similar throughout the depth of each core and across all four cores, between 0.40 to 0.45. Since the slab was placed over a plastic vapor retarder in all four cores, and was dense trowel-finished, the internal moisture of concrete from mix water was used to well hydrated the cement and create a dense concrete.

Both coarse and fine aggregate particles in concrete are sound and did not contribute to any potentially deleterious reactions such as alkali-aggregate reactions to cause the reported flooring failure. Alkali-silica reaction (ASR) in concrete, often trigged by moisture and alkalis brought to the surface by moisture upwelling is often considered as the cause of floor covering failure. Present cores do not show any evidence of such a reaction, or reaction products (ASR gel), or reaction microstructures (e.g., microcracking from reactive aggregates to paste) to consider such a process to be the cause.

Profiles of water-soluble anions and alkalis across the depth of cores show no obvious increase of water-soluble ions (chloride, sulfate, sodium, potassium) towards the top of the cores, indicating perhaps moisture upwelling if occurred was not strong enough to leave its chemical fingerprint in terms of elevated alkali, chloride, sulfate levels towards the top.

Terrazzo-Concrete Interface - In Cores 2 and 3, terrazzo showed complete de-bonding from concrete irrespective of having a green reinforced bond coat in Core 3 or its complete absence in Core 2. In Cores 1 and 4, terrazzo is bonded to concrete, again irrespective of having a green bond coat in Core 1, or not having it in Core 4 (latter with a thin polymer surface film on the concrete that was probably applied as a primer or a bonding agent). The top concrete surface in all four cores showed a dense, trowel-finished surface with densified paste to a depth of 5 to 6 mm, which is darker gray and free of any air due to trowel-finishing compared to paste in the interior body. A thin film of carbonated concrete is found in all four cores, indicating inadequate removal of carbonated and trowel-densified surface from concrete slab both of which would densify the very top and potentially hinder development of a good bond to a newly placed polymer-based epoxy system.

In cores having debonded flooring from concrete no trace of terrazzo and/or bonding coat is found on the concrete surface (except only a trace in Core 3) and no trace of concrete is found on the underside of terrazzo or bonding coat. This indicates a clear separation of flooring from concrete and application of flooring on a relatively smooth flat surface found to be the dense trowel-finished surface of slab where newly placed flooring components did not penetrate into concrete or develop any good mechanical interlocking for a good bond.

In the absence of any potently deleterious reactions (e.g., alkali-aggregate reaction) in terrazzo or concrete, especially at the top surface region of concrete, and in the absence of any chemical fingerprint of moisture upwelling through the slab to bring potentially deleterious components (e.g., alkalis) towards the surface to inhibit the bond, the reported debonding of flooring is judged to be due to inadequate preparation of concrete slab surface to make it more receptive to the new flooring, e.g., with better and deeper grinding to remove the carbonated skin and dense trowel-finished surface, thorough cleaning of the prepared surface to remove any dirt or standing water, using appropriate bonding agent to actually bond to the concrete surface rather than only to the terrazzo (as is the case here) for eventual bonding of the new flooring to concrete, etc. Flooring failures driven by moisture upwelling would have caused debonding at the location of Core 4 where concrete slab is significantly thicker than that at the locations of Cores 2 and 3 and does not have a polymer bond coat except a thin film of an organic film (e.g., primer) which has helped adhere flooring to concrete (despite the fact that concrete still has a dense trowel-finished carbonated surface that should have been removed for better mechanical bond). This indicates use of proper bonding agent resistant to moisture and high alkali situations usually encountered in a concrete slab to develop good bond between a polymer terrazzo and cementitious substrate systems.

Two Types of Terrazzo Failures - Two common causes of failure of terrazzo flooring from concrete substrate are related to: (1) moisture, which could come from multiple sources, e.g., both from: (i) interior concrete slab e.g., by moisture upwelling (hydrostatic pressure, osmotic pressure, capillary rise) from concrete's batch water, underlying subbase, etc., as well as from (ii) exterior sources, e.g., ambient humidity, floor cleaning solutions, curing water, dewpoint, precipitation, etc., and (2) surface preparation of concrete. Moisture-related failure include (i) osmotic and/or hydrostatic pressures from moisture buildup beneath impermeable, nonbreathable floor covering causing blistering and delamination, (ii) alkali-silica reaction and related distress beneath the flooring causing blistering, cracking, and debonding, (iii) moisture-upwelling-induced increased alkali level at the surface causing destabilization and failure of flooring adhesives, adhesive

staining, etc. Moisture upwelling to cause accumulation beneath terrazzo flooring and blistering can occur under: (a) a relative humidity gradient from a wet slab to dry ambient air above, or (b) by osmotic pressure where moisture travels through a semi-permeable membrane into a solution of higher solute concentration, which is driven by a force that tends to equalize the concentrations of dissolved solute (typically salts) on the two sides of the membrane. Both processes can lead to formation of liquid-filled blisters.

Surface preparation-related failures include: (i) presence of dust, dirt, or other surface contaminants from improper cleaning and surface preparation, or surface-parallel near-surface microcracks from surface scarification processes, all of which could act as bond breaker to prevent adhesion of new flooring, (ii) absence of a bonding agent to develop a good 'chemical bond' of flooring to concrete, (iii) inadequate roughening or scarification of concrete surface to prevent development of a good 'mechanical bond' between flooring and concrete, etc.

All these options were considered to investigate possible causes of reported failure of terrazzo flooring. Cores received showed 'clean separation' of terrazzo with or without an underlying green bond coat from lightly scarified concrete surface where the concrete surface still has a thin carbonated skin and a dense trowel-finished surface to a depth of 5 to 6 mm. No blistering, or moisture-induced alkali-silica reaction in the concrete surface are found to cause the floor failure.

Blister Liquid - High alkalis (2.05% Na_2O and 3.28% K_2O), alkalinity (pH 11.2), and organic components found in the liquid reportedly collected from a blister can come from multiple sources, e.g., from interior concrete slab by moisture upwelling from concrete's batch water, as well as from exterior sources, e.g., ambient humidity, floor cleaning solutions, curing water, dewpoint, precipitation, etc. Without knowing the source of the liquid, or for that matter examining a so-called 'blister' itself, analysis of liquid in a vial cannot provide clues to the moisture-induced flooring failure. If it is from an external source then it has no direct role on terrazzo failure except perhaps destabilization of bonding agent by its high alkalinity. However, if it is indeed from an internal source, e.g., from concrete's batch water that has risen by moisture upwelling under a relative humidity gradient then moisture build up beneath an impermeable terrazzo floor can create enough pressure to cause blistering or debonding. Liquid in vial received was reported by maintenance personnel to be collected by first dry drilling through the terrazzo then applying pressure on the terrazzo to release the liquid from underneath the terrazzo to collect in the vial, which indicates the presence of moisture and moisture buildup beneath the terrazzo. Four cores examined, however, showed no evidence of 'blistering' as dome-shaped upwelling of terrazzo or possible extrusion by buildup of moisture and/or other ingredients (e.g., alkali-silica gel) that are commonly suspected from blister formation. Terrazzo in all four cores is epoxy-based, very dense, hard and showed complete smooth clear, flat separation from the underlying lightly ground concrete surface with a mated flat underside. Such clear separation of flooring from concrete has occurred irrespective of presence or absence of an intermediate bond coat (latter, when present, showed good adhesion to terrazzo but not to concrete). Cores 1 and 3 show the presence of a thin (2.5 to 3 mm thickness) green polymer bond coat well-adhered to the underside of terrazzo but completely debonded from concrete. Liquid in a vial reportedly received from a blister having water beneath the terrazzo, however, keep the possibility of moisture-related blistering open, which was not possible to investigate from the cores alone.

Conclusion - Therefore, based on detailed laboratory examinations of: (a) a liquid reportedly collected from a blister, and (b) four cores, terrazzo failure is determined to be a combination of:

a. ***Moisture buildup beneath the terrazzo flooring*** that has reportedly caused blistering and accumulation of liquid beneath the terrazzo having high alkalis that can potentially damage the bonding agent used to apply terrazzo flooring on concrete. *Concrete surface region in four cores showed no evidence of any deleterious alkali-silica reaction* from high alkalis in the liquid to cause blistering, which appeared to have formed from moisture buildup alone. Common quantitative moisture tests should be done prior to terrazzo installation according to ASTM F1869, *Standard Test Method for Measuring Moisture Vapor Emission Rate of Concrete Subfloor Using Anhydrous Calcium Chloride* or F2170, *Standard Test Method for Determining Relative Humidity in Concrete Floor Slabs Using in situ Probes*. Qualitative, comparative methods such as a plastic sheet test (ASTM D 4263), mat bond test, or handheld electronic moisture meters for electrical resistance test or electrical impedance test, nuclear moisture gauge, may be useful as survey tools but should not be used to accept a floor prior to terrazzo installation.

b. ***Inadequate surface preparation of concrete slab*** where absence of a bonding agent on the concrete surface (instead of only at the base of terrazzo in Cores 1 and 3) and presence of a thin carbonated skin and a dense trowel-finished surface to a depth of 5 to 6 mm from lightly scarified surface in all four cores, which has prevented development of a good *chemical bond* by a suitable bonding agent, or a *mechanical bond* by a surface roughened enough to create mechanical interlocking with the flooring components.

INTRODUCTION

Reported herein are the results of detailed laboratory studies of four terrazzo-concrete composite cores reportedly collected from Knott Hall of Loyola Blakefield located in Towson, Maryland.

KNOTT HALL – LOYOLA BLAKEFIELD

Figure 1 shows photograph of the subject building at Loyola Blakefield in Towson, Maryland.

Figure 1: Knott Hall at Loyola Blakefield in Towson, Maryland.

BACKGROUND INFORMATION

Loyola Blakefield, formerly Loyola High School, is an American Catholic, college preparatory school for boys established by the Society of Jesus. It is located in Towson, Maryland, within the Archdiocese of Baltimore. Building on a distinguished historic tradition, the new Knott Hall at Loyola Blakefield serves as a striking first impression for visitors. Situated atop a hill along Charles Street, the facility—which houses an Alumni Hall, dining facility, gymnasium and Student Commons—has become the heart of the school on this picturesque campus imbued with tradition.

Terrazzo floor across the hall has reportedly shown blistering and bonding issues from the underlying concrete slab-on-grade. As a result, four terrazzo-concrete composite cores drilled through the entire slab thickness were provided to investigate all possible reasons for the reported terrazzo failures.

FIELD PHOTOGRAPHS

The following schematic drawing shows approximate locations of four cores received, proximity of Core 2 from a nearby blister on terrazzo, drilling of Core 1 from over control joints, and of Core 4 from a sound area.

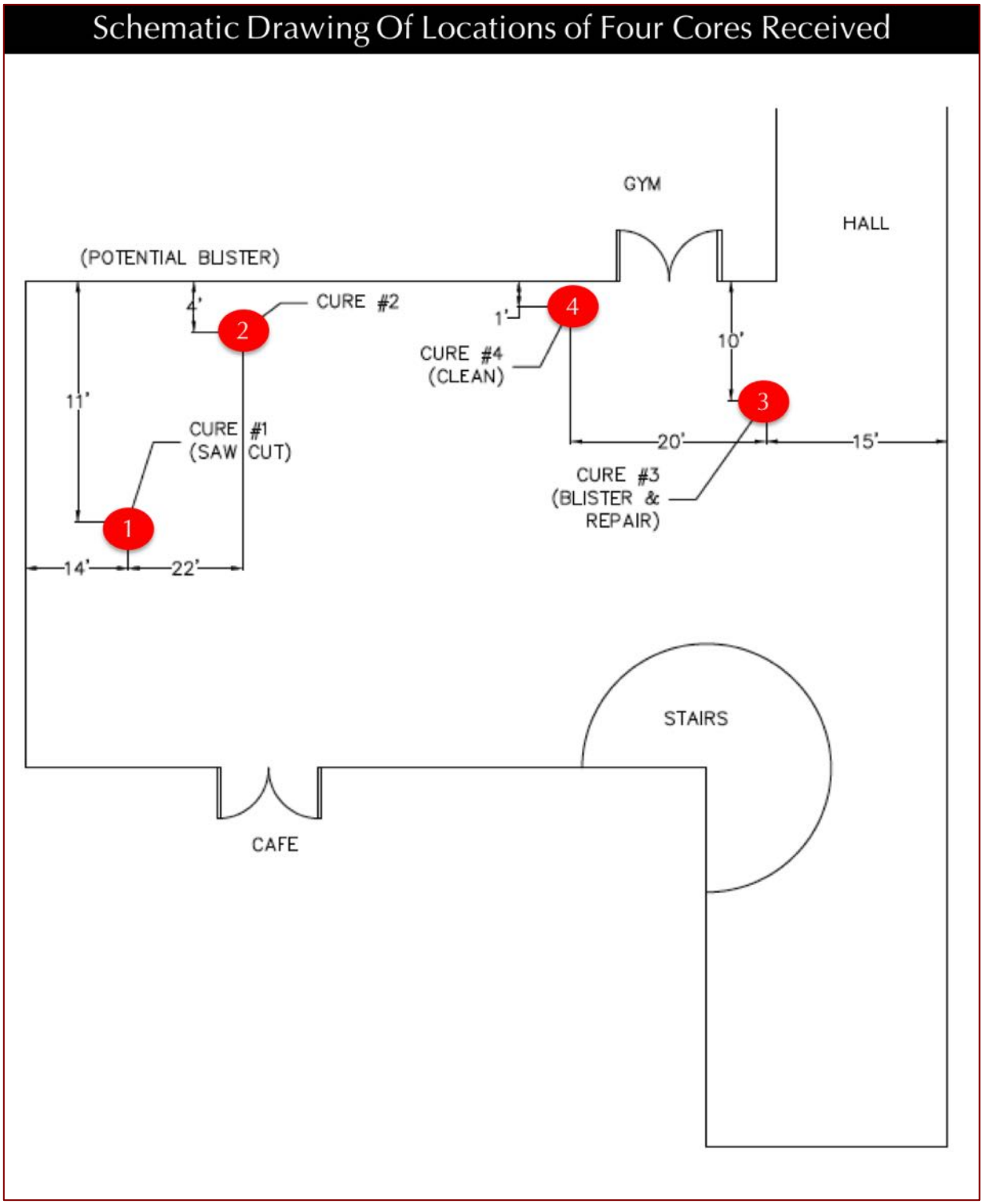

Figure 2: Schematic hand drawing showing approximate locations of four cores received.

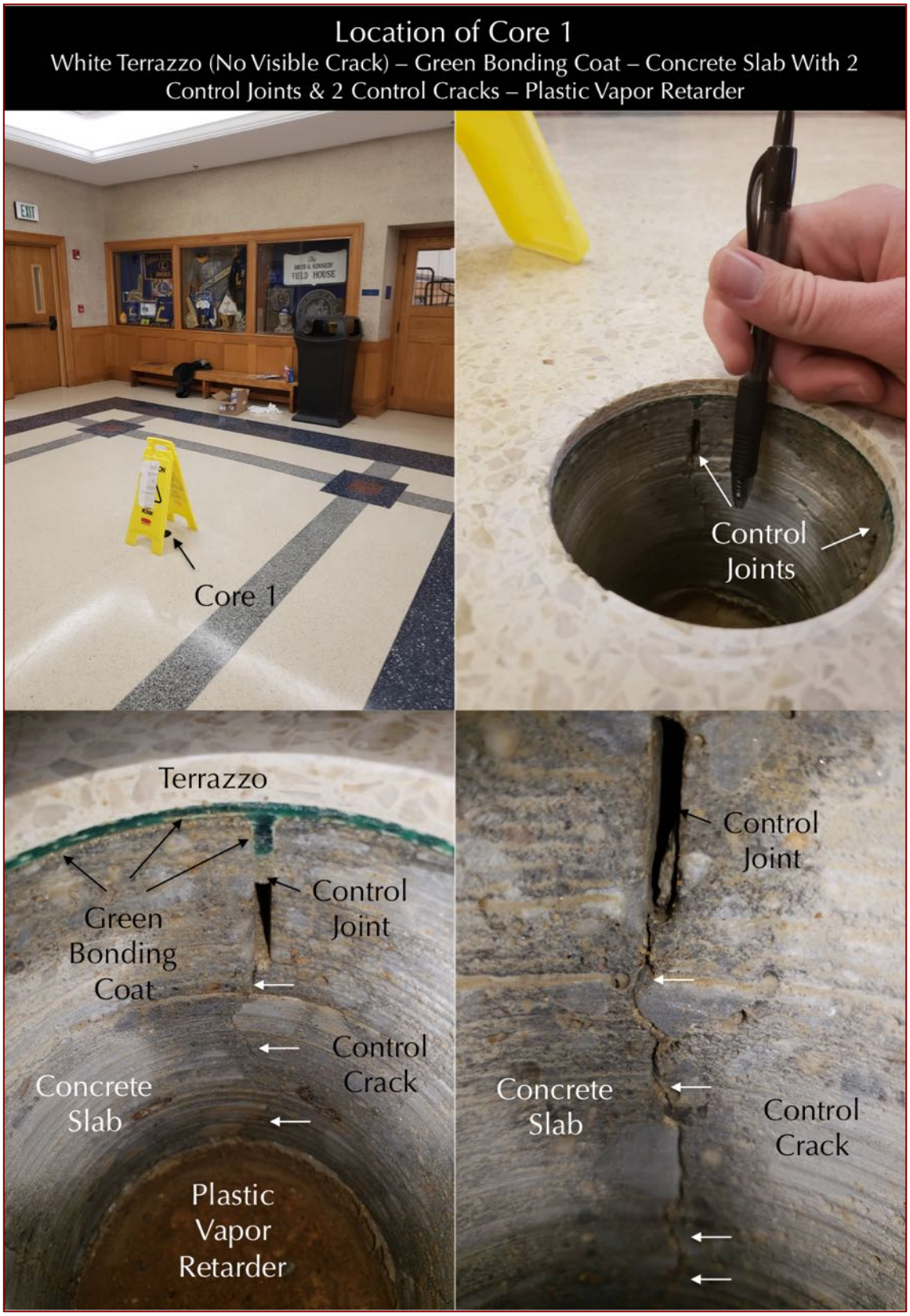

Figure 3: Location of Core 1 from a white terrazzo floor (top left), interior slab after removing the core (top right) showing two control joints with associated cracks (bottom photos), and a green bond coat beneath the terrazzo, and a subbase on which a plastic vapor retarder was placed (not shown in bottom left) before placement of the slab.

Figure 4: Location of Core 2 from a dark blue band of terrazzo floor (top left), interior slab after removing the core (top right) showing complete debonding of terrazzo from concrete with no intermediate bond coat (top right and bottom photos).

Figure 5: Location of Core 3 from a white terrazzo floor (top left), interior slab after removing the core (top right) showing terrazzo and concrete (bottom photos), and a green bond coat beneath the terrazzo (bottom left), and a subbase on which a plastic vapor retarder was placed (not shown in bottom right) before placement of the slab.

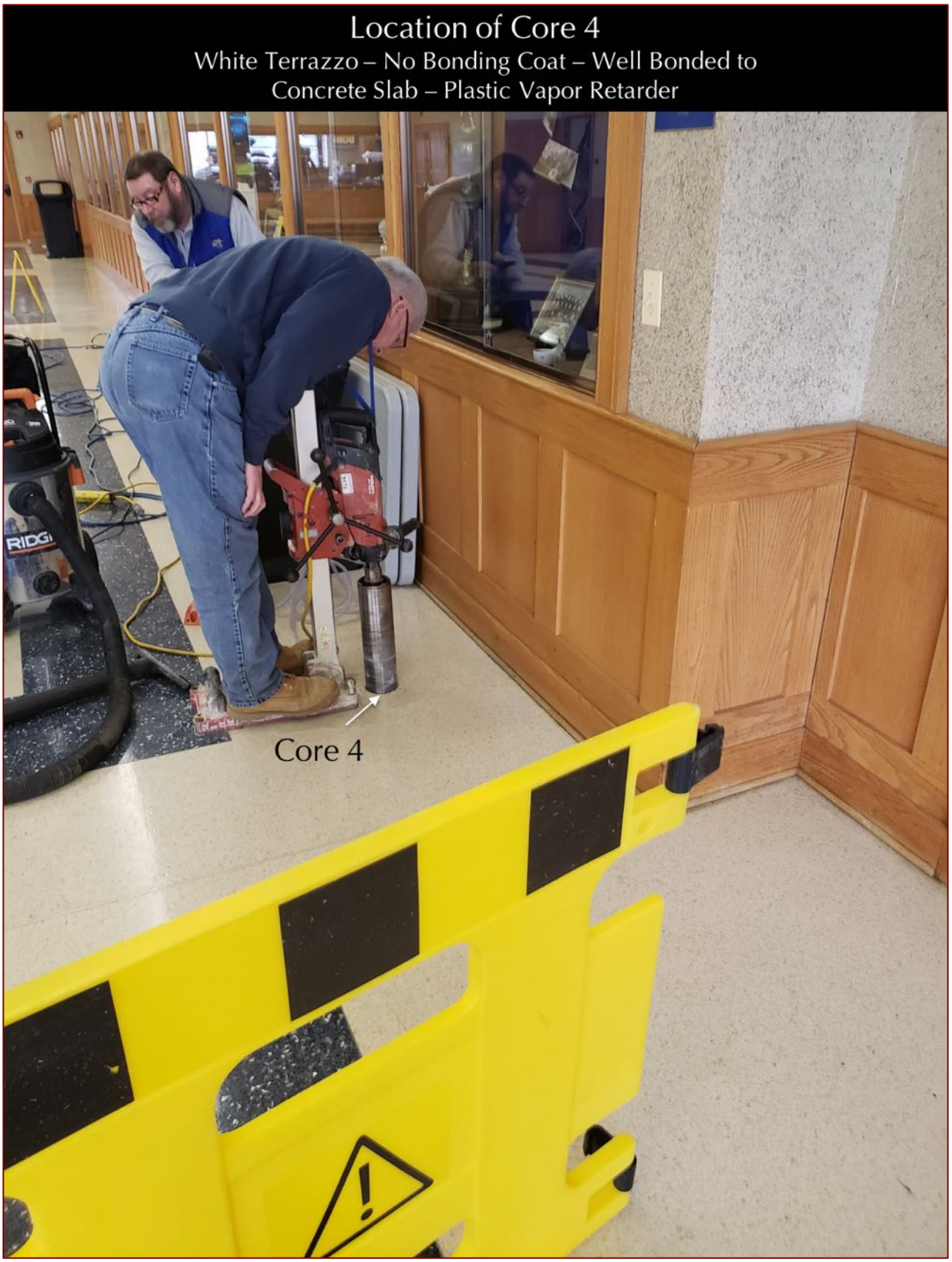

Figure 6: Location of Core 4 from a white terrazzo floor during drilling of the core.

PURPOSES OF EXAMINATION

The purposes of the laboratory investigation are to determine:

a) The overall composition of the terrazzo flooring and concrete slab, including the type, size, and composition of aggregates and binder used in the terrazzo flooring and concrete substrate;
b) Evidence of any physical and/or chemical deterioration of the terrazzo, and underlying concrete, including potential alkali-aggregate reaction in terrazzo and/or concrete;
c) Role of terrazzo, if any, in the reported blistering and observed de-bonding of the terrazzo flooring;
d) Evaluation of any potential moisture infiltration and moisture-related terrazzo failure from chemical analyses of water-soluble ions through the concrete slab;
e) Evidence of any improper curing of the terrazzo, including any improper materials or workmanship issues to evaluate if terrazzo materials and installation process have contributed to the flooring failure;
f) Evaluation of workmanship during terrazzo installation, including concrete surface preparation from depth of removal of concrete to condition of the prepared concrete surface prior to terrazzo installation; and
g) Analyses of the liquid in a vial reportedly collected from beneath terrazzo in a blister.

SAMPLES

Core ID	Diameter	Length	Top Surface	Bottom Surface	Embedded Items	Cracks, Joints, Lg. Voids	Condition
#1	3 5/8 in. (90 mm)	5 1/2 in. (140 mm)	Sound Terrazzo	Formed, wavy concrete base with a plastic vapor retarder detached from concrete, indicating direct placement of slab on a vapor retarder	Two perpendicular 3/16 in. diameter mesh at a depth of 4 in. from the top surface	Two perpendicular control joins with associated cracks below	Intact
#2	3 5/8 in. (90 mm)	4 3/8 in. (110 mm)	Sound Terrazzo with a 3/8 in. diameter drill hole		None	None	Terrazzo debonded from concrete, a visible crack in Terrazzo in Core 3 but none in Core 4
#3	3 5/8 in. (90 mm)	5 in. (120 mm)	Visible crack in terrazzo, terrazzo debonded from concrete		1/4 in. mesh at a depth of 4 1/2 in. from the top surface	One crack in terrazzo only	
#4	3 5/8 in. (90 mm)	8 3/4 in. (220 mm)	Sound Terrazzo		3/16 in. wire mesh at a depth of 6 3/4 in. from the top surface	None	Intact

Table 1: Descriptions of cores as received.

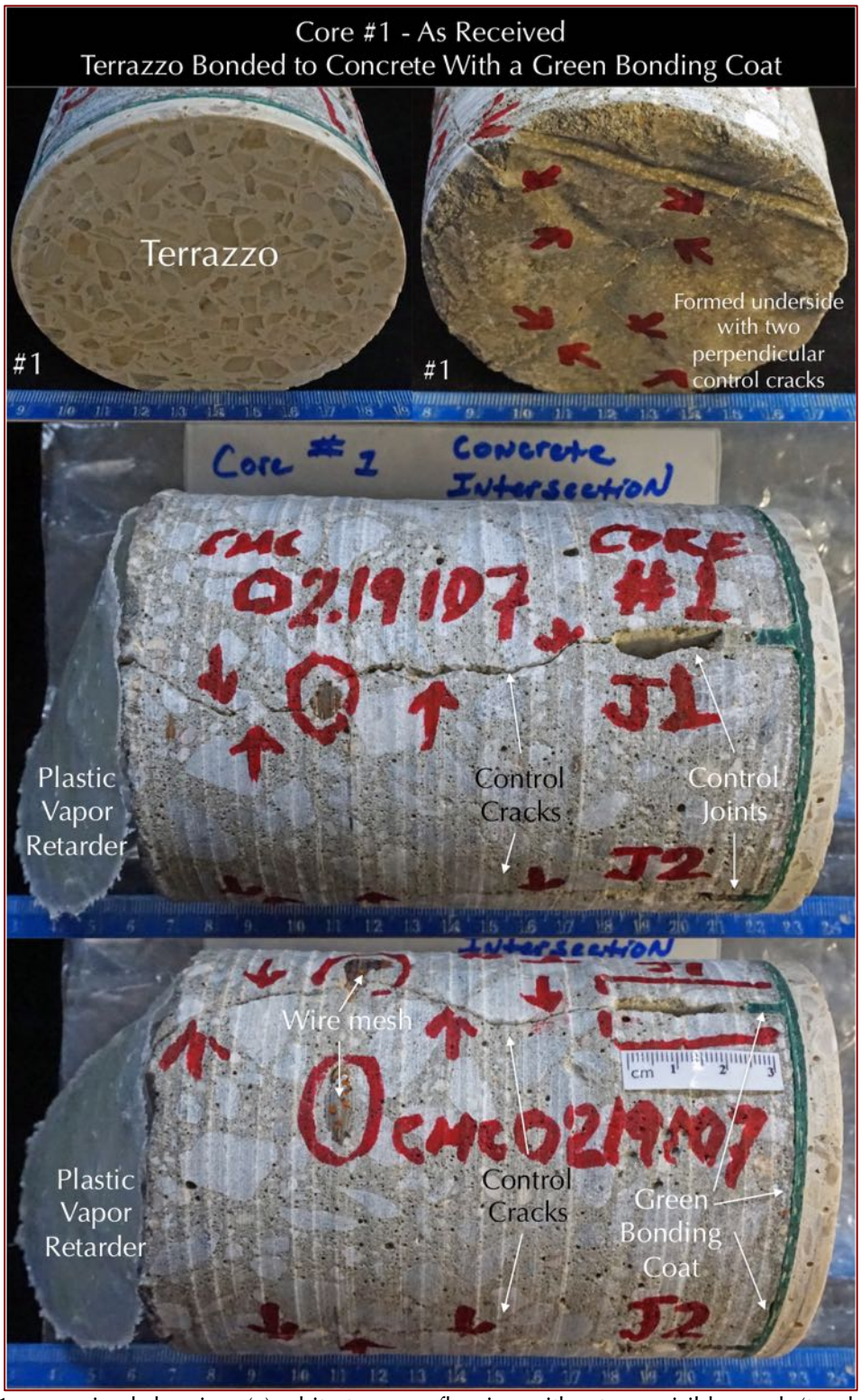

Figure 7: Core 1 as received showing: (a) white terrazzo flooring without any visible crack (top left); (b) smooth, wavy formed bottom end of concrete with impression of placement of slab on a plastic vapor retarder, and two visible perpendicular cracks from two control joints in the core (top right); (c) terrazzo, a green bond coat, and concrete with a control joint and associated crack and a plastic sheet at the base (middle row); and (d) another side view of terrazzo-green bond coat–concrete composite where two control joints and cracks beneath joints are seen (bottom).

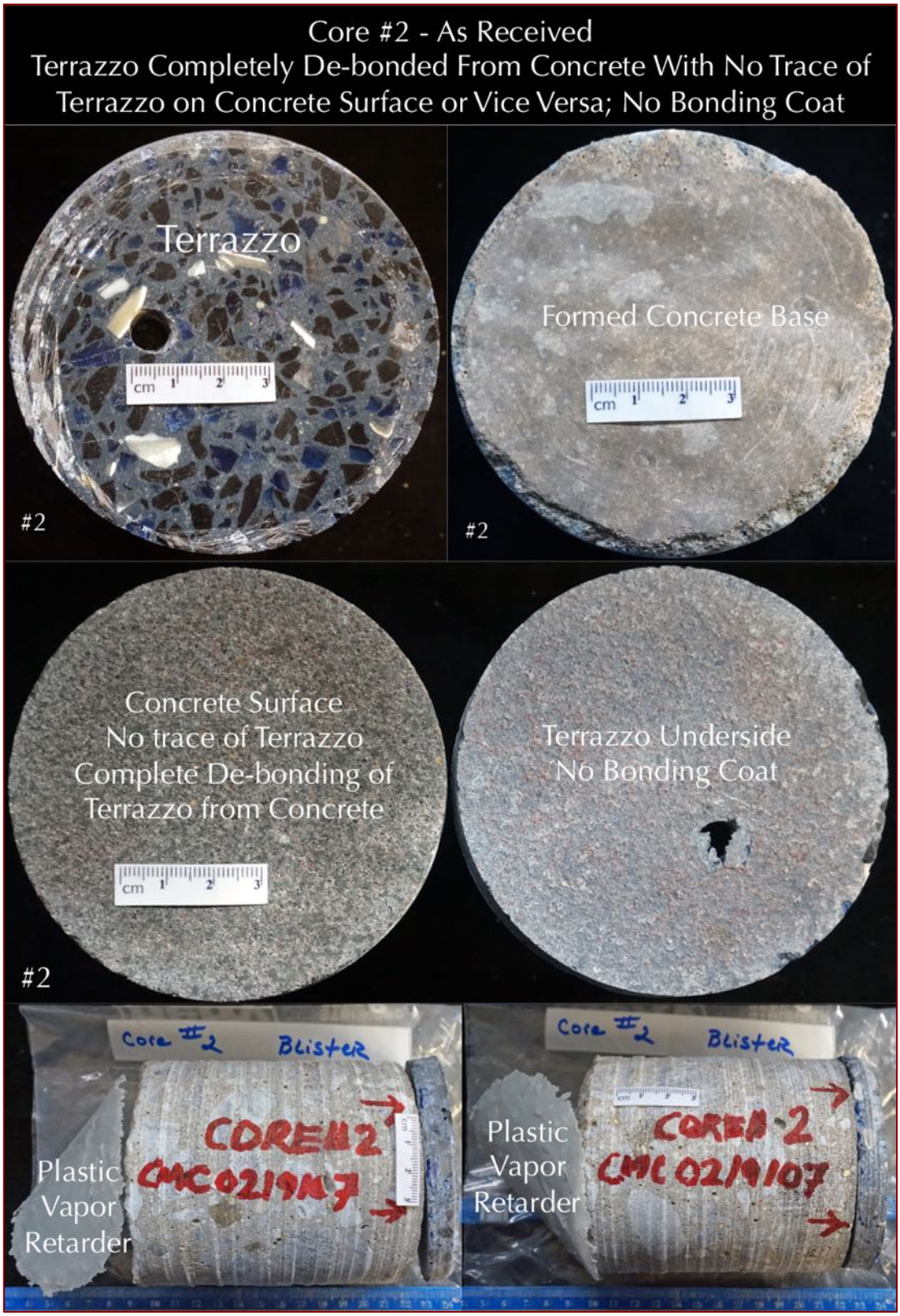

Figure 8: Core 2 as received showing: (a) blue terrazzo flooring without any visible crack but a drill hole (top left); (b) smooth, wavy formed bottom end of concrete with impression of placement of slab on a plastic vapor retarder (top right); (c) top concrete surface (middle left) and underside of terrazzo (middle right) showing clean separation of two, and (d) side views of terrazzo, complete de-bonding from concrete, and plastic sheet at the base of concrete.

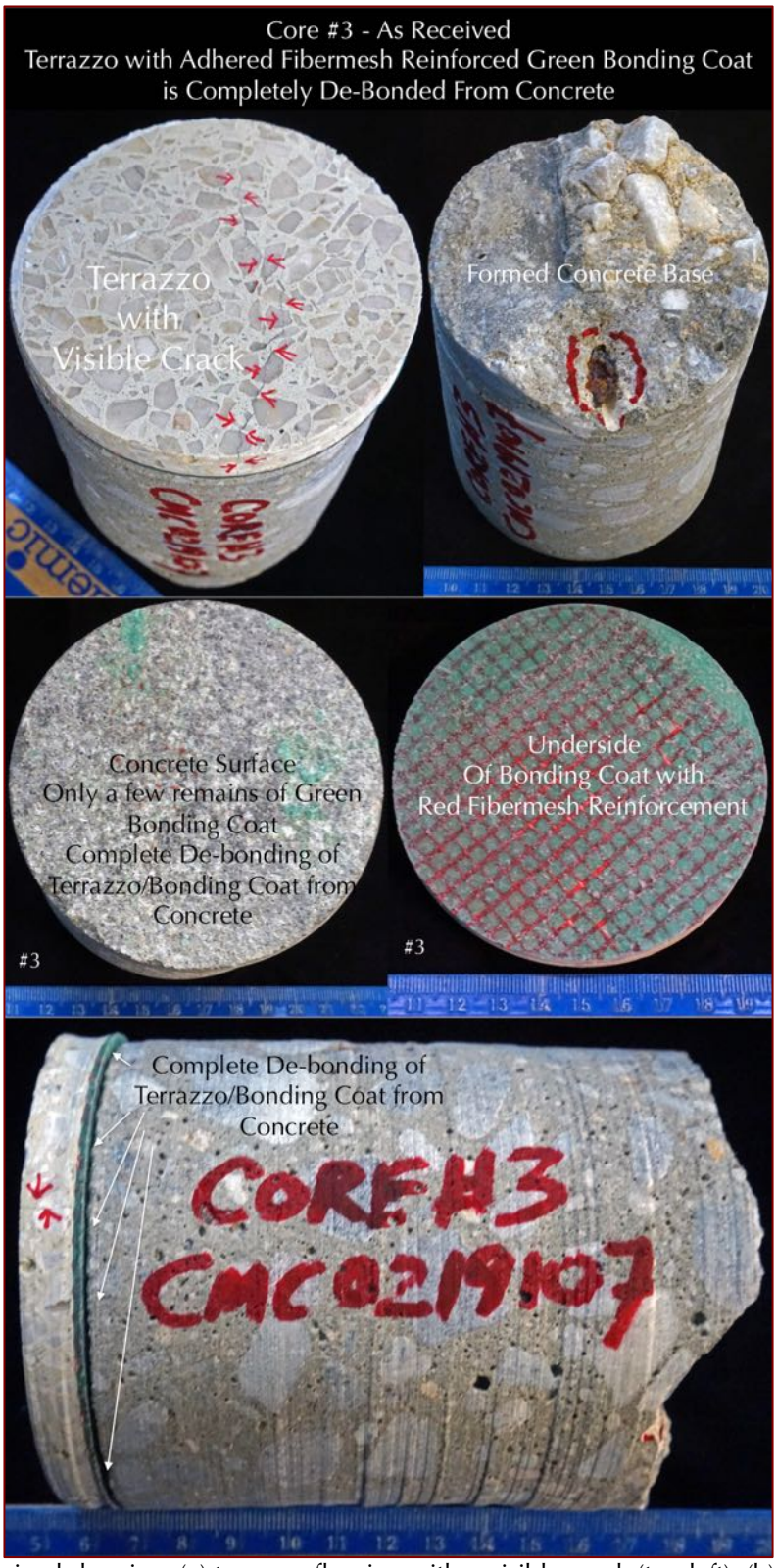

Figure 9: Core 3 as received showing: (a) terrazzo flooring with a visible crack (top left); (b) smooth, wavy formed bottom end of concrete with impression of placement of slab on a plastic vapor retarder (top right); (c)) top concrete surface (middle left) and underside of terrazzo showing a green bond coat with red fibermesh reinforcement (middle right) showing clean separation of concrete from terrazzo-green coat composite (middle row); and (d) a side view of terrazzo-green bond coat – complete separation plane and concrete composite (bottom row).

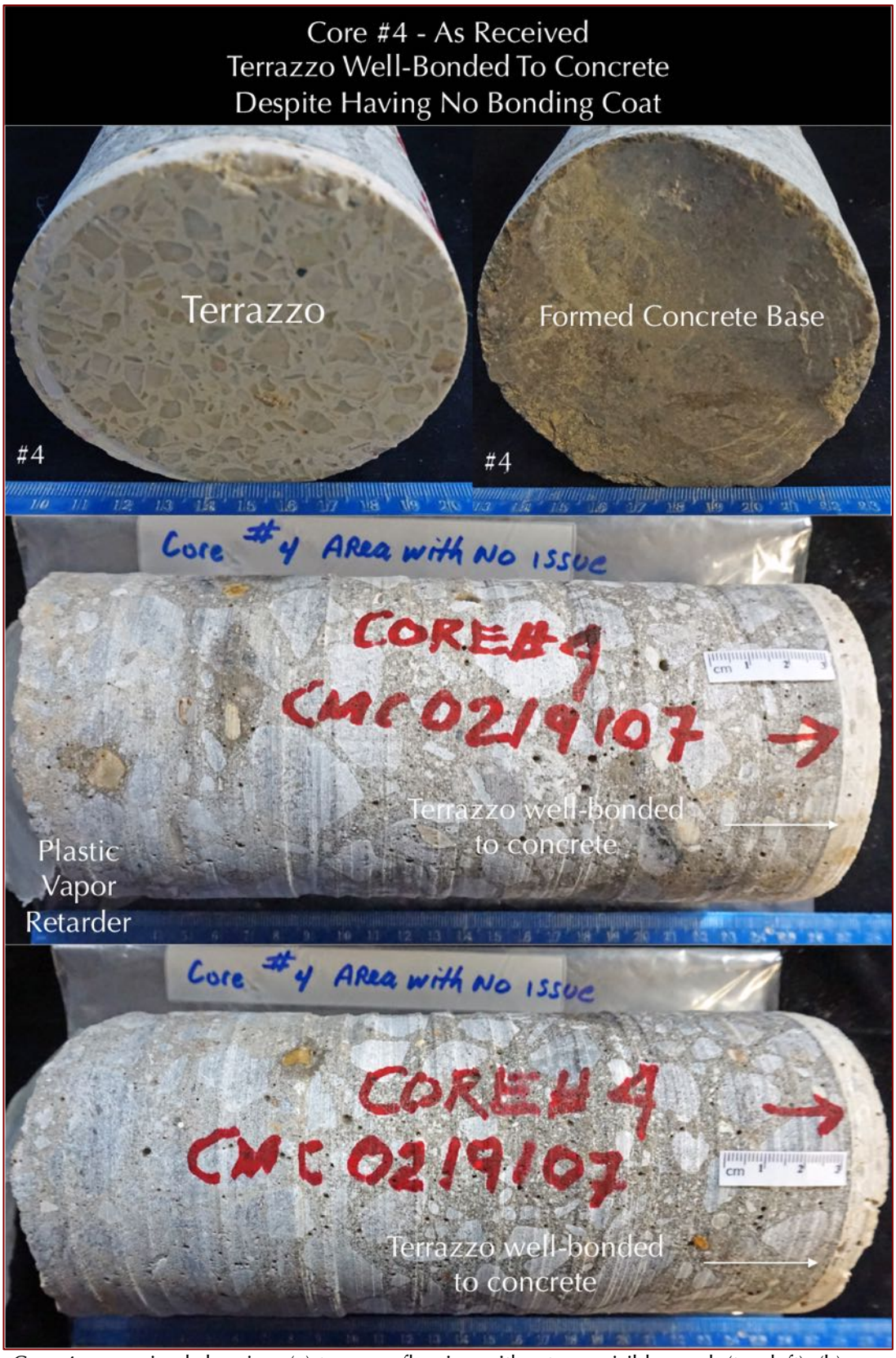

Figure 10: Core 4 as received showing: (a) terrazzo flooring without any visible crack (top left); (b) smooth, wavy formed bottom end of concrete with impression of placement of slab on a plastic vapor retarder (top right); and (c) two side views of terrazzo and concrete substrate with good bond between the top (middle and bottom rows).

LABORATORY EXAMINATIONS

LAPPED CROSS SECTIONS

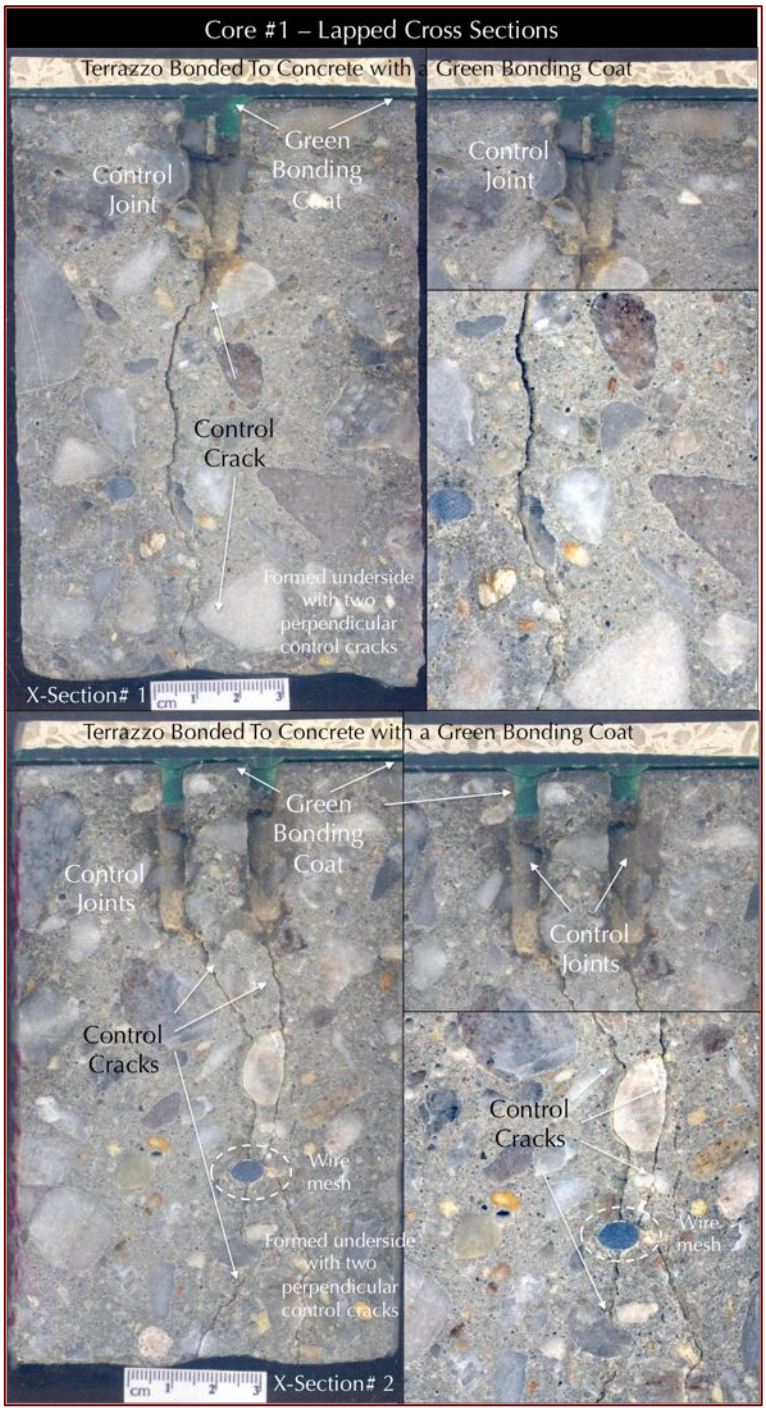

Figure 11: Lapped cross section of Core 1 showing: (a) white terrazzo flooring without any visible crack and smooth, wavy formed bottom end of concrete with impression of placement of slab on a plastic vapor retarder; (c) terrazzo, a green bond coat, and concrete with control joints and associated cracks; (d) good grading and well-distribution of crushed stone coarse aggregate in concrete, (e) dense terrazzo having crushed aggregate chips and white binder, (f) well-bonding of terrazzo to concrete by the green bond coat that has penetrated into control joints.

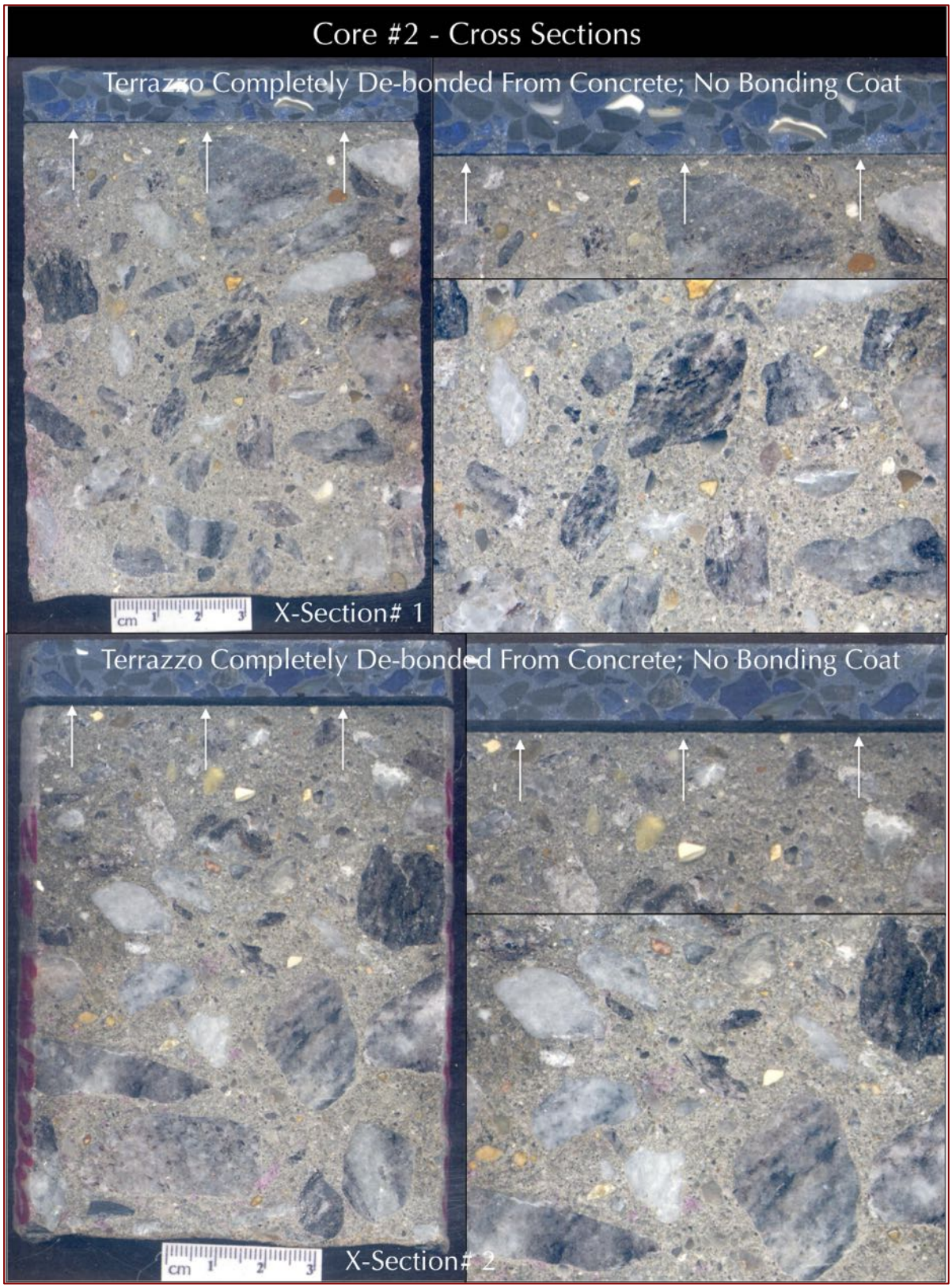

Figure 12: Lapped cross section of Core 2 showing: (a) blue terrazzo flooring without any visible crack and smooth, wavy formed bottom end of concrete with impression of placement of slab on a plastic vapor retarder; (c) complete separation of terrazzo from concrete; (d) good grading and well-distribution of crushed stone coarse aggregate in concrete, and (e) dense terrazzo having crushed aggregate chips and dark blue polymer binder.

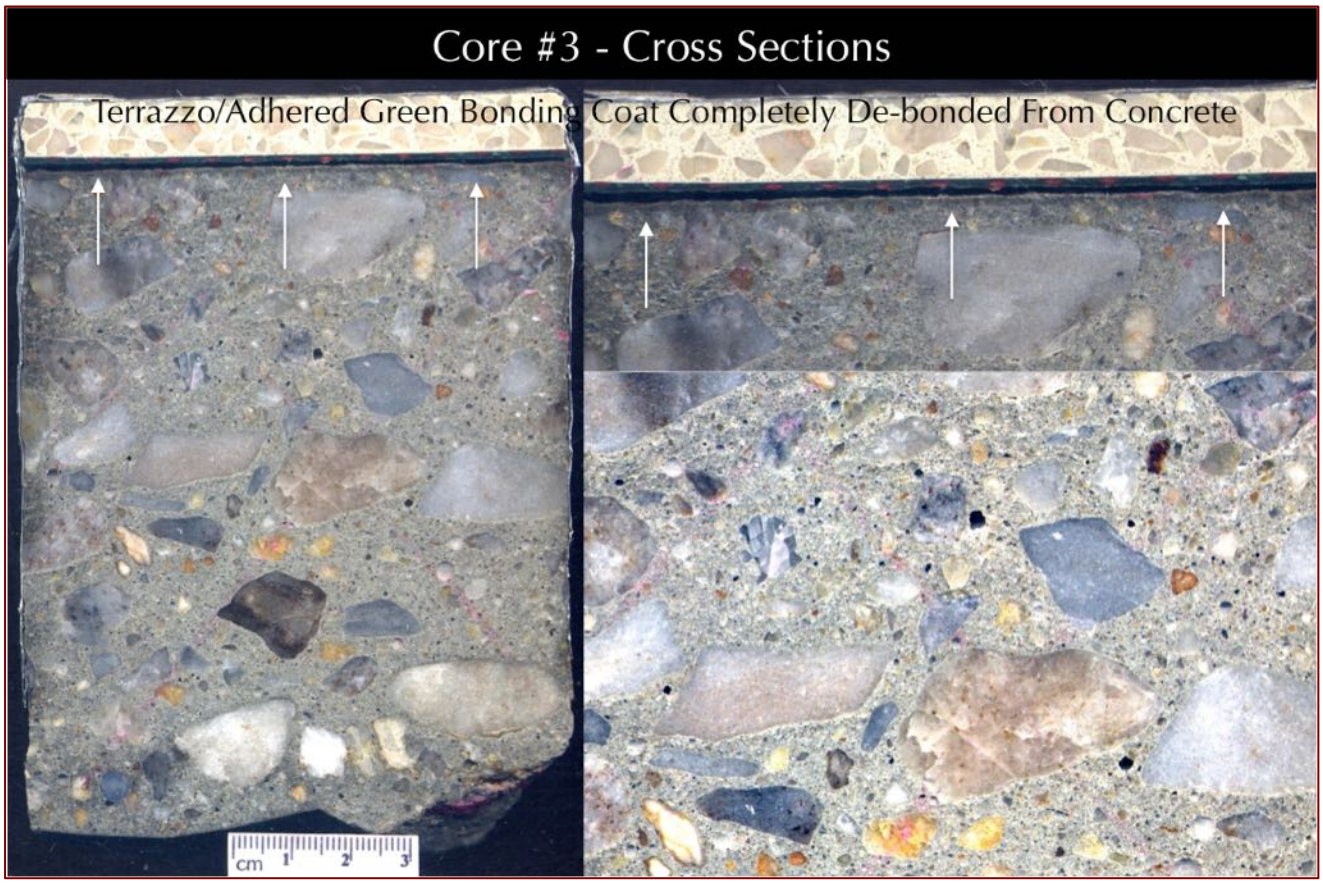

Figure 13: Lapped cross section of Core 3 showing: (a) white terrazzo flooring and smooth, wavy formed bottom end of concrete with impression of placement of slab on a plastic vapor retarder; (c) terrazzo, and a green bond coat, which are mutually bonded but together de-bonded from concrete; (d) good grading and well-distribution of crushed stone coarse aggregate in concrete, and (e) dense terrazzo having crushed aggregate chips and white binder.

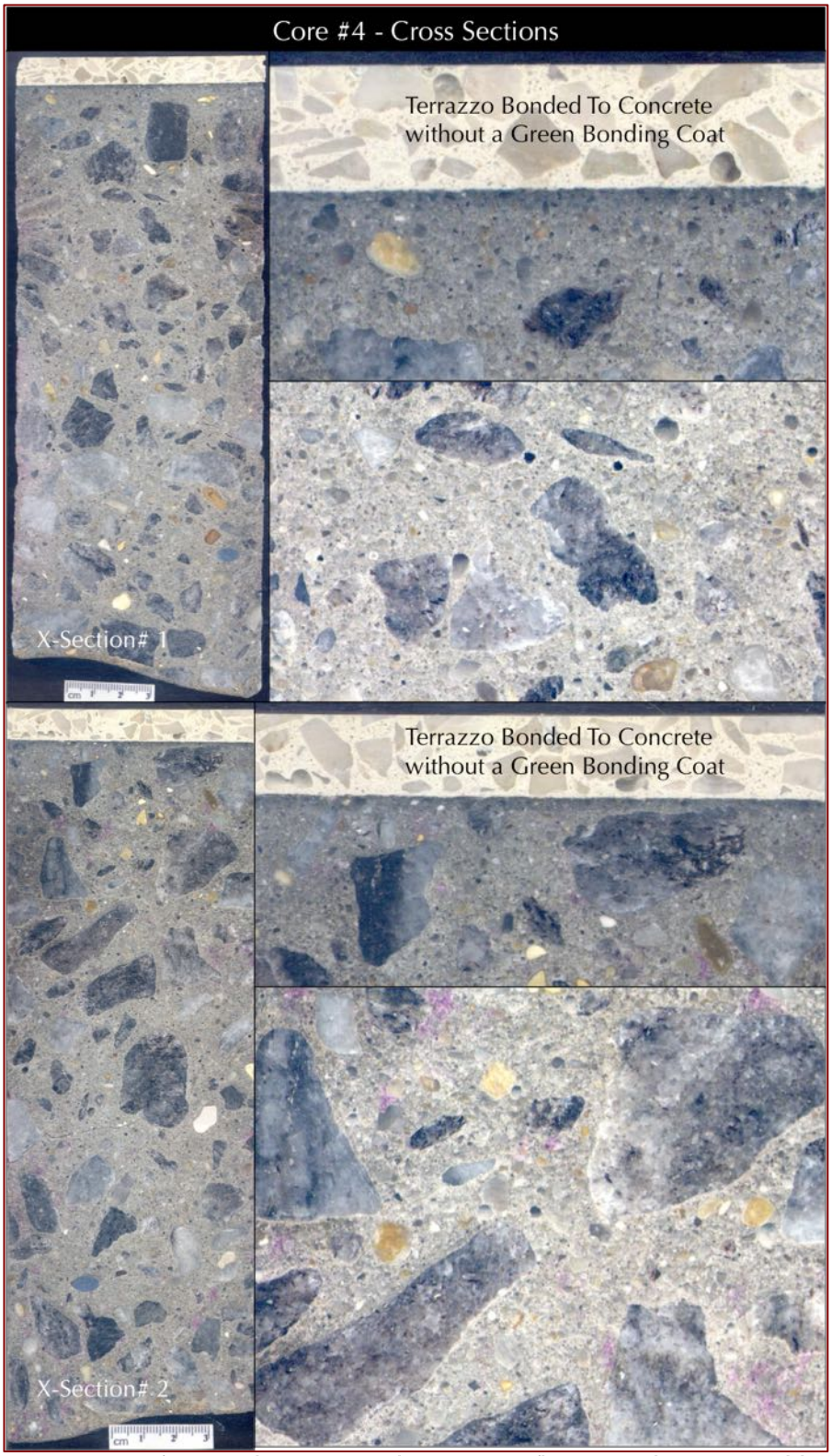

Figure 14: Lapped cross section of Core 4 showing: (a) white terrazzo flooring without any visible crack and smooth, wavy, formed bottom end of concrete with impression of placement of slab on a plastic vapor retarder; (c) good bond of terrazzo to concrete despite having no green bond coat between the two as found in other cores; (d) good grading and well-distribution of crushed stone coarse aggregate in concrete, and (e) dense terrazzo having crushed aggregate chips and white binder.

SAW-CUT SECTIONS

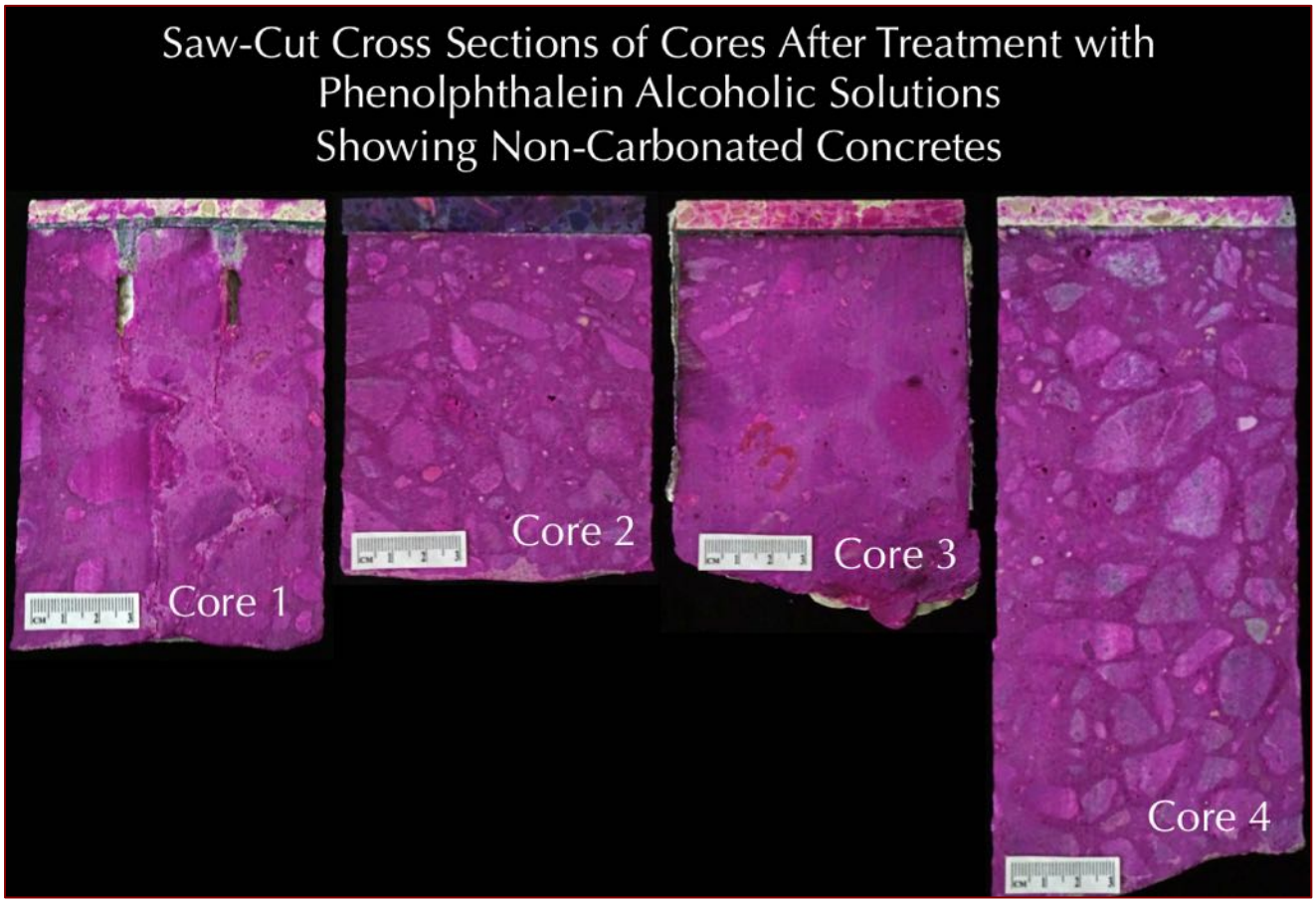

Figure 15: Saw-cut cross sections of four cores after treatment with phenolphthalein alcoholic solutions showing lack of carbonation of concrete where concrete turned dark pink after treatment, and carbonated aggregate chips in terrazzo which remain clear after treatment except for some contaminated stain from underlying concrete.

PHOTOMICROGRAPHS OF LAPPED CROSS SECTIONS

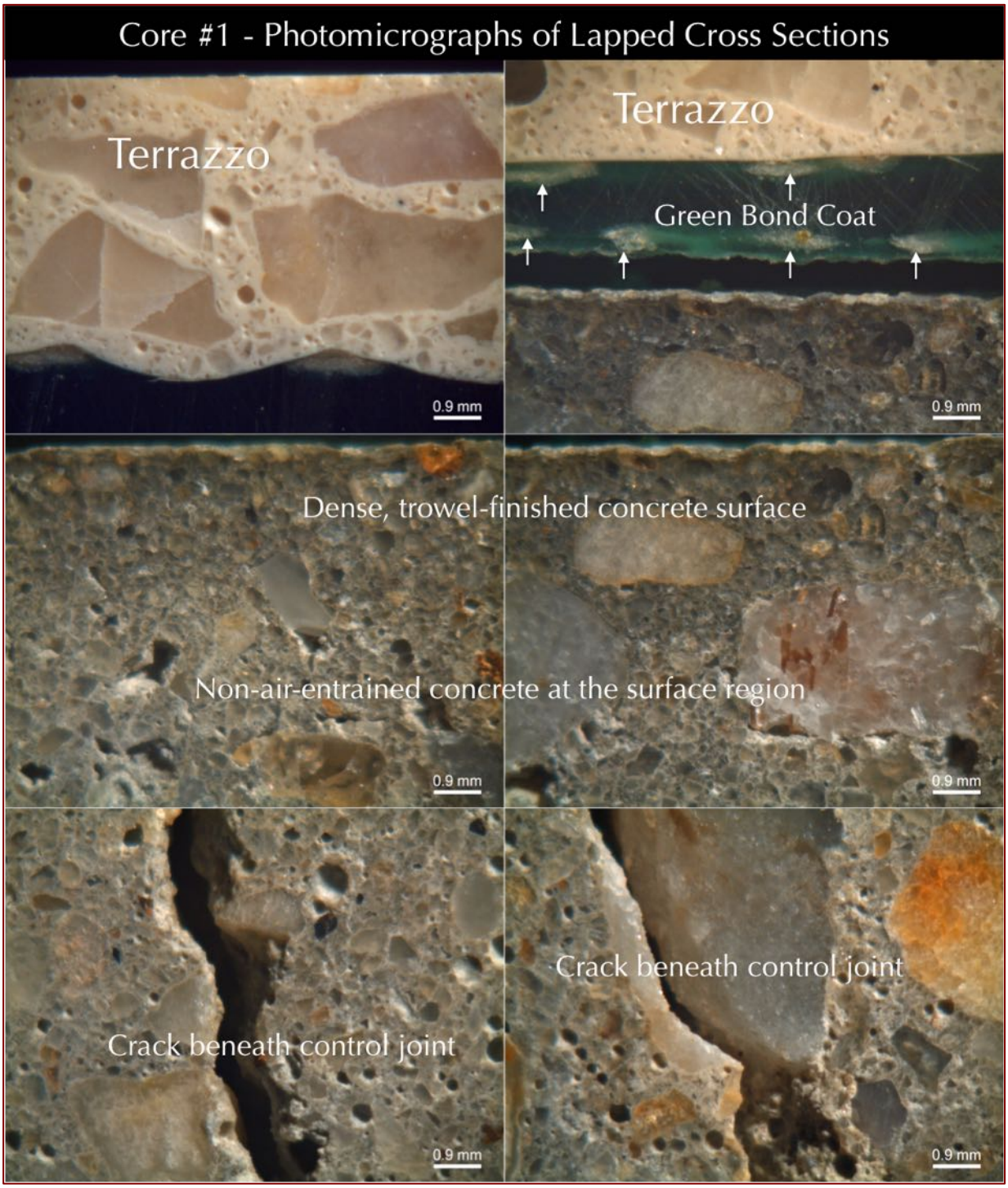

Figure 16: Photomicrographs of lapped cross section of Core 1 showing: (a) terrazzo flooring 7 mm in thickness, having crushed limestone/marble chips (3 mm nominal size) in white polymer binder, and dense, non-air-entrained nature of terrazzo; (b) green bond coat adhered to the base of terrazzo (nominal 2.5 to 3 mm thick) but completely de-bonded from concrete (the coat has fiber reinforcement at its top and bottom ends as shown by arrows at the cross sections); (c) dense, dark gray, air-free trowel-finished surface region of concrete floor with no trace of bonding coat on it; (d) non-air-entrained nature of concrete; and (e) extension of crack in concrete from control joints.

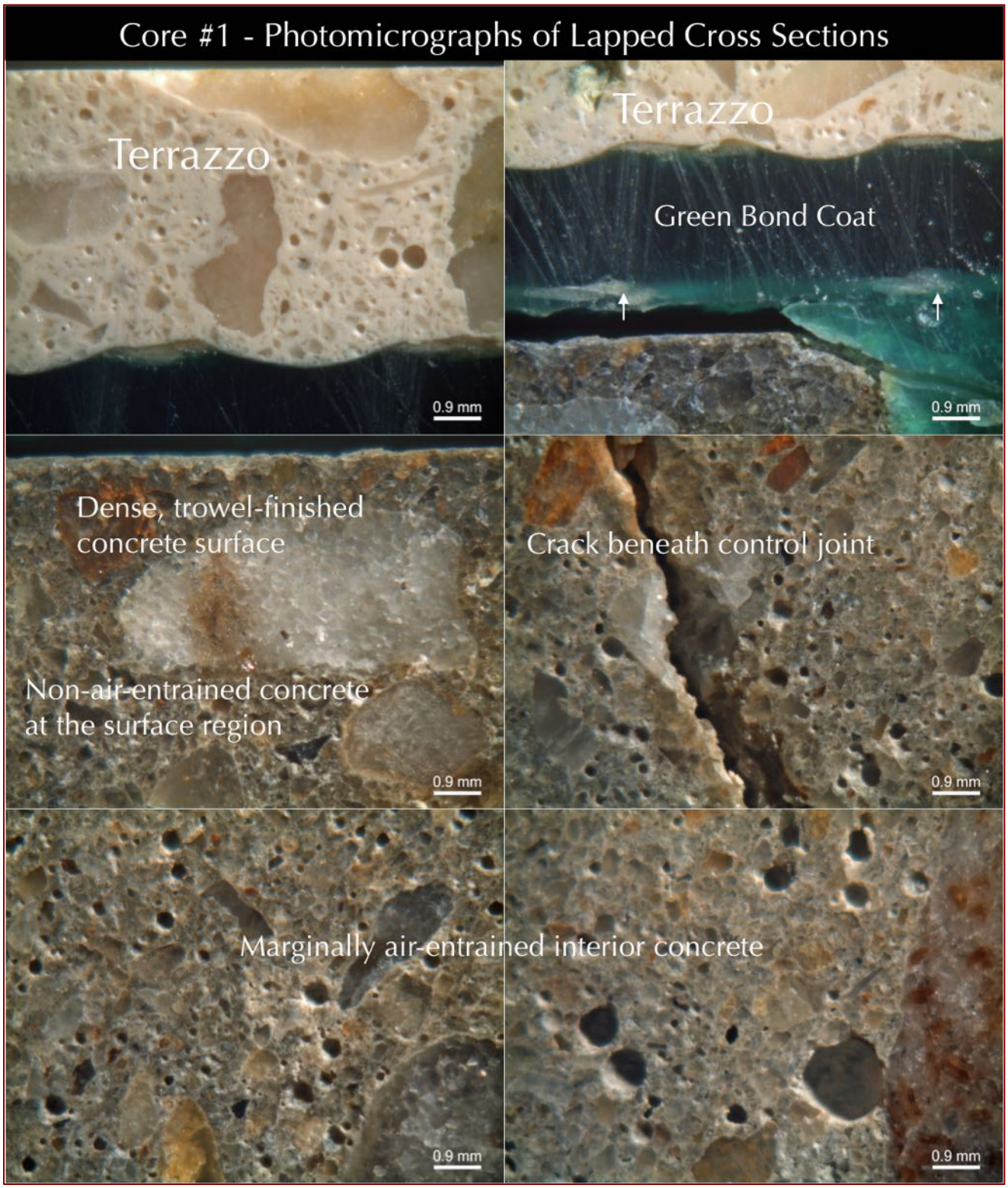

Figure 17: Photomicrographs of lapped cross section of Core 1 showing: (a) terrazzo flooring 7 mm in thickness, having crushed limestone/marble chips (3 mm nominal size) in white polymer binder, and dense, non-air-entrained nature of terrazzo; (b) green bond coat adhered to the base of terrazzo (nominal 2.5 to 3 mm thick) but completely de-bonded from concrete (fiber reinforcement at the base of this coat is marked by arrows); (c) dense, dark gray, air-free trowel-finished surface region of concrete floor with no trace of bonding coat on it; (d) non-air-entrained to marginally air entrained nature of concrete; and (e) extension of crack in concrete from control joints.

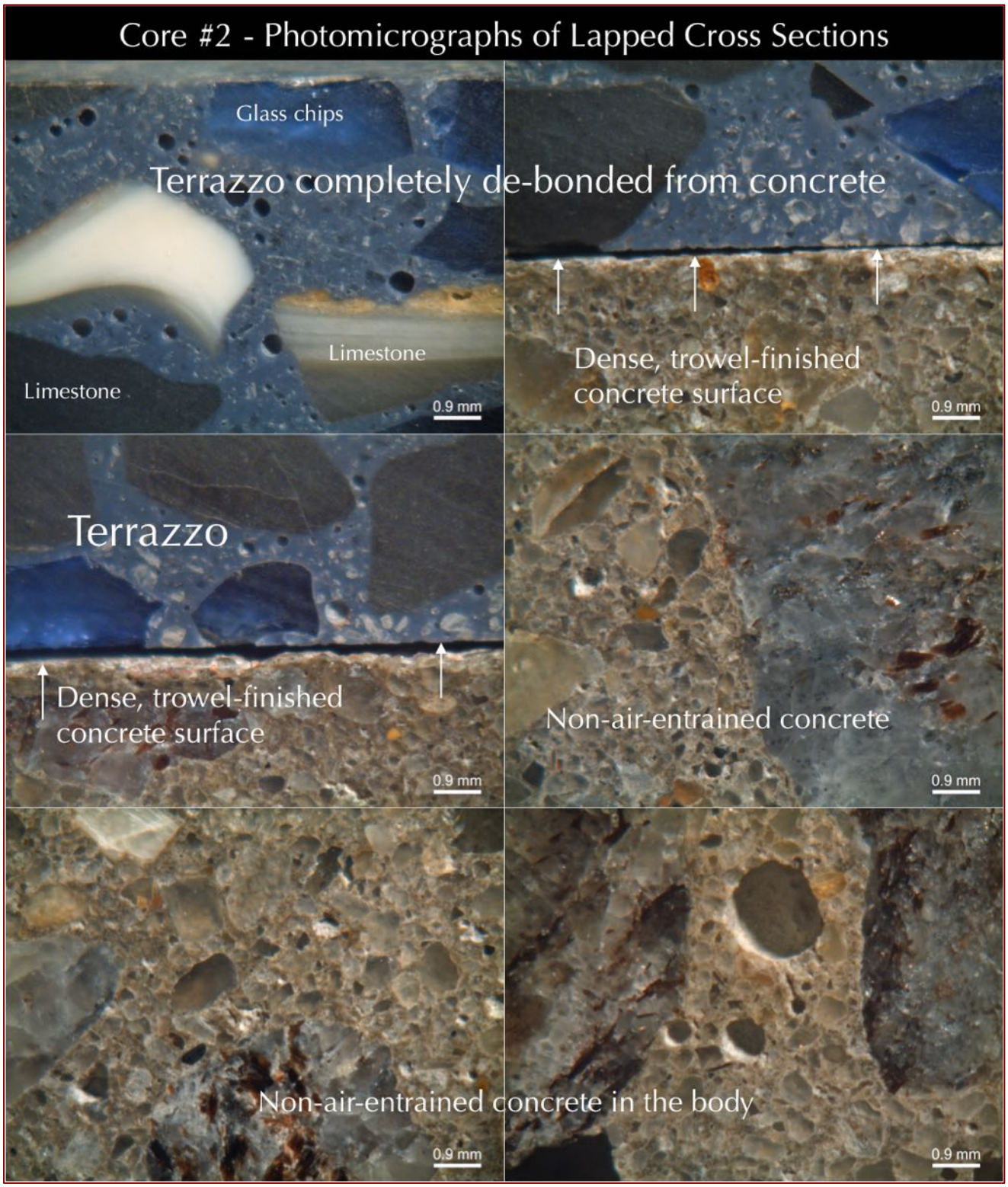

Figure 18: Photomicrographs of lapped cross section of Core 2 showing: (a) terrazzo flooring 12 mm in thickness, having crushed limestone/marble/glass chips (5 mm nominal size) in dark blue pigmented polymer binder, and dense, non-air-entrained nature of terrazzo; (b) lack of any bond coat beneath terrazzo, and complete de-bonding of terrazzo from concrete; (c) dense, dark gray, air-free trowel-finished surface region of concrete floor with no trace of terrazzo on it; and (d) non-air-entrained nature of concrete.

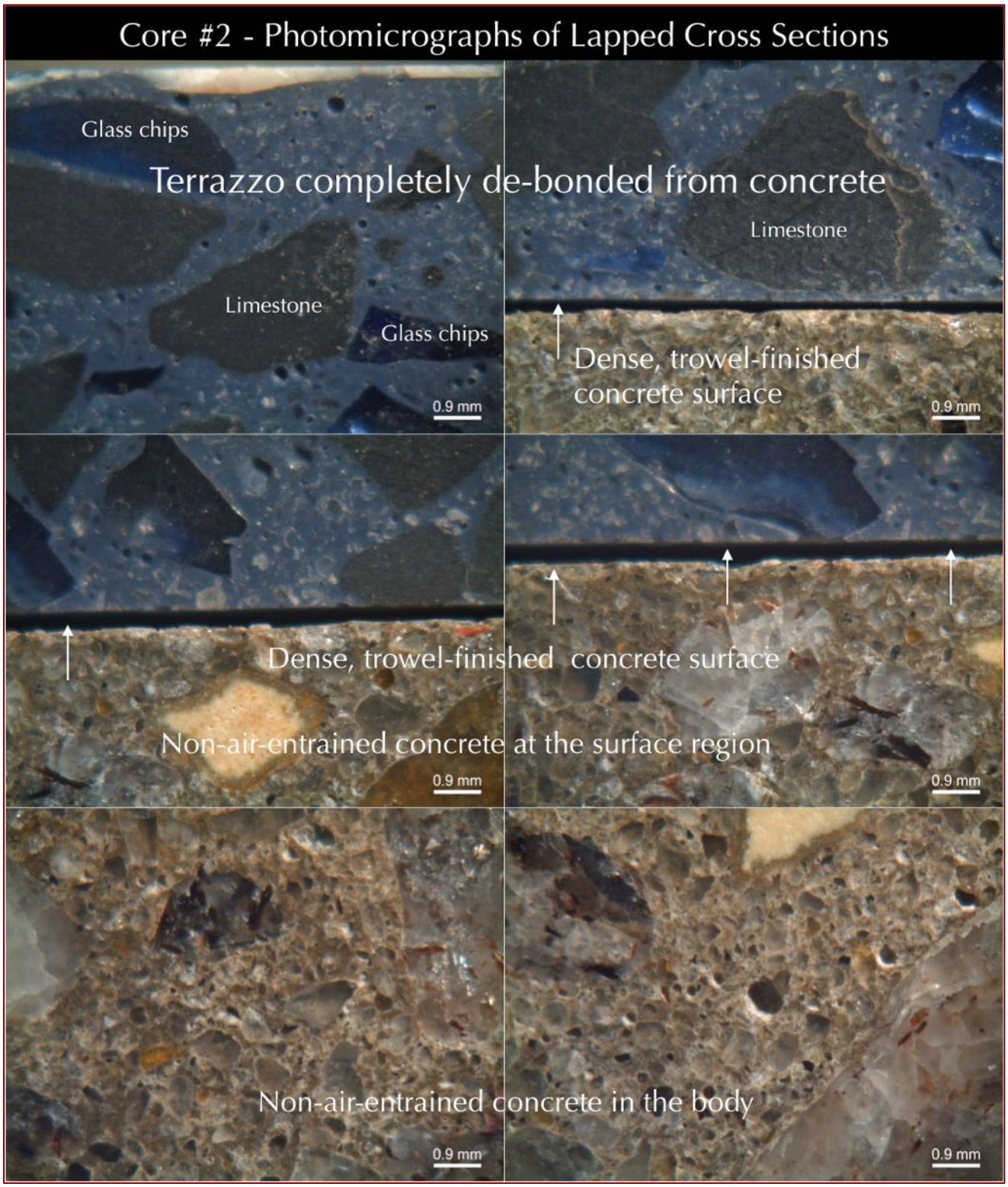

Figure 19: Photomicrographs of lapped cross section of Core 2 showing: (a) terrazzo flooring 12 mm in thickness, having crushed limestone/marble/glass chips (5 mm nominal size) in dark blue pigmented polymer binder, and dense, non-air-entrained nature of terrazzo; (b) lack of any bond coat beneath terrazzo, and complete de-bonding of terrazzo from concrete; (c) dense, dark gray, air-free trowel-finished surface region of concrete floor with no trace of terrazzo on it; and (d) non-air-entrained nature of concrete.

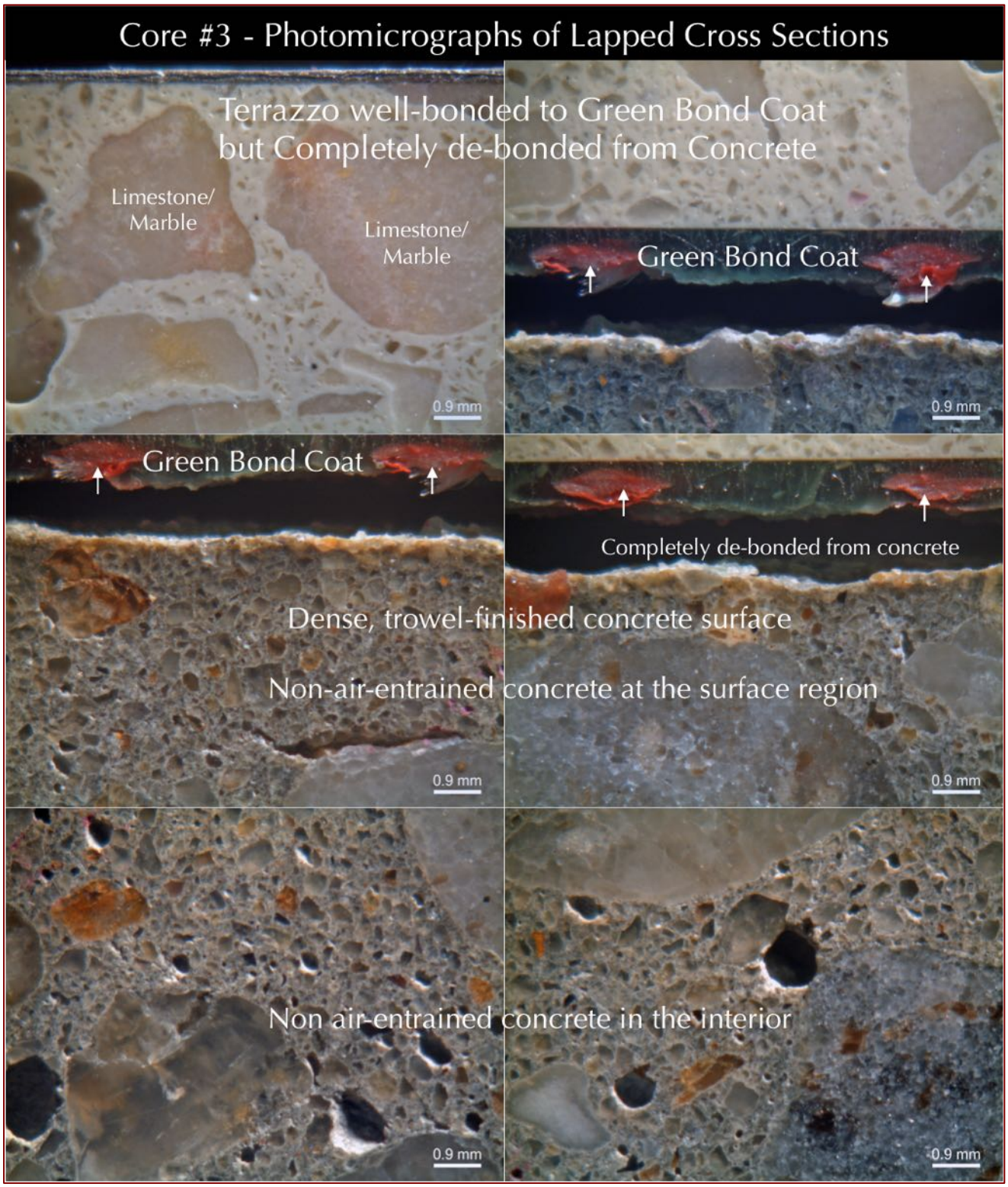

Figure 20: Photomicrographs of lapped cross section of Core 3 showing: (a) terrazzo flooring 10 mm in thickness, having crushed limestone/marble chips (3 mm nominal size) in white polymer binder, and dense, non-air-entrained nature of terrazzo; (b) green bond coat with red fibermesh reinforcement adhered to the base of terrazzo (nominal 2.5 to 3 mm thick) but completely de-bonded from concrete; (c) dense, dark gray, air-free trowel-finished surface region of concrete floor with no trace of bonding coat on it; and (d) non-air-entrained nature of concrete.

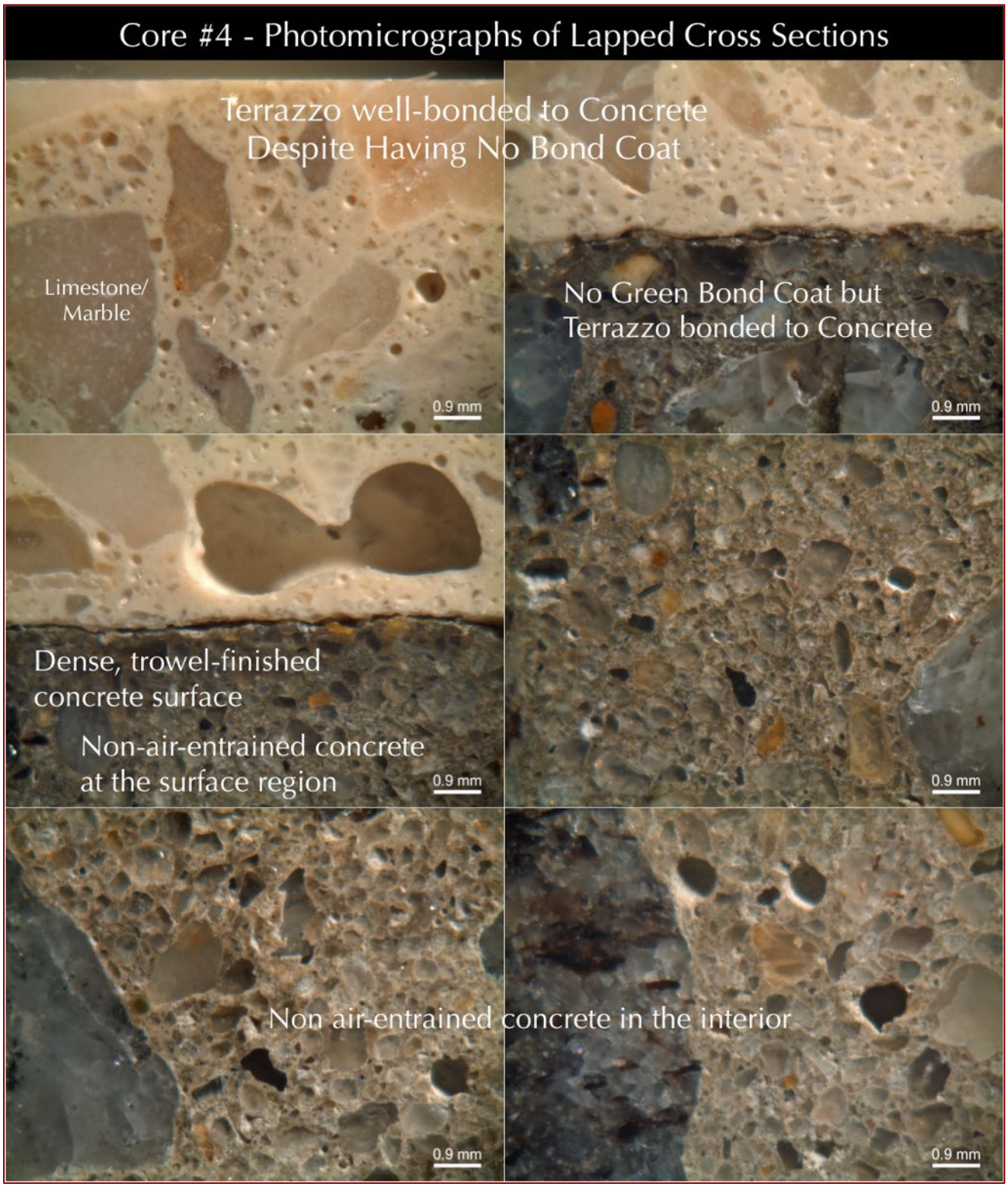

Figure 21: Photomicrographs of lapped cross section of Core 4 showing: (a) terrazzo flooring 10 mm in thickness, having crushed limestone/marble chips (3 mm nominal size) in white polymer binder, and dense, non-air-entrained nature of terrazzo; (b) no green bond coat at the base of terrazzo, yet terrazzo is well-bonded to concrete; (c) dense, dark gray, air-free trowel-finished surface region of concrete floor; and (d) non-air-entrained nature of concrete.

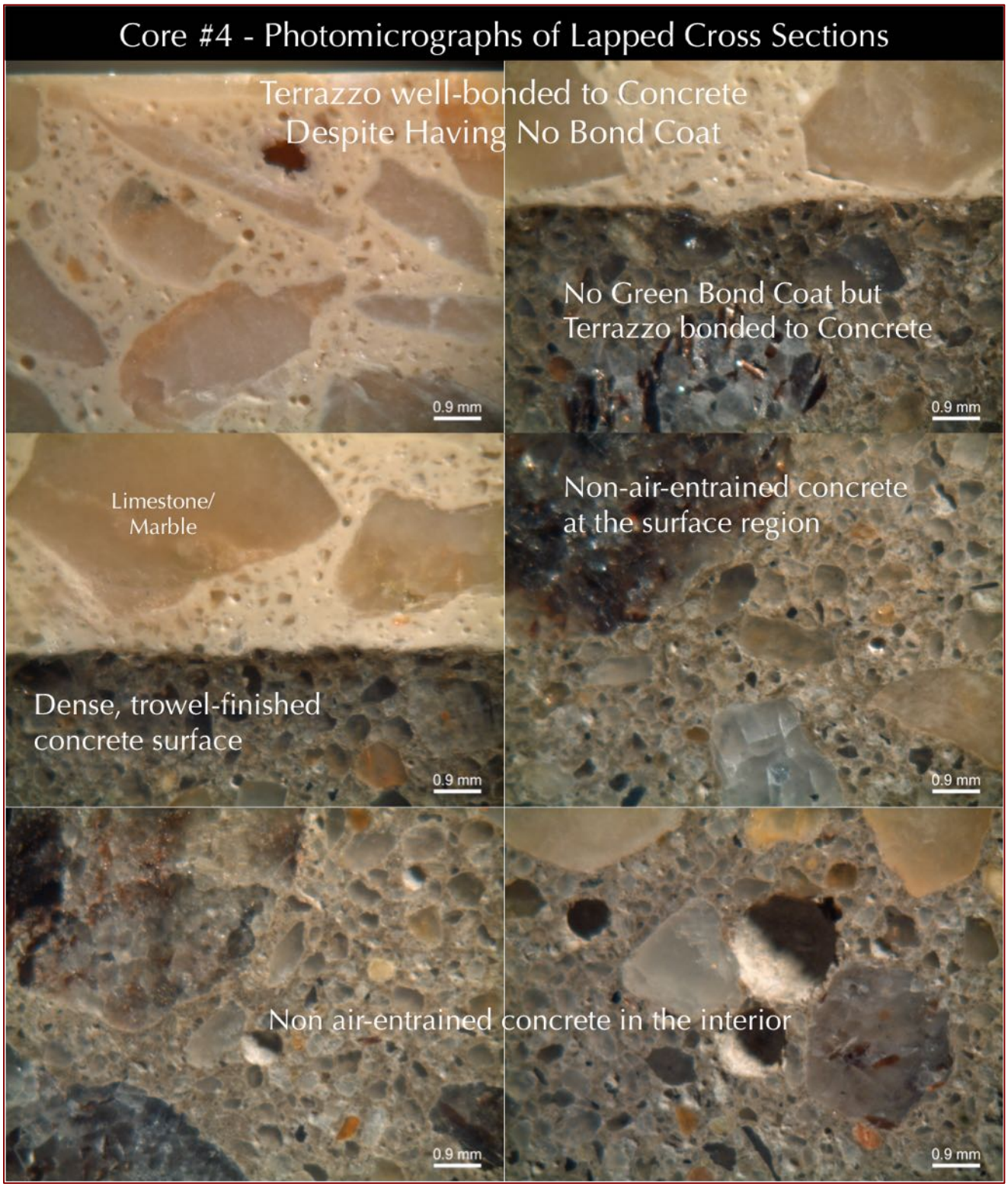

Figure 22: Photomicrographs of lapped cross section of Core 4 showing: (a) terrazzo flooring 10 mm in thickness, having crushed limestone/marble chips (3 mm nominal size) in white polymer binder, and dense, non-air-entrained nature of terrazzo; (b) no green bond coat at the base of terrazzo, yet terrazzo is well-bonded to concrete; (c) dense, dark gray, air-free trowel-finished surface region of concrete floor; and (d) non-air-entrained nature of concrete.

THIN SECTIONS

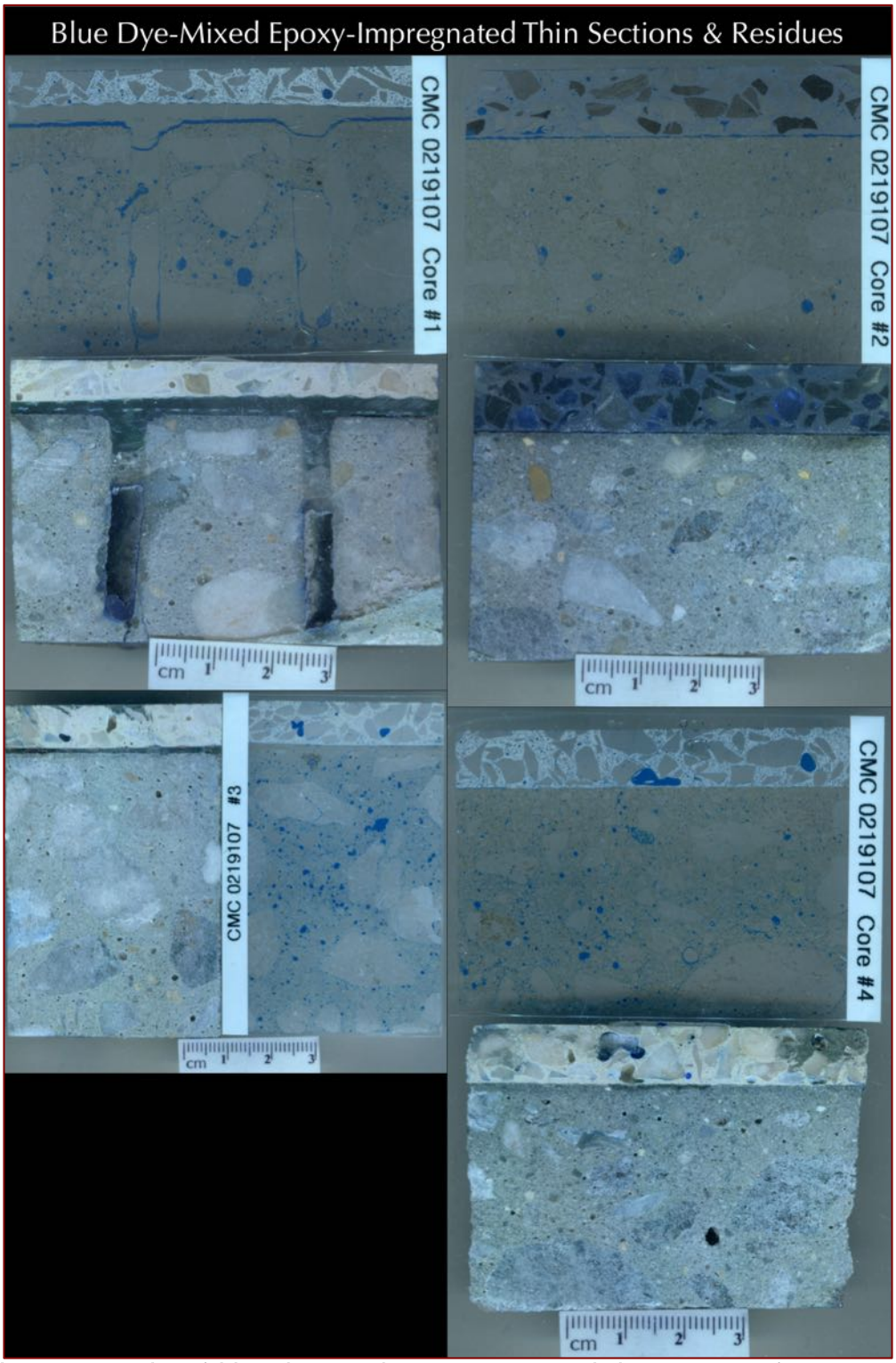

Figure 23: Photomicrographs of blue dye-mixed epoxy-impregnated thin sections of terrazzo and concrete composite cores showing size, shape, angularity, gradation, and distribution of marble/limestone chip particles in polymer binder in terrazzo, the underlying concrete where voids and cracks, if any are highlighted by blue epoxy. The top 2 inches from all four cores were sectioned and encapsulated with blue epoxy to prepare thin sections.

PHOTOMICROGRAPHS OF THIN SECTIONS

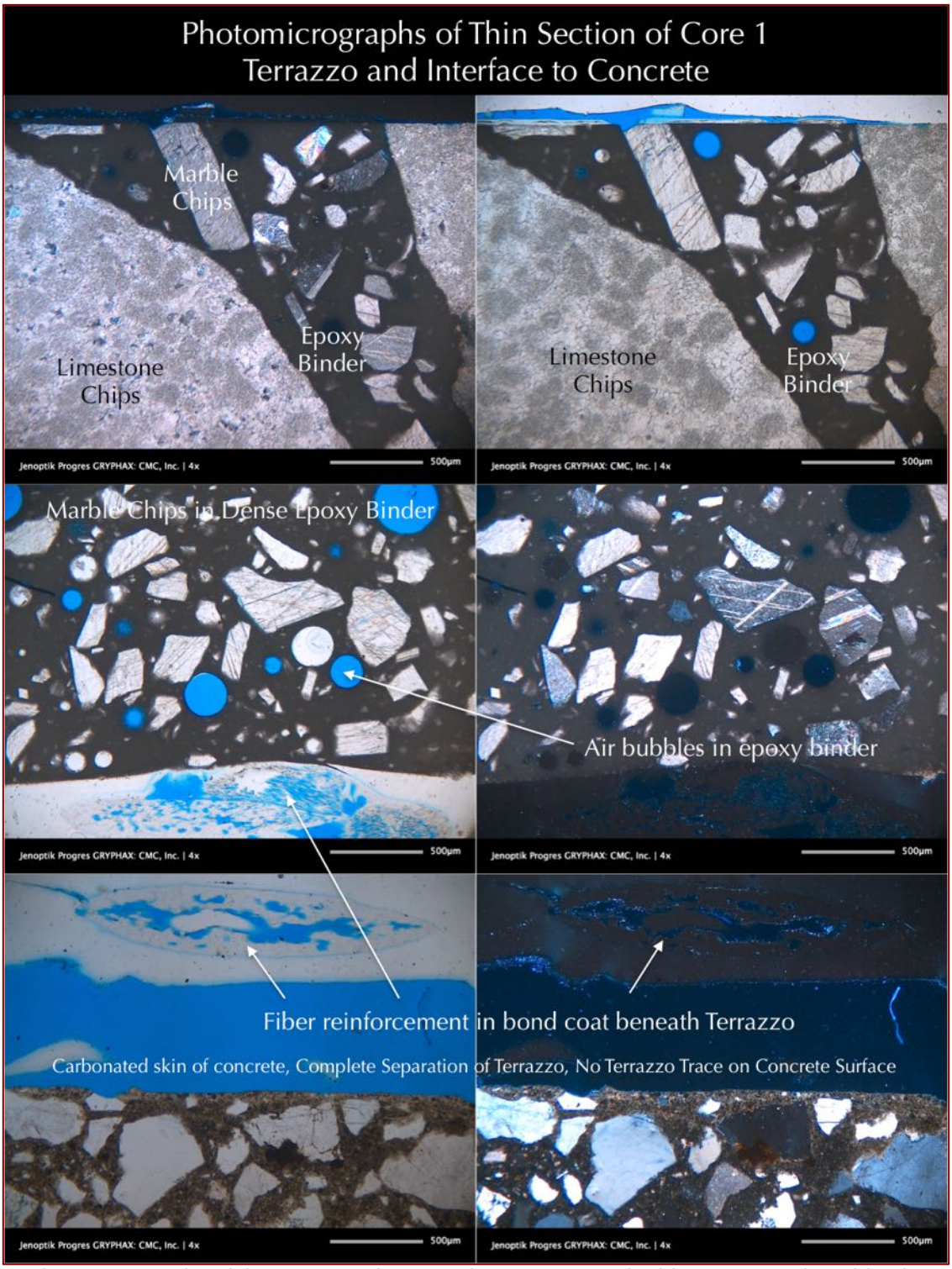

Figure 24: Photomicrographs of thin section of Core 1 showing: (a) crushed limestone and marble chips in dense polymer binder with occasional spherical entrapped voids in terrazzo; (b) fibermesh reinforcement of a bond coat at the base of terrazzo; (c) complete debonding of terrazzo and adhered bond coat from underlying concrete; (d) dense trowel-finished concrete surface with a carbonated skin at the top on which terrazzo was placed, indicating inadequate removal of concrete surface prior to terrazzo installation.

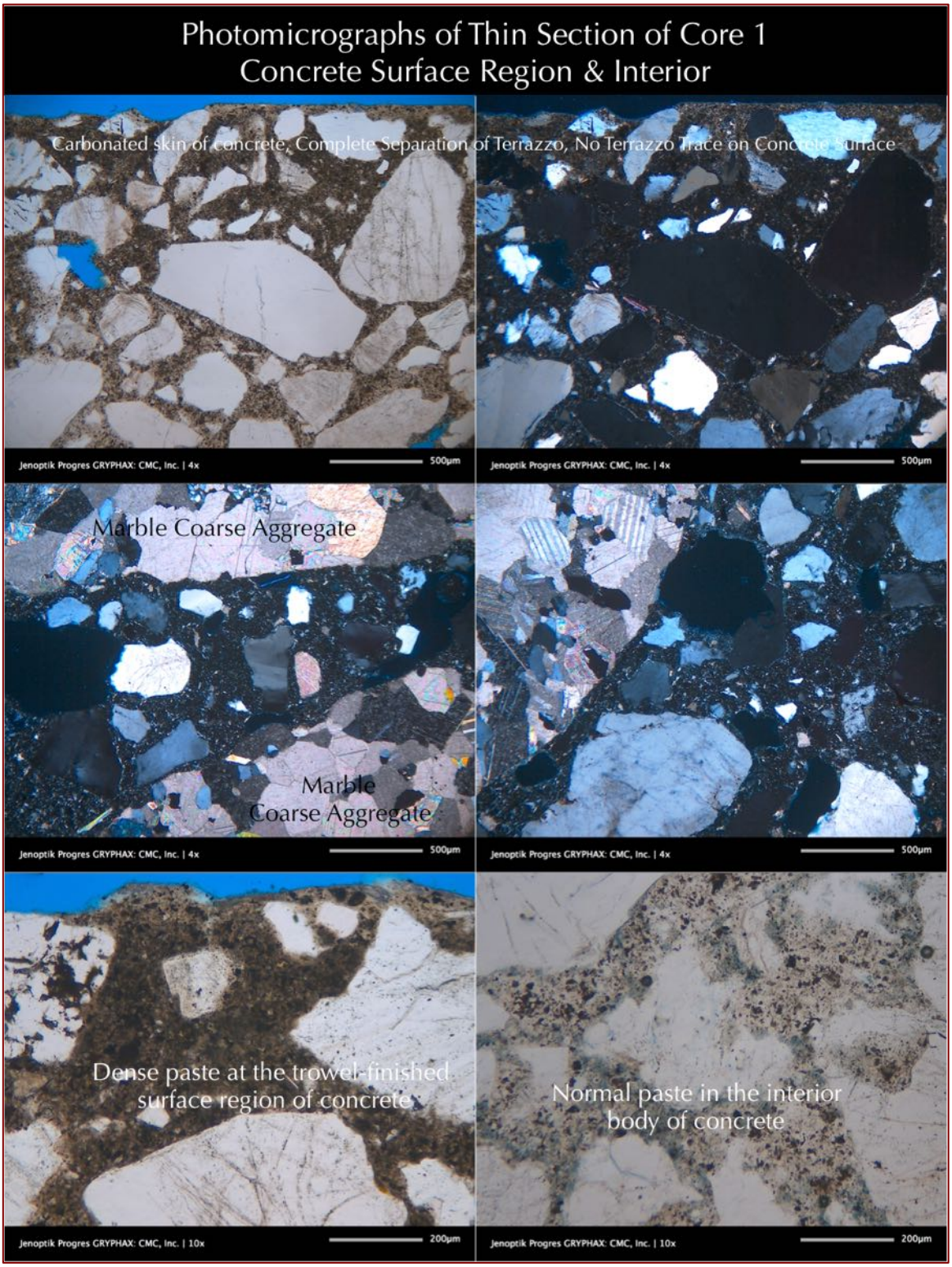

Figure 25: Photomicrographs of thin section of Core 1 showing: (a) dense trowel-finished concrete surface with a carbonated skin at the top on which terrazzo was placed, indicating inadequate removal of concrete surface prior to terrazzo installation; (b) crushed marble coarse aggregate and natural siliceous (quartz-quartzite) sand fine aggregate in concrete (middle row); (c) contrasting dense paste at the surface region versus normal paste in the body of concrete indicating incomplete removal of the dense paste at the surface that has prevented development of a good bond to the flooring components (as well as removal of any moisture build up from concrete).

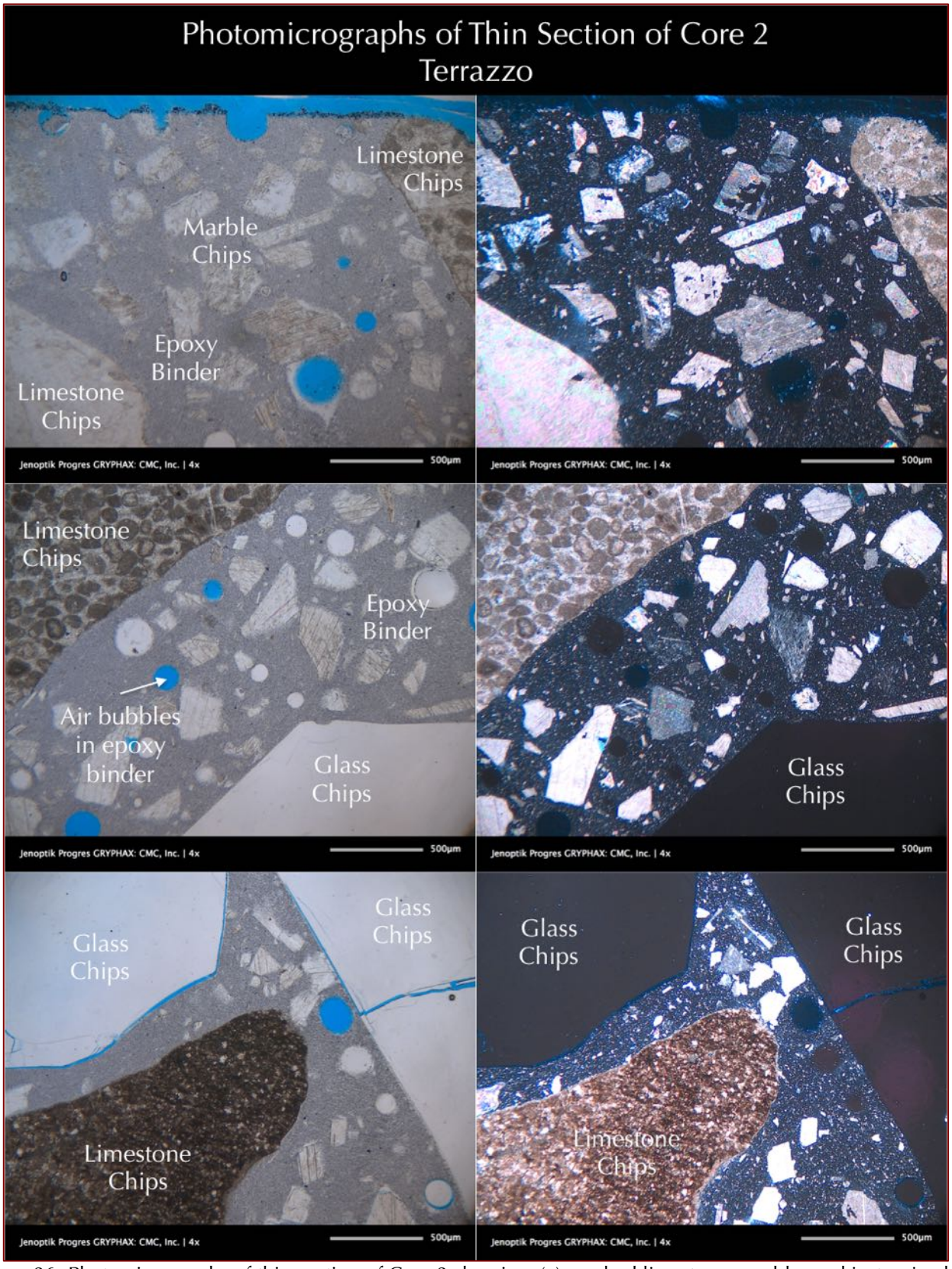

Figure 26: Photomicrographs of thin section of Core 2 showing: (a) crushed limestone, marble, and isotropic glass chips in dense polymer binder (appear much lighter toned than the binder in other three cores of white terrazzo flooring) with occasional spherical entrapped voids in terrazzo.

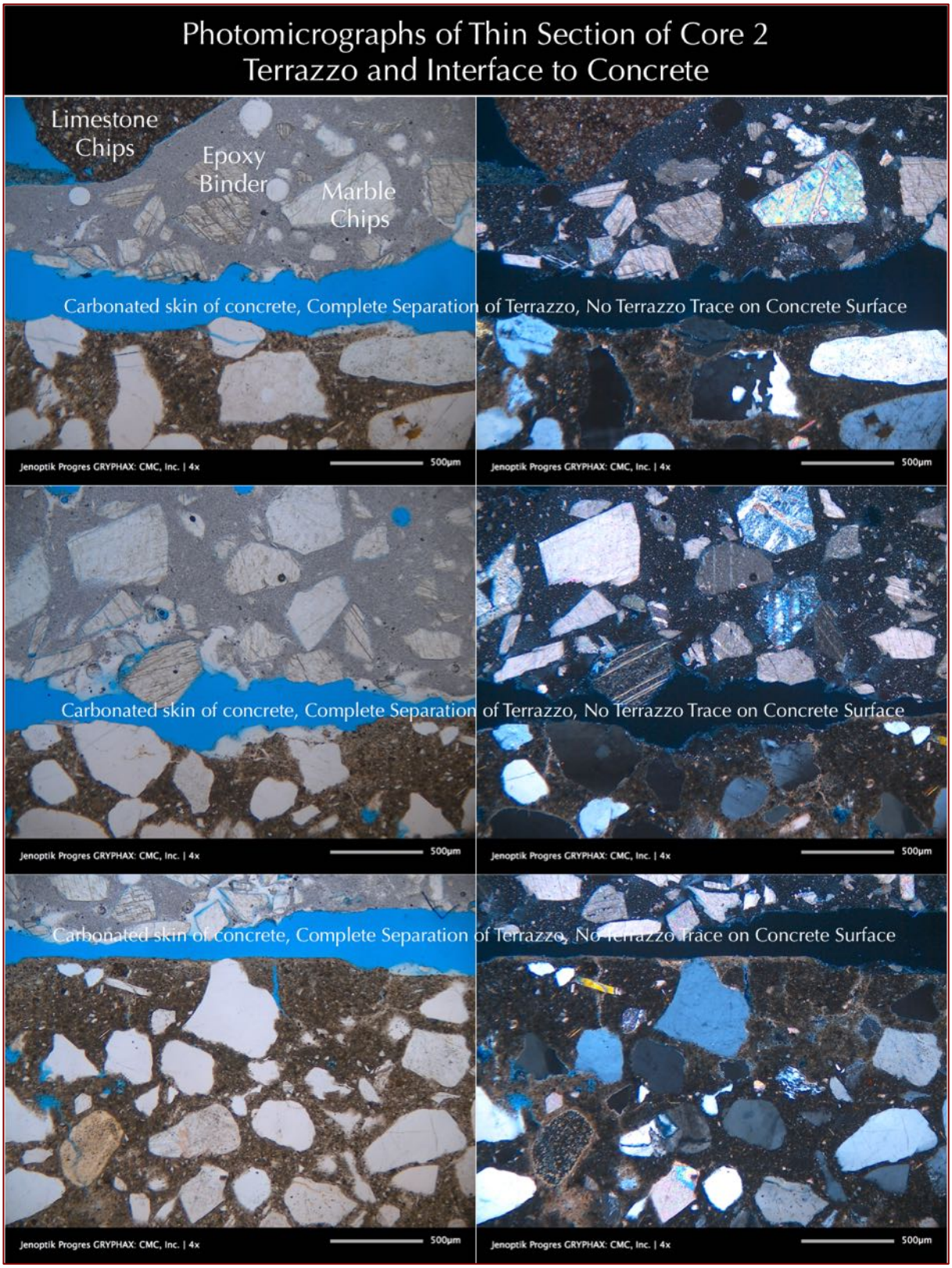

Figure 27: Photomicrographs of thin section of Core 2 showing: (a) crushed limestone, marble, and isotropic glass chips in dense polymer binder; (b) complete debonding of terrazzo from underlying concrete; (c) dense trowel-finished concrete surface with a carbonated skin (having occasional vertical shrinkage microcracks) at the top on which terrazzo was placed, indicating inadequate removal of concrete surface prior to terrazzo installation.

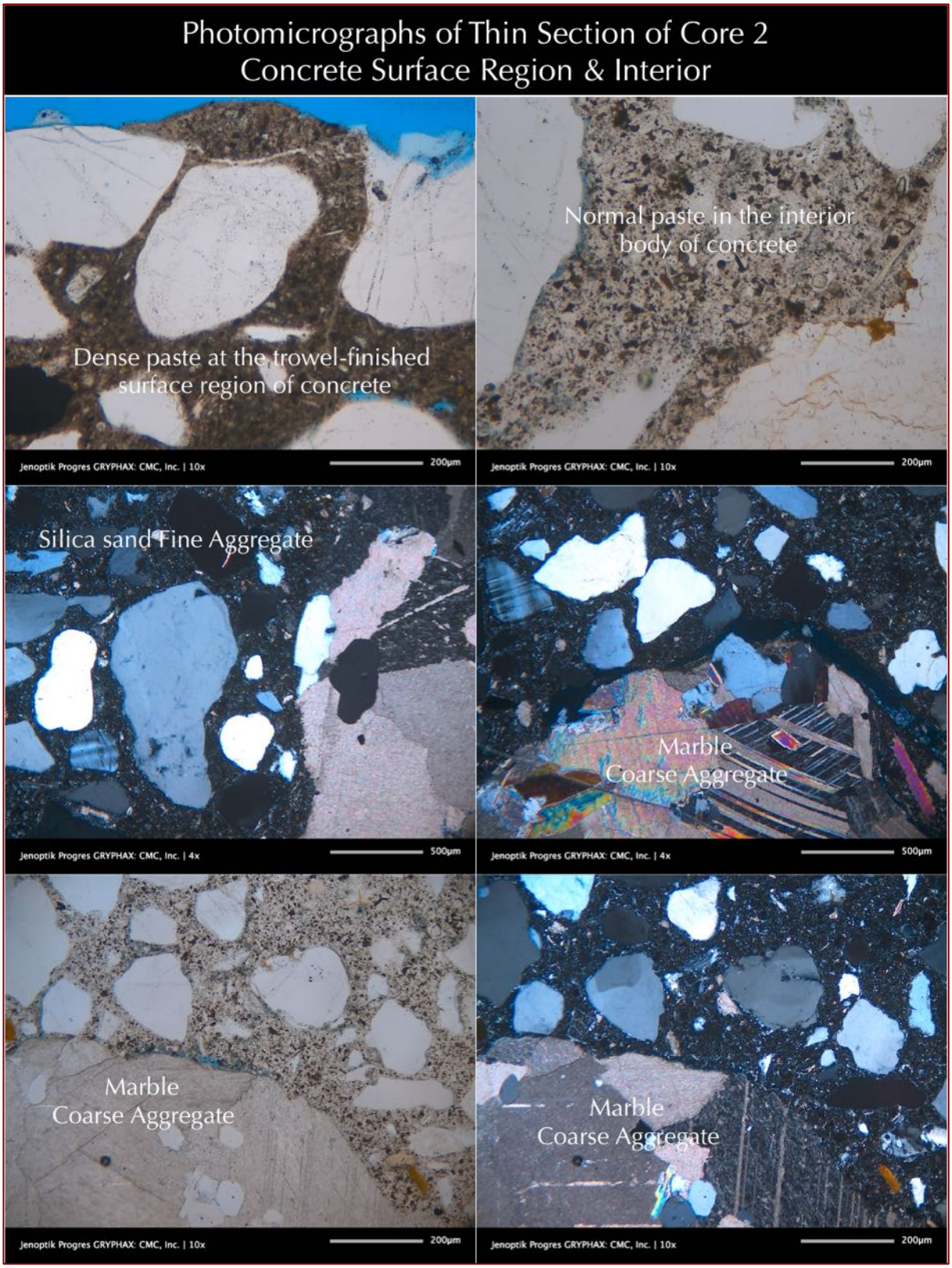

Figure 28: Photomicrographs of thin section of Core 2 showing: (a) dense trowel-finished concrete surface with a carbonated skin at the top on which terrazzo was placed, indicating inadequate removal of concrete surface prior to terrazzo installation; (b) crushed marble coarse aggregate and natural siliceous (quartz-quartzite) sand fine aggregate in concrete (middle row); (c) crushed marble and normal Portland cement paste in the body of concrete.

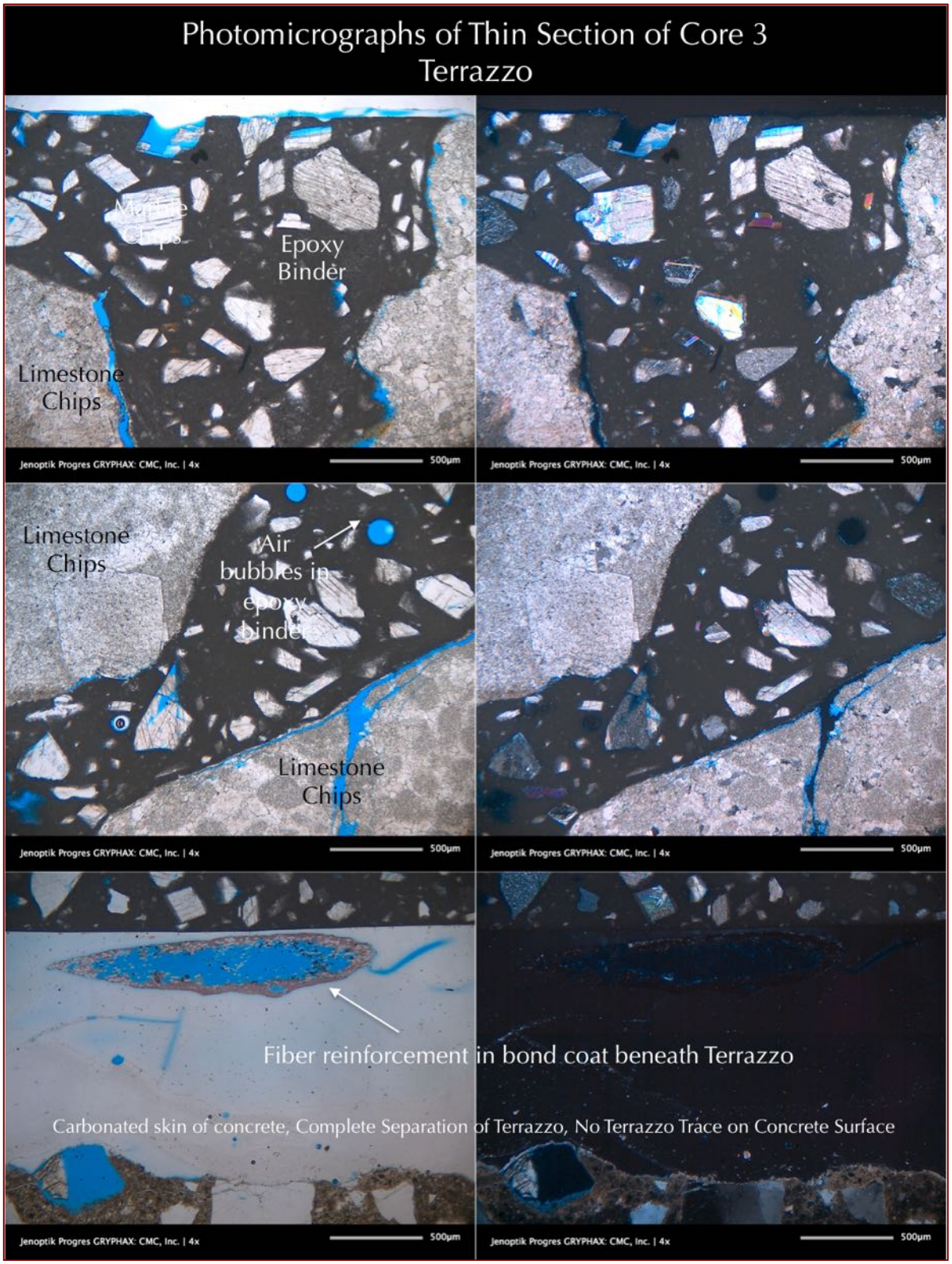

Figure 29: Photomicrographs of thin section of Core 3 showing: (a) crushed limestone and marble chips in dense polymer binder with occasional spherical entrapped voids in terrazzo; (b) fibermesh reinforcement of a bond coat at the base of terrazzo; (c) complete debonding of terrazzo and adhered bond coat from underlying concrete; (d) dense trowel-finished concrete surface with a carbonated skin at the top on which terrazzo was placed, indicating inadequate removal of concrete surface prior to terrazzo installation.

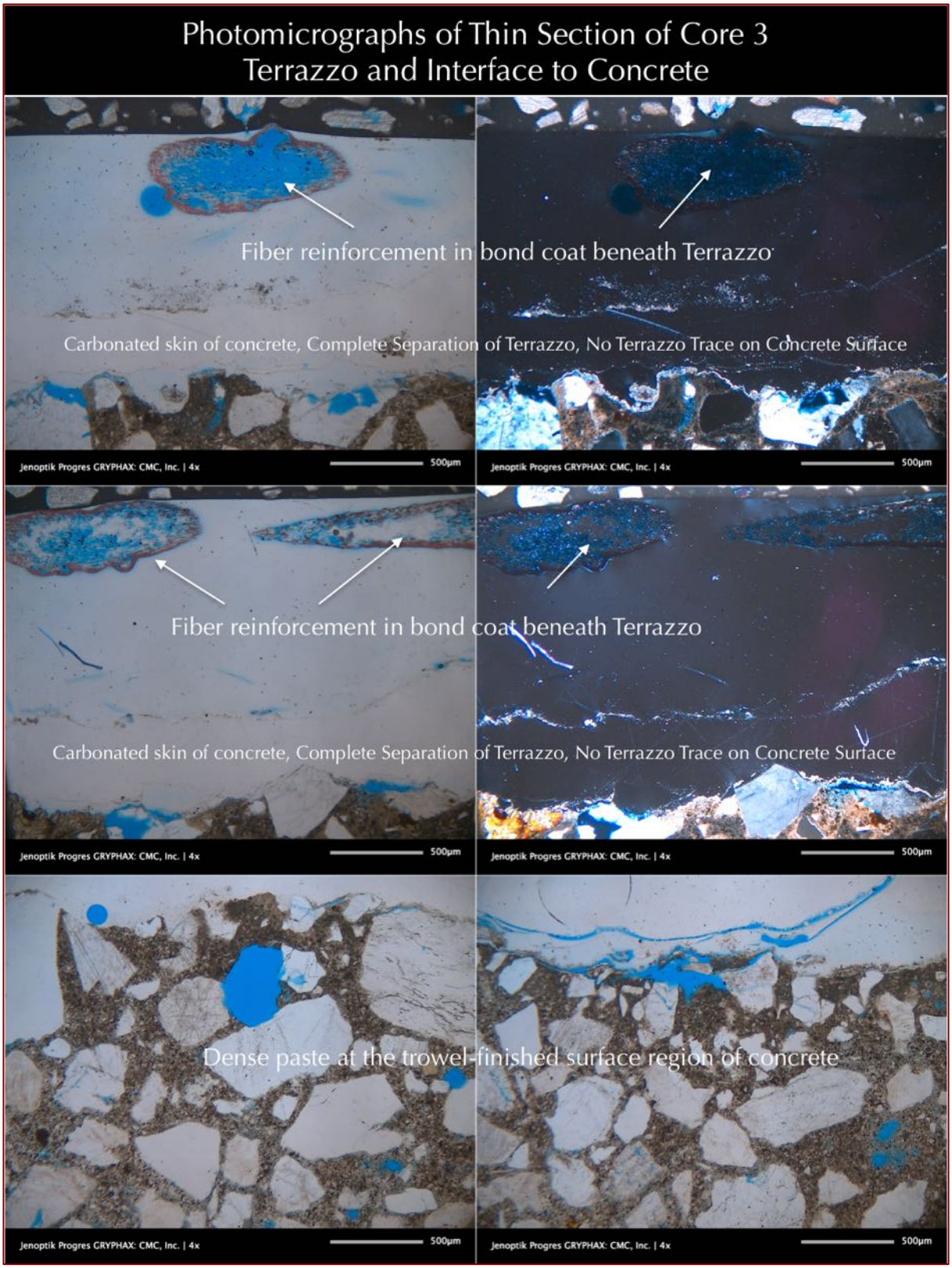

Figure 30: Photomicrographs of thin section of Core 3 showing: (a) fibermesh reinforcement of a bond coat at the base of terrazzo; (b) complete debonding of terrazzo and adhered bond coat from underlying concrete; (c) dense trowel-finished concrete surface with a carbonated skin at the top on which terrazzo was placed, indicating inadequate removal of concrete surface prior to terrazzo installation.

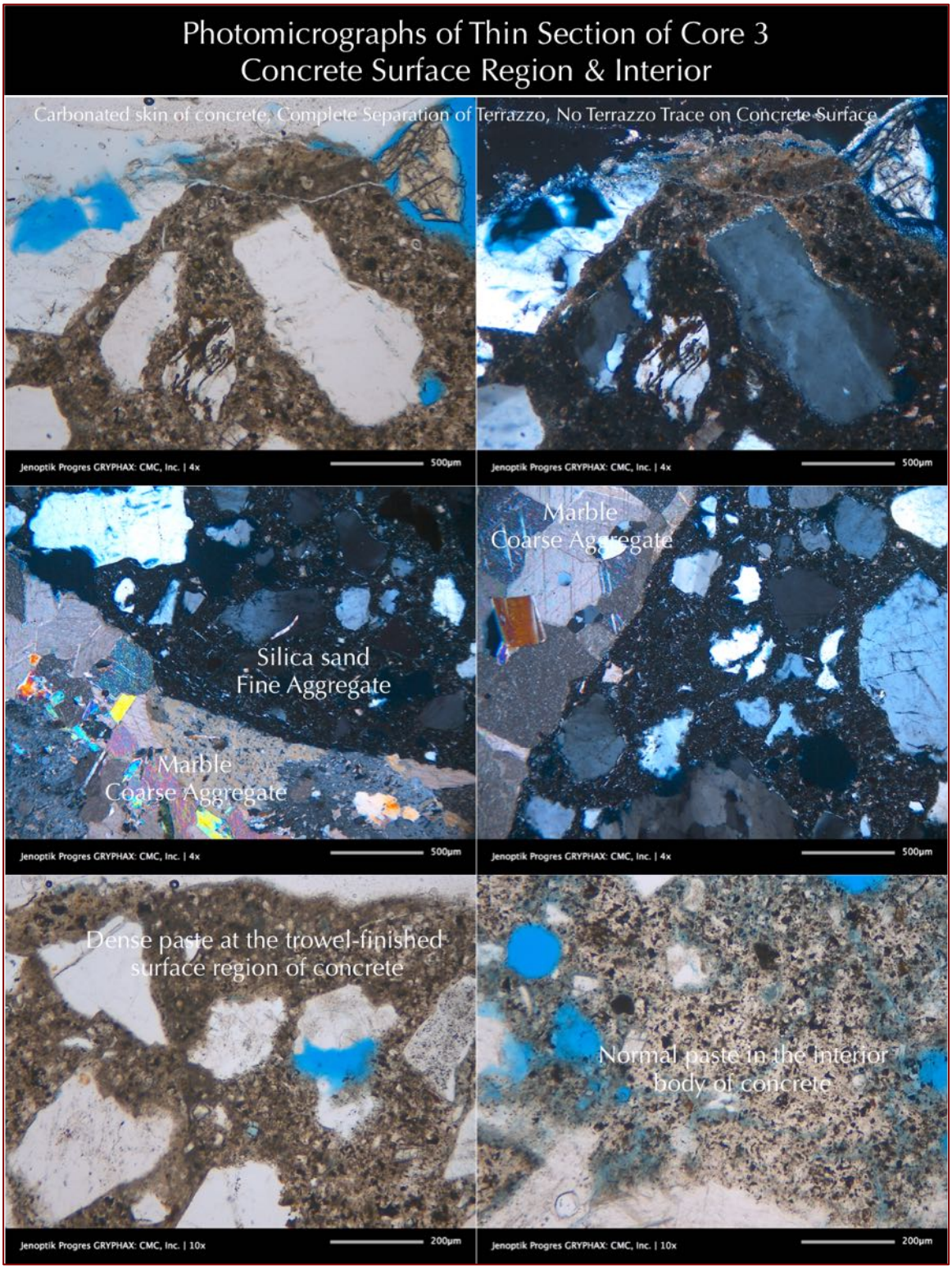

Figure 31: Photomicrographs of thin section of Core 3 showing: (a) dense trowel-finished concrete surface with a carbonated skin at the top on which terrazzo was placed, indicating inadequate removal of concrete surface prior to terrazzo installation; (b) crushed marble coarse aggregate and natural siliceous (quartz-quartzite) sand fine aggregate in concrete (middle row); (c) contrasting dense paste at the surface region versus normal paste in the body of concrete indicating incomplete removal of the dense paste at the surface that has prevented development of a good bond to the flooring components (as well as removal of any moisture build up from concrete).

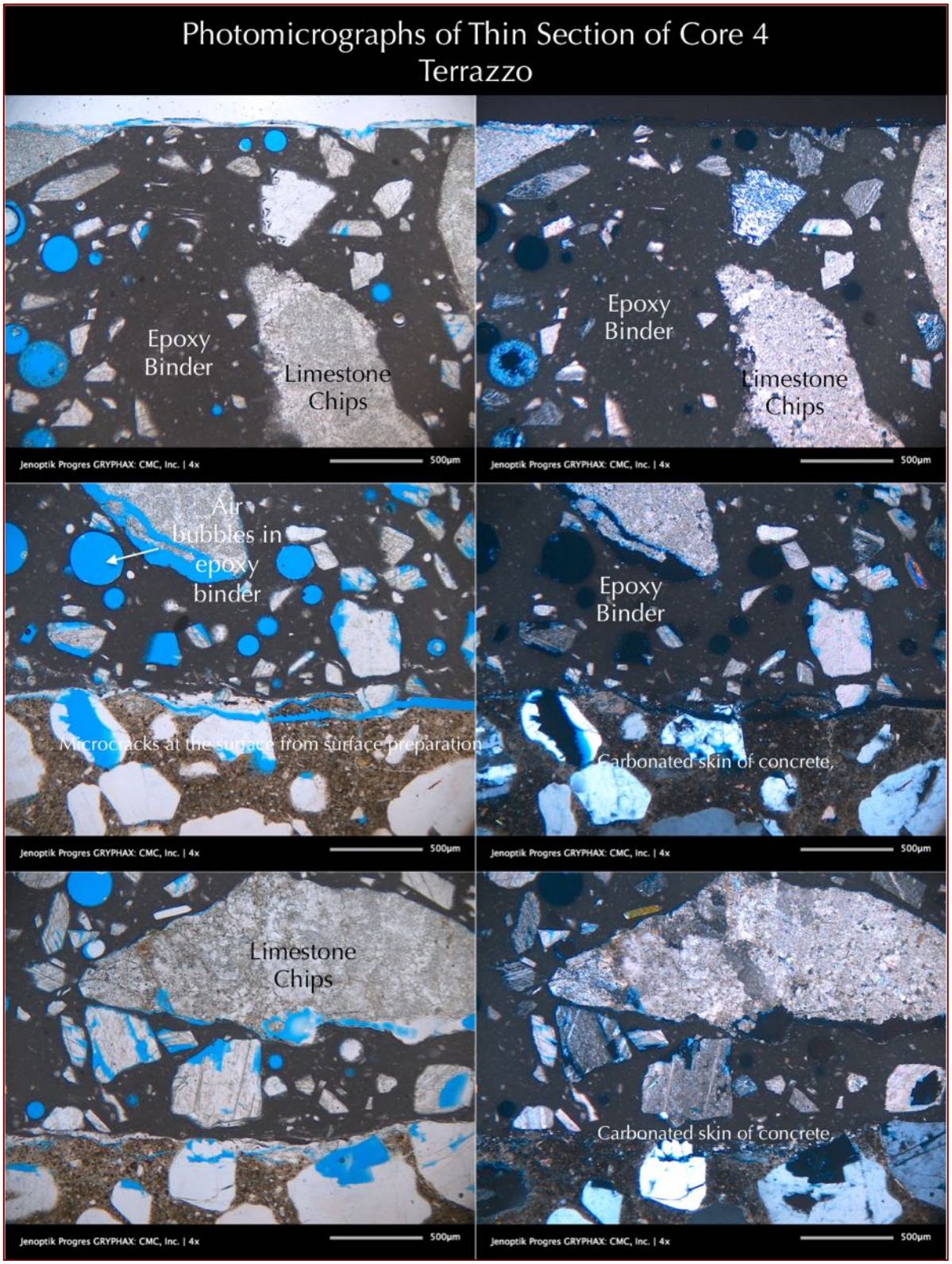

Figure 32: Photomicrographs of thin section of Core 4 showing: (a) crushed limestone and marble chips in dense polymer binder with occasional spherical entrapped voids in terrazzo; (b) occasional fine, hairline microcracks at terrazzo-concrete interface despite relatively good bond between the two; (c) dense trowel-finished concrete surface with a carbonated skin at the top on which terrazzo was placed, indicating inadequate removal of concrete surface prior to terrazzo installation, which, however, did not prevent good bond between terrazzo and concrete.

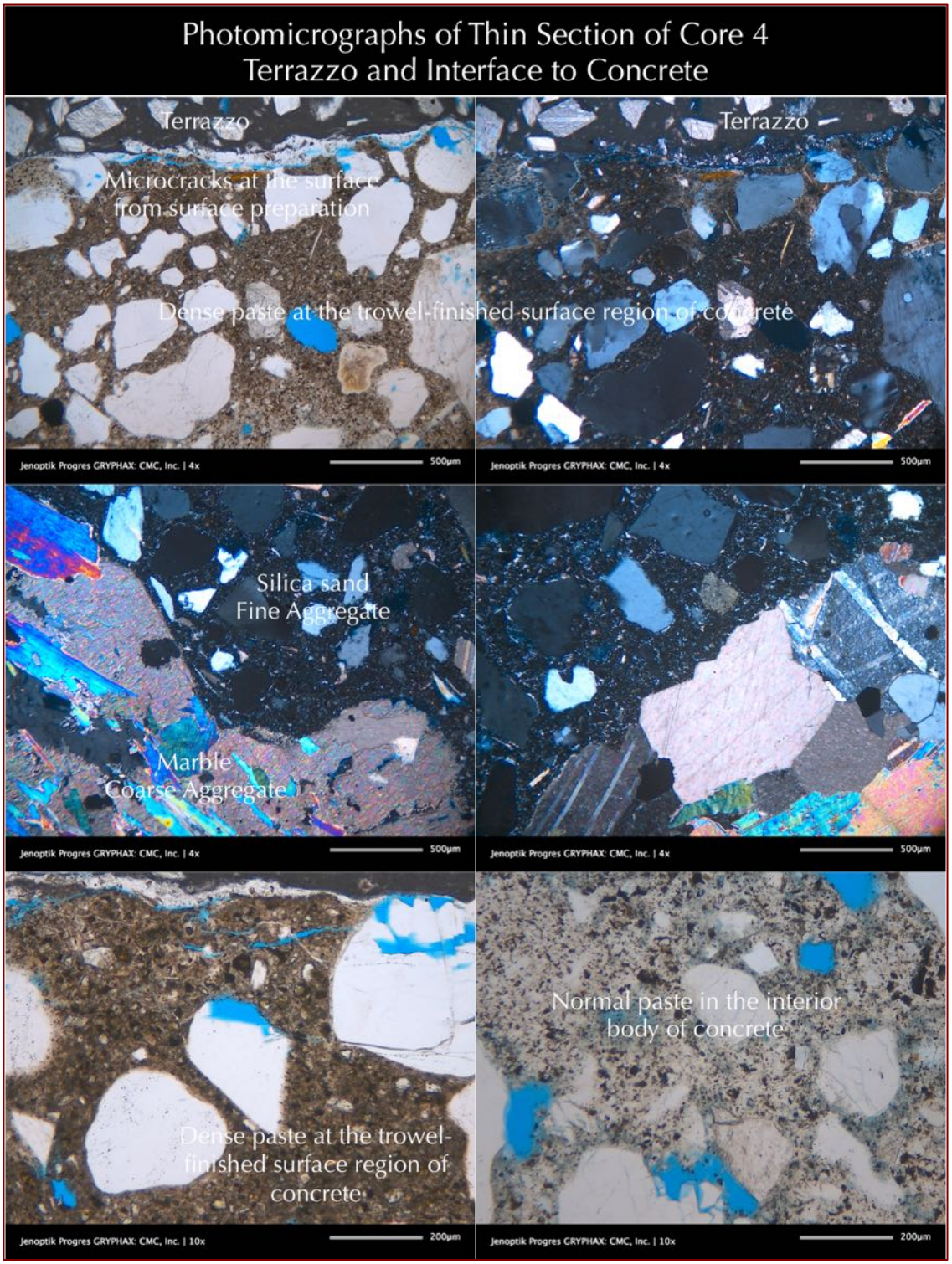

Figure 33: Photomicrographs of thin section of Core 4 showing: (a) dense trowel-finished concrete surface with a carbonated and microcracked skin at the top and a thin film of a possible primer at the top on which terrazzo was placed, indicating inadequate removal of concrete surface prior to primer and terrazzo installation; (b) crushed marble coarse aggregate and natural siliceous (quartz-quartzite) sand fine aggregate in concrete (middle row); (c) contrasting dense paste at the surface region versus normal paste in the body of concrete indicating incomplete removal of the dense paste at the surface that has prevented development of a good bond to the flooring components (as well as removal of any moisture build up from concrete).

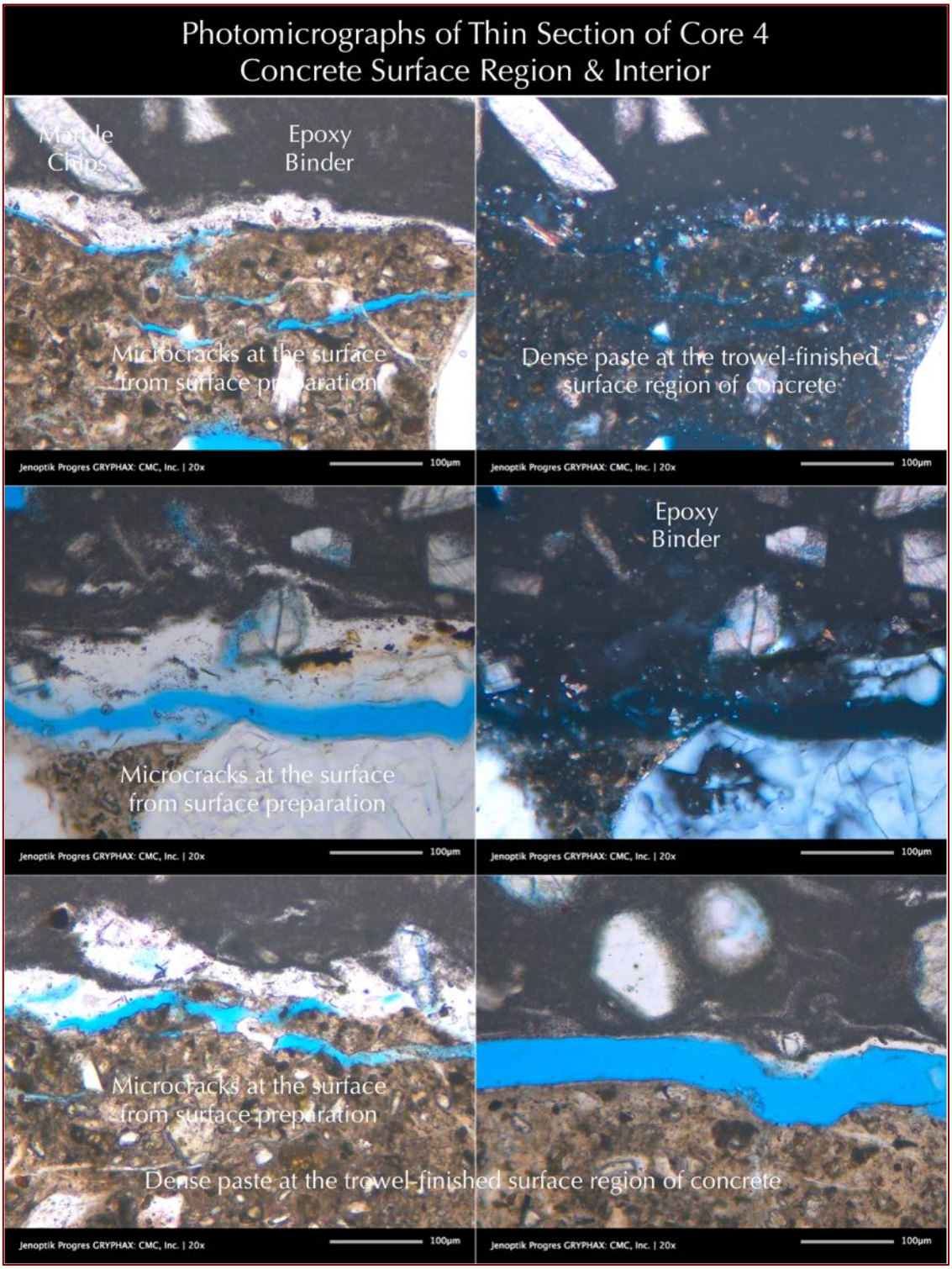

Figure 34: Photomicrographs of thin section of Core 4 showing: (a) dense trowel-finished concrete surface with a carbonated and microcracked skin at the top and a thin film of a possible primer at the top on which terrazzo was placed, indicating inadequate removal of concrete surface prior to primer and terrazzo installation; (b) crushed marble coarse aggregate and natural siliceous (quartz-quartzite) sand fine aggregate in concrete (middle row); (c) contrasting dense paste at the surface region versus normal paste in the body of concrete indicating incomplete removal of the dense paste at the surface that has prevented development of a good bond to the flooring components (as well as removal of any moisture build up from concrete).

SCANNING ELECTRON MICROSCOPY & X-RAY MICROANALYSES

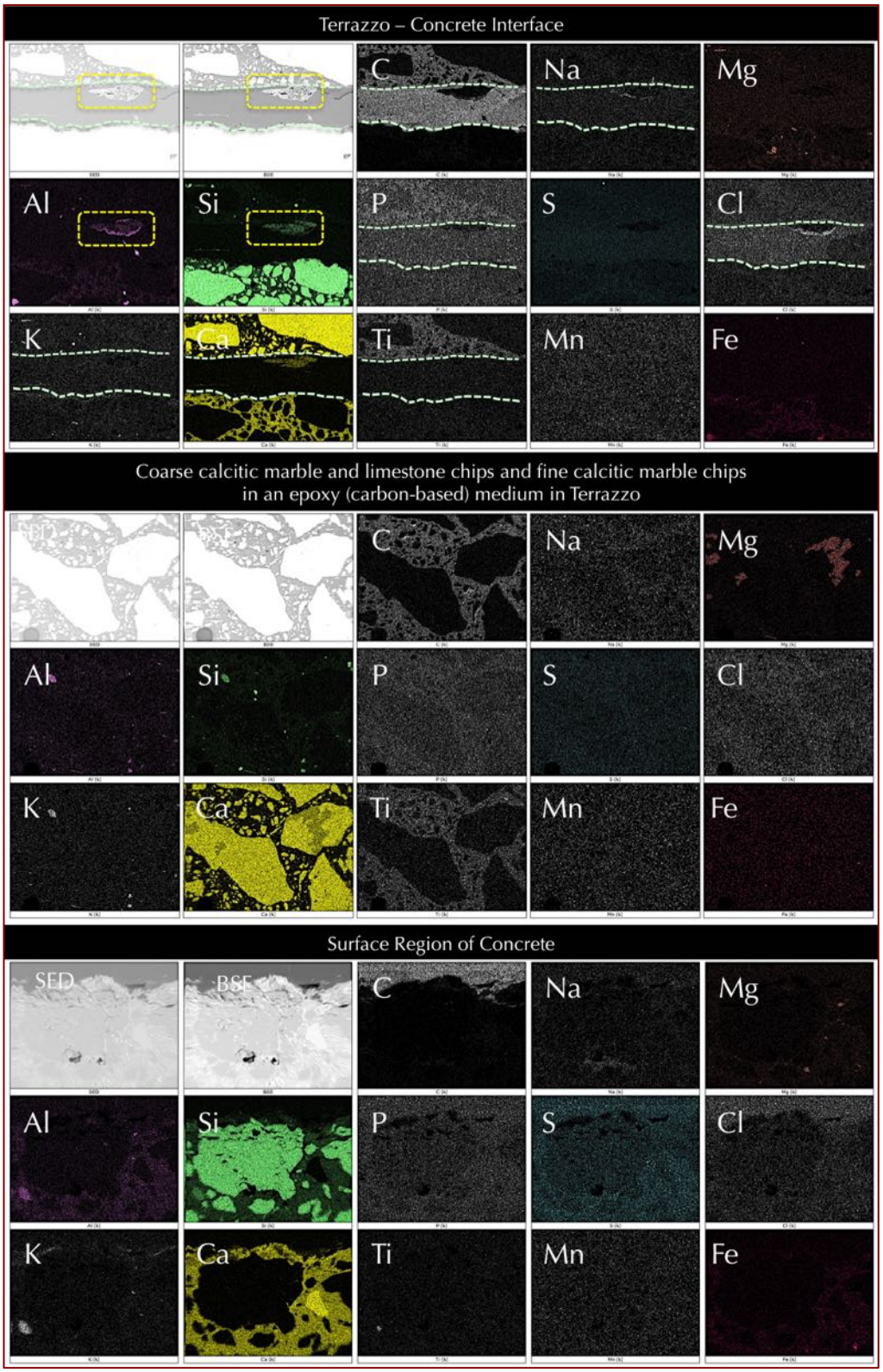

Figure 35: X-ray elemental maps of Terrazzo-concrete interface (top), interior of terrazzo (middle), and surface region of concrete (bottom) collected from energy-dispersive X-ray spectroscopy of scanning electron microscope.

X-ray elemental maps of terrazzo, concrete, and terrazzo-concrete interface in Core 3 from a scanning electron microscope shown in Figure 35 revealed a number of information that are listed below:

Terrazzo:

a. Calcitic marble chips in fine fractions from Ca-map
b. Calcitic limestone with patches of dolomite in coarse chips from Ca and Mg maps of coarse fractions
c. Titanium oxide based pigment from Ti-map
d. Carbon-based polymer binder (epoxy) from C-map

Bonding Agent Beneath Terrazzo:

a. Carbon-based bonding agent from C-map
b. Presence of calcium-aluminum silica-based glass fiber reinforcement mesh from Ca, Al, and Si maps that are depleted in C as opposed to high-C in the bonding agent itself
c. An elevated chlorine level in the bonding agent compared to terrazzo above or concrete below from Cl-map

Concrete:

a. Absence of any noticeable enrichment of alkalis at the surface region from Na and K maps
b. Absence of any enrichment of chloride at the surface from Cl-map
c. Portland cement-based composition of the binder from Ca-map
d. Siliceous sand aggregate in concrete from Si-map

BULK TERRAZZO MINERALOGY FROM XRD

Figure 36 shows the X-ray diffraction pattern of the bulk terrazzo, which shows calcite as the main detectable phase from calcitic marble and limestone having with 87.3% calcite and 12.7% calcite, which is consistent with discovery of finer calcitic marble chips and coarser limestone fractions in optical microscopy (Figures 24 to 34) and X-ray elemental maps (Figure 35).

BULK TERRAZZO COMPOSITION FROM XRF

Table 2 shows results of bulk oxide composition of the terrazzo from an energy-dispersive XRF showing dominant lime from calcitic marble chips and limestone chips, noticeable titanium oxide from white pigment, and minor magnesia for calcitic marble and limestone in the chips. High loss on ignition (balance) accounts for epoxy binder.

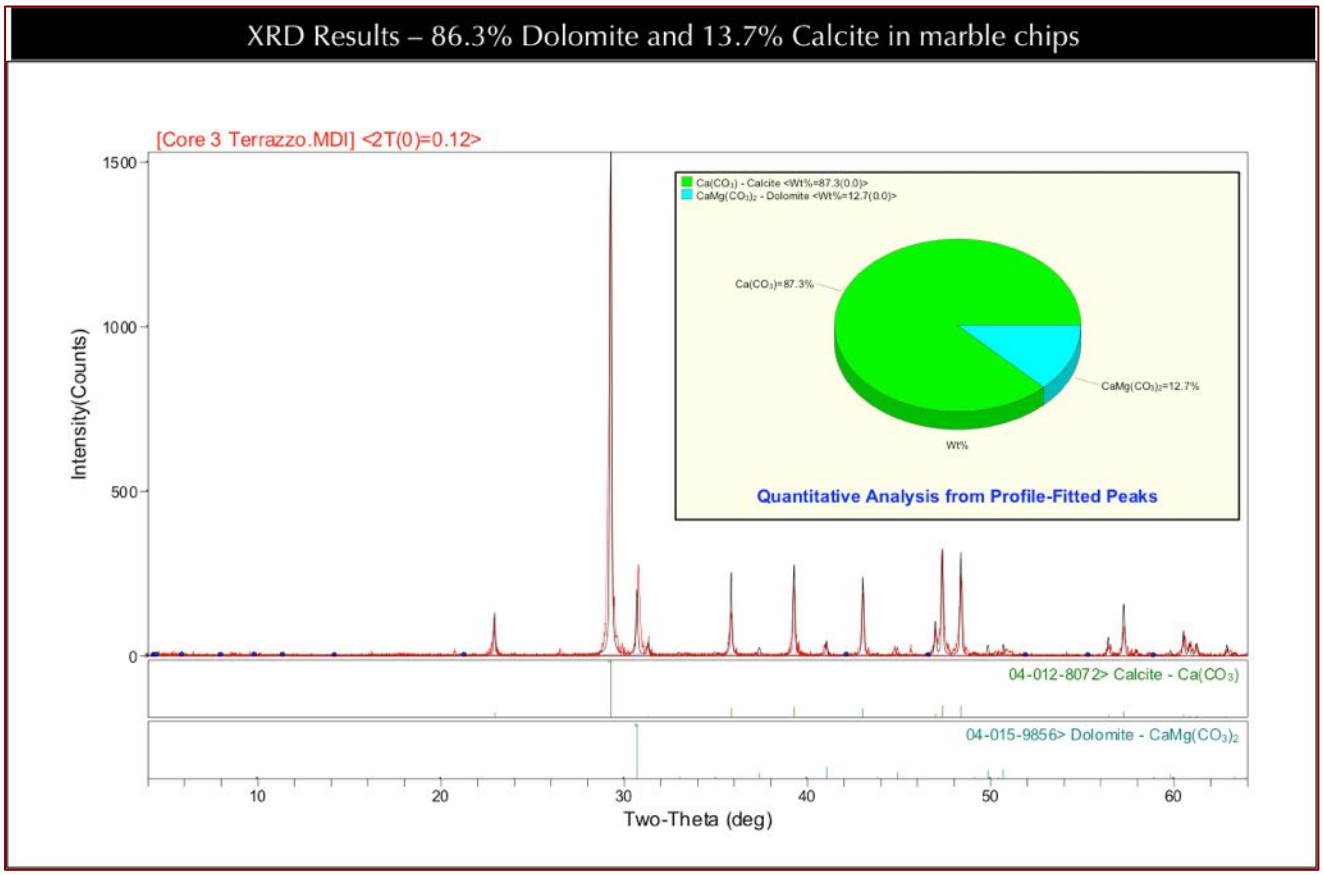

Figure 36: X-ray diffraction pattern of bulk terrazzo showing dolomite as the dominant mineral followed by calcite both from the marble chips.

Oxides (wt.%)	Bulk Terrazzo in Core 3
Silica - SiO_2	-
Alumina - Al_2O_3	0.153
Iron - Fe_2O_3	0.397
Lime - CaO	49.2 (Calcite, Limestone)
Magnesia - MgO	3.6 (Limestone)
Sodium - Na_2O	-
Potassium - K_2O	0.182
Titanium - TiO_2	0.78 (Pigment)
Phosphorus - P_2O_5	0.212
Sulfate - SO_3	-
Balance	46.1 (CO_2, polymer binder)
Total	100

Table 2: Bulk oxide compositon of terrazzo from XRF. High balance corresponds to the losses on ignition (CO_2, H_2O) from carbonates in marble chips and organics in the resin polymer.

THERMAL ANALYSIS

One major application of thermal analysis (e.g., thermogravimetric analysis, TGA) is in the assessment of the filler content in polymers, such as in this present case the proportions of epoxy resin and marble chips. The level of fillers can have a significant impact on the end use properties (thermal expansion, stiffness, damping) of the final product. Because the amount of filler is one of the possible causes to changes in the thermal expansion, TGA is used to determine the amount of filler present. The epoxy resin undergoes thermal degradation beginning at 440 ˚C with a mass loss of 55 to 60 percent.

Figure 37 shows TGA (bold black), DSC (dotted red), and DTG (dashed blue) curves of terrazzo from losses in weights due to various decompositions during controlled heating in a Mettler-Toledo's simultaneous TGA/DSC 1 unit from 30ºC to 1000ºC in a ceramic crucible (alumina 70µl, no lid) at a heating rate of 10ºC/min in a nitrogen purge at a rate of 75 mL/min.

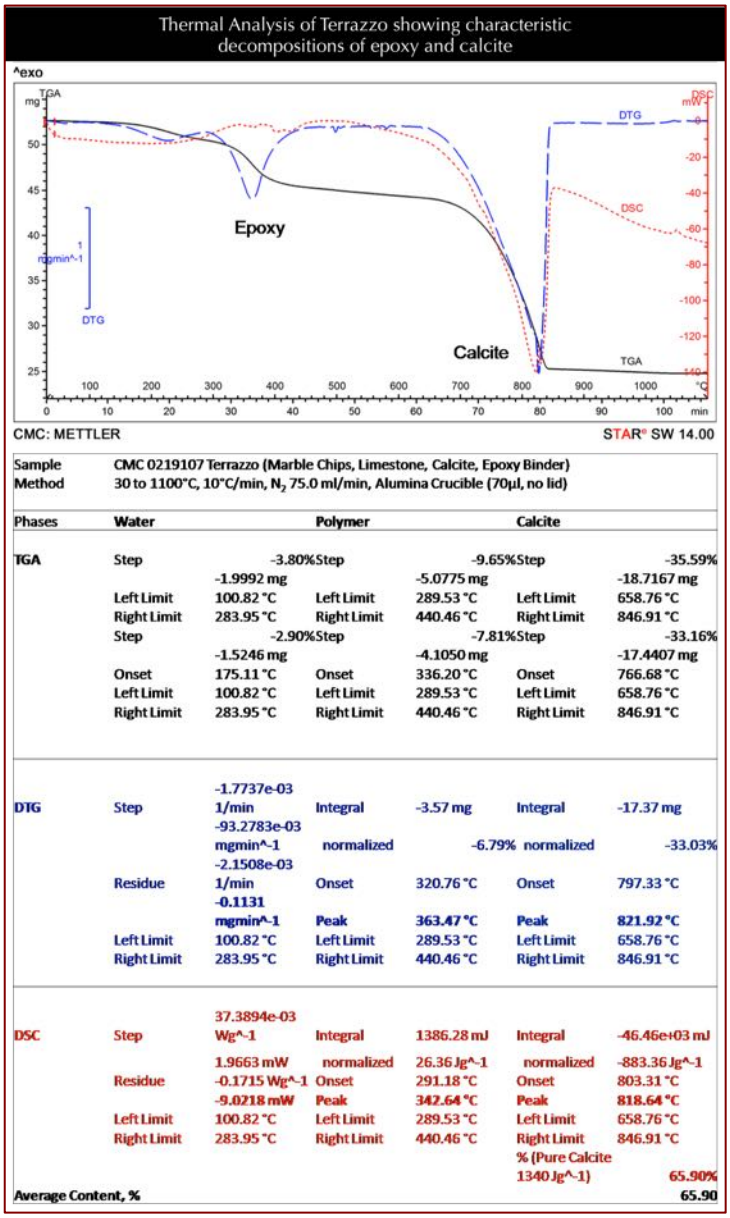

Sample	CMC 0219107 Terrazzo (Marble Chips, Limestone, Calcite, Epoxy Binder)					
Method	30 to 1100°C, 10°C/min, N_2 75.0 ml/min, Alumina Crucible (70µl, no lid)					
Phases	**Water**		**Polymer**		**Calcite**	
TGA	Step	-3.80%	Step	-9.65%	Step	-35.59%
		-1.9992 mg		-5.0775 mg		-18.7167 mg
	Left Limit	100.82 °C	Left Limit	289.53 °C	Left Limit	658.76 °C
	Right Limit	283.95 °C	Right Limit	440.46 °C	Right Limit	846.91 °C
	Step	-2.90%	Step	-7.81%	Step	-33.16%
		-1.5246 mg		-4.1050 mg		-17.4407 mg
	Onset	175.11 °C	Onset	336.20 °C	Onset	766.68 °C
	Left Limit	100.82 °C	Left Limit	289.53 °C	Left Limit	658.76 °C
	Right Limit	283.95 °C	Right Limit	440.46 °C	Right Limit	846.91 °C
DTG	Step	-1.7737e-03 1/min	Integral	-3.57 mg	Integral	-17.37 mg
		-93.2783e-03 mgmin^-1	normalized	-6.79%	normalized	-33.03%
	Residue	-2.1508e-03 1/min	Onset	320.76 °C	Onset	797.33 °C
		-0.1131 mgmin^-1	Peak	363.47 °C	Peak	821.92 °C
	Left Limit	100.82 °C	Left Limit	289.53 °C	Left Limit	658.76 °C
	Right Limit	283.95 °C	Right Limit	440.46 °C	Right Limit	846.91 °C
DSC	Step	37.3894e-03 Wg^-1	Integral	1386.28 mJ	Integral	-46.46e+03 mJ
		1.9663 mW	normalized	26.36 Jg^-1	normalized	-883.36 Jg^-1
	Residue	-0.1715 Wg^-1	Onset	291.18 °C	Onset	803.31 °C
		-9.0218 mW	Peak	342.64 °C	Peak	818.64 °C
	Left Limit	100.82 °C	Left Limit	289.53 °C	Left Limit	658.76 °C
	Right Limit	283.95 °C	Right Limit	440.46 °C	Right Limit	846.91 °C
					% (Pure Calcite 1340 Jg^-1)	65.90%
Average Content, %						65.90

The results show two major decompositions from: (a) decomposition of the epoxy binder (from an endothermic peak around 363.7ºC in the DTG curve), and (b) decarbonation of calcite (from an endothermic peak around 821.9ºC in the DTG curve). Thermal analysis detected about 8 percent weight loss from resin binder, and about 66 percent calcite in the filler chips.

Figure 37: TGA (bold black), DSC (dotted red), and DTG (dashed blue) curves of terrazzo showing losses in weight due to various decompositions (loss of water and cardon dioxide) during controlled heating in a Mettler-Toledo's simultaneous TGA/DSC 1 unit from 30ºC to 1000ºC in a ceramic crucible (alumina 70µl, no lid) at a heating rate of 10ºC/min in a nitrogen purge at a rate of 75 mL/min. The results show three major decompositions from: (a) the loss of combined water from polymer binder at the lower temperature (from a low temperature peak in DTG curve), (b) decomposition of the epoxy-resin itself at the intermediate temperature (from a peak in the DTG curve), and (c) decarbonation of calcite and dolomite at higher temperature (from the major peak in the DTG curve).

MIGRATION OF WATER-SOLUBLE IONS THROUGH CONCRETE SLAB

In order to investigate moisture migration and upwelling through the concrete slab-on-grade, water-soluble anions (e.g., chloride, sulfate), and cations (sodium, potassium) were leached out from 10.00 grams of pulverized concrete. Samples taken from the top, mid-depth, and bottom ends of four cores and ions were determined by potentiometric titration (for water-soluble chloride contents), anion chromatography (for water-soluble chloride and sulfate), and X-ray fluorescence spectroscopy for water-soluble alkalis (Na, k). Pulverized concrete from three depths per core were passed through No. 50 sieve, then digested in deionized water first for 15-minute at near boiling temperatures, then for 24-hour in room temperature. Digested samples were filtered through two 2.5-micron filter papers, followed by additional filtration through two 0.22-micron filter papers. Aliquots of filtrates thus obtained were used for potentiometric titration for chloride content (*a la* ASTM C 1218), ion chromatography (*a la* ASTM D 4327) for water-soluble anion (chloride and sulfate) contents, and X-ray fluorescence for water-soluble alkali (Na, K) contents.

Figures 38 through 40 and Table 3 show results of water-soluble chloride contents at the top, mid-depth, and formed bottom ends of four cores determined from potentiometric titration *a la* ASTM C 1218. Chloride profiles of four cores show no systematic increase of chloride towards the surface (except perhaps in Core 4 to a small degree), as would have been anticipated for moisture upwelling and thus moisture-driven migration of water-soluble chloride towards the surface. Absolute chloride levels are all low at three depths for each core, indicating no preferential contamination of concrete by chloride at the surface.

Figure 41 shows results of water-soluble chloride and sulfate contents from ion chromatography, where chloride results are all low, consistent with chloride results from titration. Similar to chloride, sulfate contents are also found to be very low.

Based on both titration and ion chromatography water-soluble anions are found to be low in concrete at all depths and do not indicate any systematic increase towards the surface from moisture upwelling through concrete slab.

Figure 42 shows water-soluble alkali content measured from X-ray fluorescence spectroscopy, first in the light yellow liquid from a reported blister received in a vial and then through three depths in Core 2, which was reportedly retrieved from a blistered location. Liquid from blister showed oxides of 2.05 percent sodium and 3.28 percent potassium. By contrast, alkali levels in water digested concrete from three depths are all found to be below the detection limit of XRF. There was no evidence of increasing water-soluble alkali contents towards the top end of the core.

The dense trowel-finished surface of concrete slab at the top reduced breathability of concrete from its exposed surface. Placement of slab over a plastic vapor retarder prevented moisture migration between concrete and subbase. Therefore, relative humidity gradient in slab was judged to be lower than that needed to drive any moisture

upwelling. Concrete's inherent moisture has participated in cement hydration and hence formation of a dense paste throughout the slab as opposed to moving soluble ingredients towards the top under a humidity gradient.

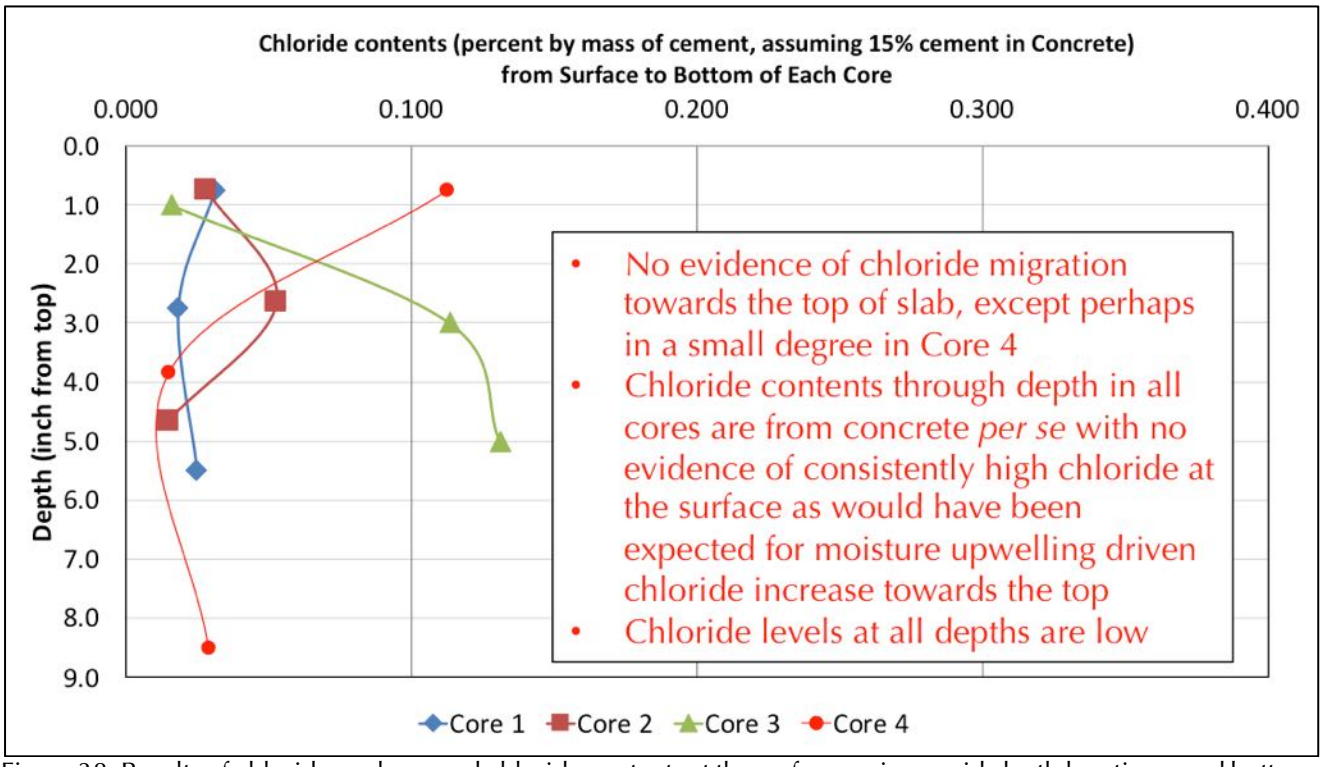

Figure 38: Results of chloride analyses and chloride contents at the surface regions, mid-depth locations, and bottom ends of cores. Chloride contents are expressed as percentages by mass of cement assuming a cement content of 15 percent in normal-weight concretes.

Sample ID	Depth (in.)	Sample weight (g)	Equivalent Point of Titration	Cal.culated Chloride, % by mass of concrete	Chloride by mass of cement, 15% cement	Chloride, ppm	Eqv. Flake $CaCl_2$
1 Top	0.75	7.943	0.2100	0.0047	0.031	47	0.01
1 Middle	2.75	10.080	0.1553	0.0027	0.018	27	0.01
1 Bottom	5.50	10.029	0.2103	0.0037	0.025	37	0.01
2 Top	0.75	10.016	0.2385	0.0042	0.028	42	0.01
2 Middle	2.66	10.012	0.4480	0.0079	0.053	79	0.02
2 Bottom	4.66	10.053	0.1262	0.0022	0.015	22	0.00
3 Top	1.00	10.007	0.1351	0.0024	0.016	24	0.00
3 Middle	3.00	10.030	0.9631	0.0170	0.113	170	0.04
3 Bottom	5.00	10.076	1.1178	0.0196	0.131	196	0.04
4 Top	0.75	10.015	0.9530	0.0168	0.112	168	0.03
4 Middle	3.85	10.025	0.1273	0.0022	0.015	22	0.00
4 Bottom	8.50	10.057	0.2460	0.0043	0.029	43	0.01

Table 3: Results of chloride analyses of concrete cores.

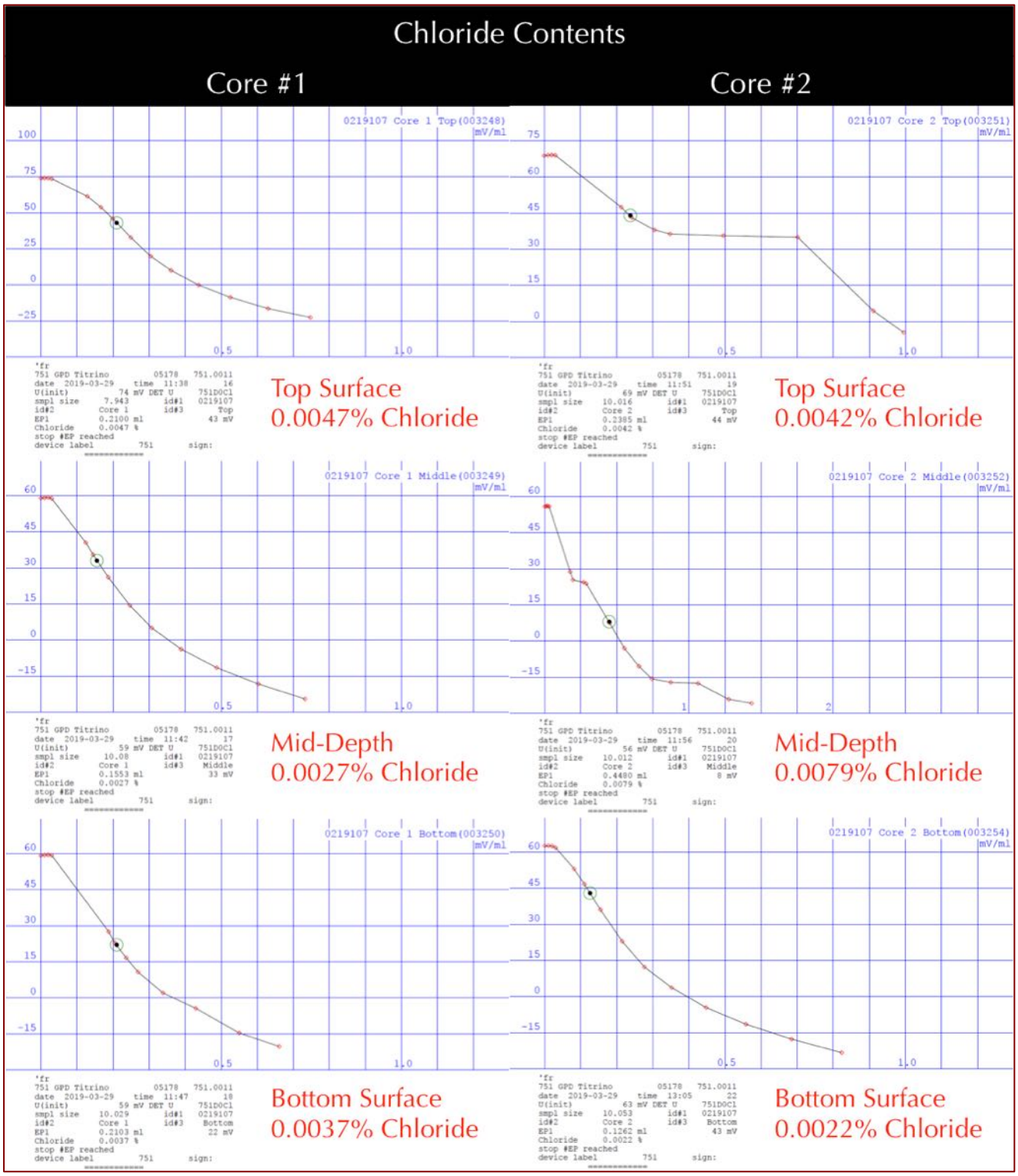

Figure 39: The potentiometric titration curves of chloride analyses from the top surface region (top plots), mid-depth locations (middle plots), and bottom ends (bottom plots) of Cores 1 and 2. In all titration curves, the equivalent points of titration are marked with a dot and circle on the mV-vs-mL $AgNO_3$ plots. Chloride contents are shown both in the data from the Metrohm Titrator as well as in red.

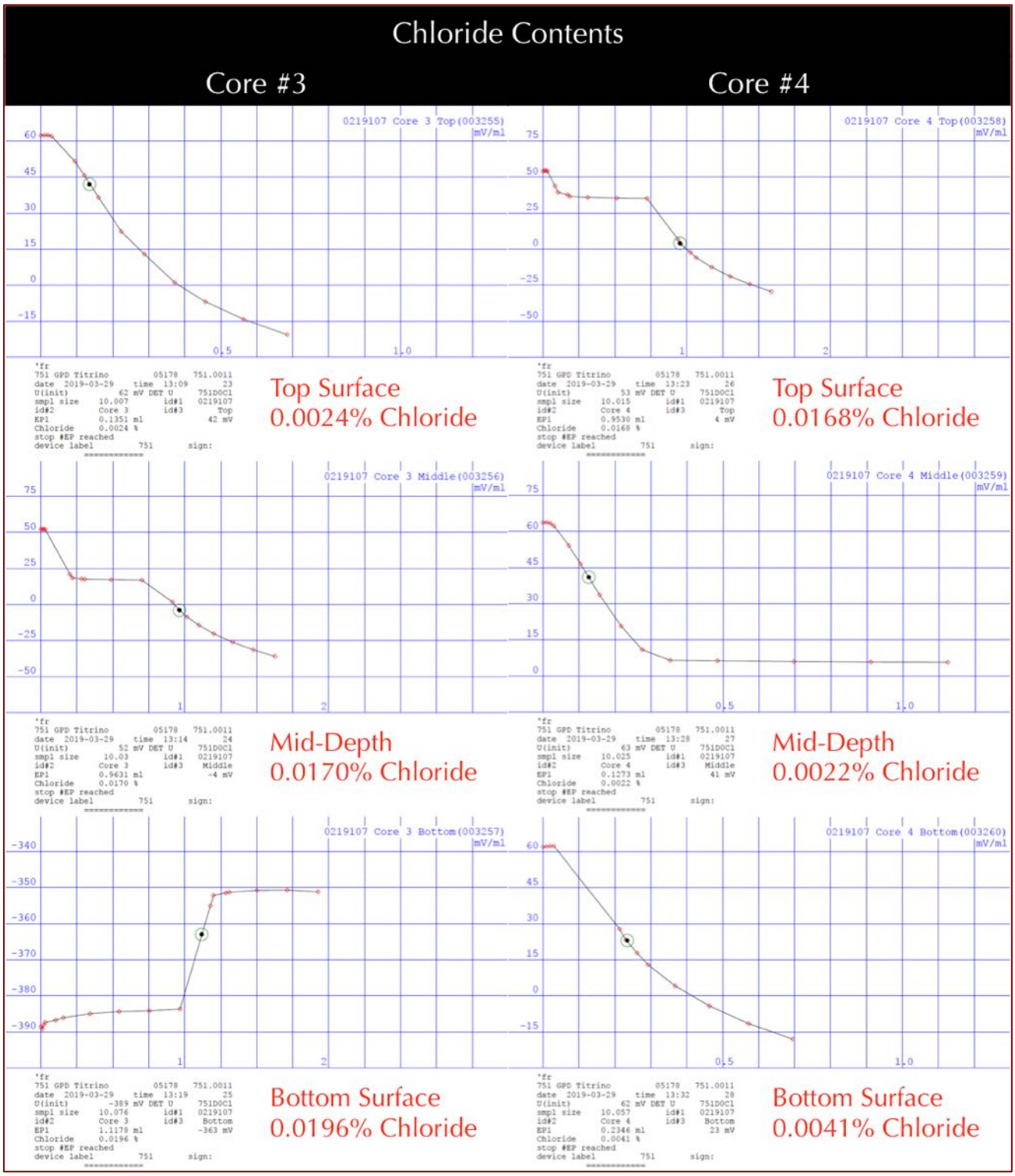

Figure 40: The potentiometric titration curves of chloride analyses from the top surface region (top plots), mid-depth locations (middle plots), and bottom ends (bottom plots) of Cores 3 and 4. In all titration curves, the equivalent points of titration are marked with a dot and circle on the mV-vs-mL $AgNO_3$ plots. Chloride contents are shown both in the data from the Metrohm Titrator as well as in red.

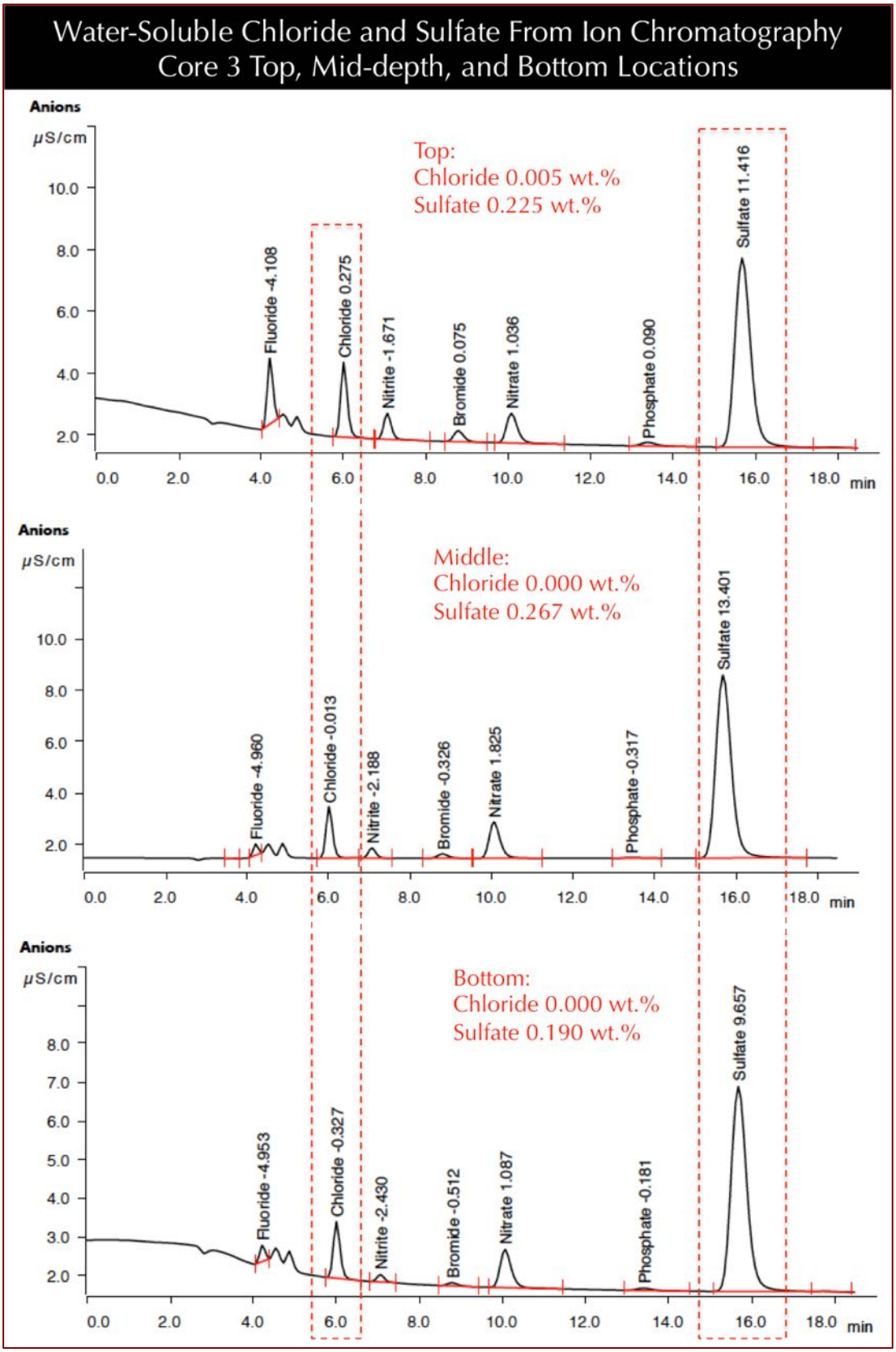

Figure 41: Ion chromatograms of water-soluble chloride and sulfate ions from top, mid-depth, and bottom locations of Core 3 showing no systematic variations of chloride or sulfate contents from bottom to top.

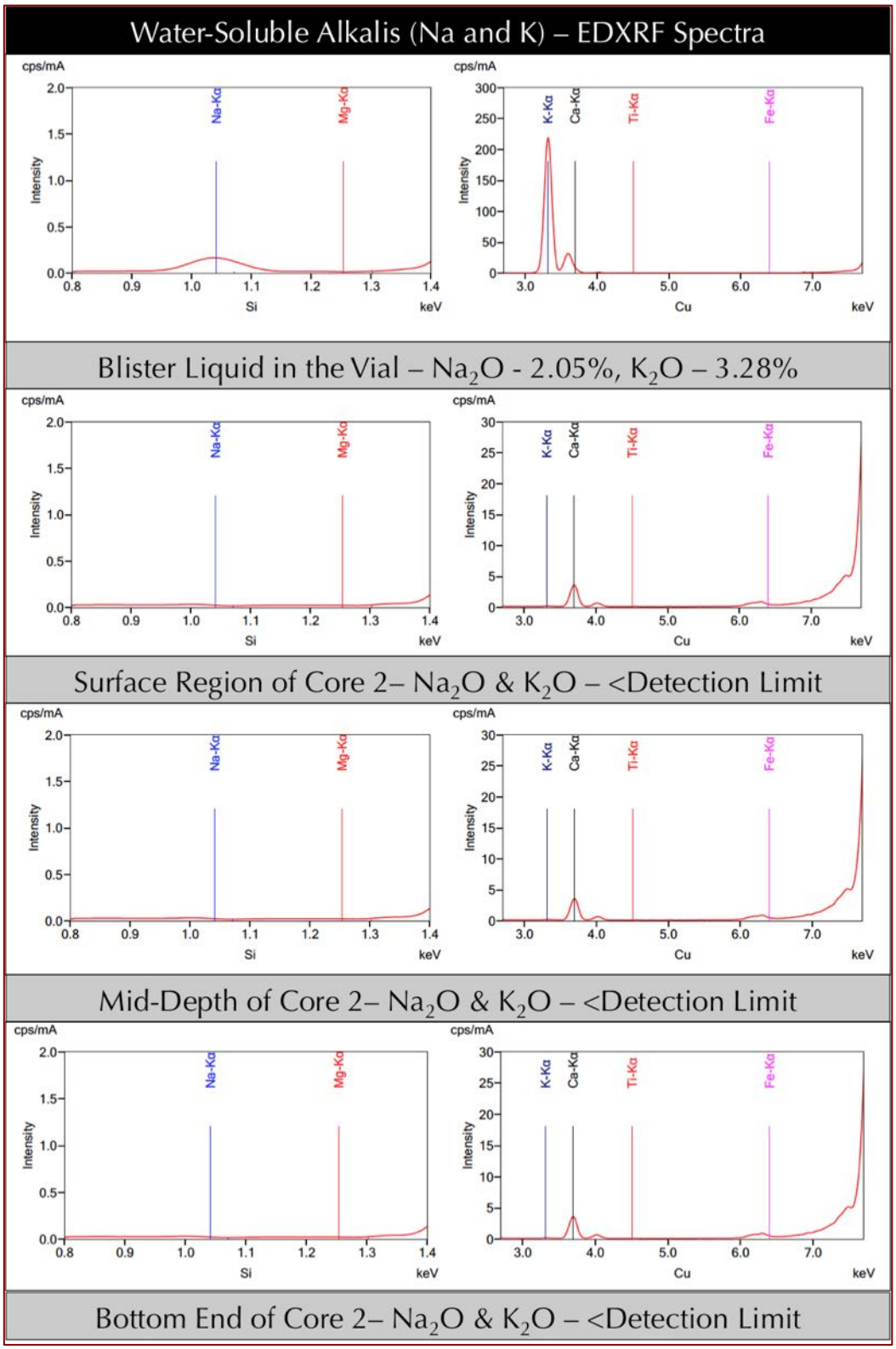

Figure 42: Results of water-soluble alkali contents from X-ray fluorescence spectroscopy: (a) the top spectrum is for the liquid from blister, and (b) three successive spectra are from three successive depths in Core 2, which was retrieved from a blistered location. Notice the presence of clear discernable peaks of sodium and potassium in the liquid from vial in the top spectrum, but no such peaks in the water-soluble filtrates of concrete in the bottom three spectra.

LIQUID FROM A BLISTER

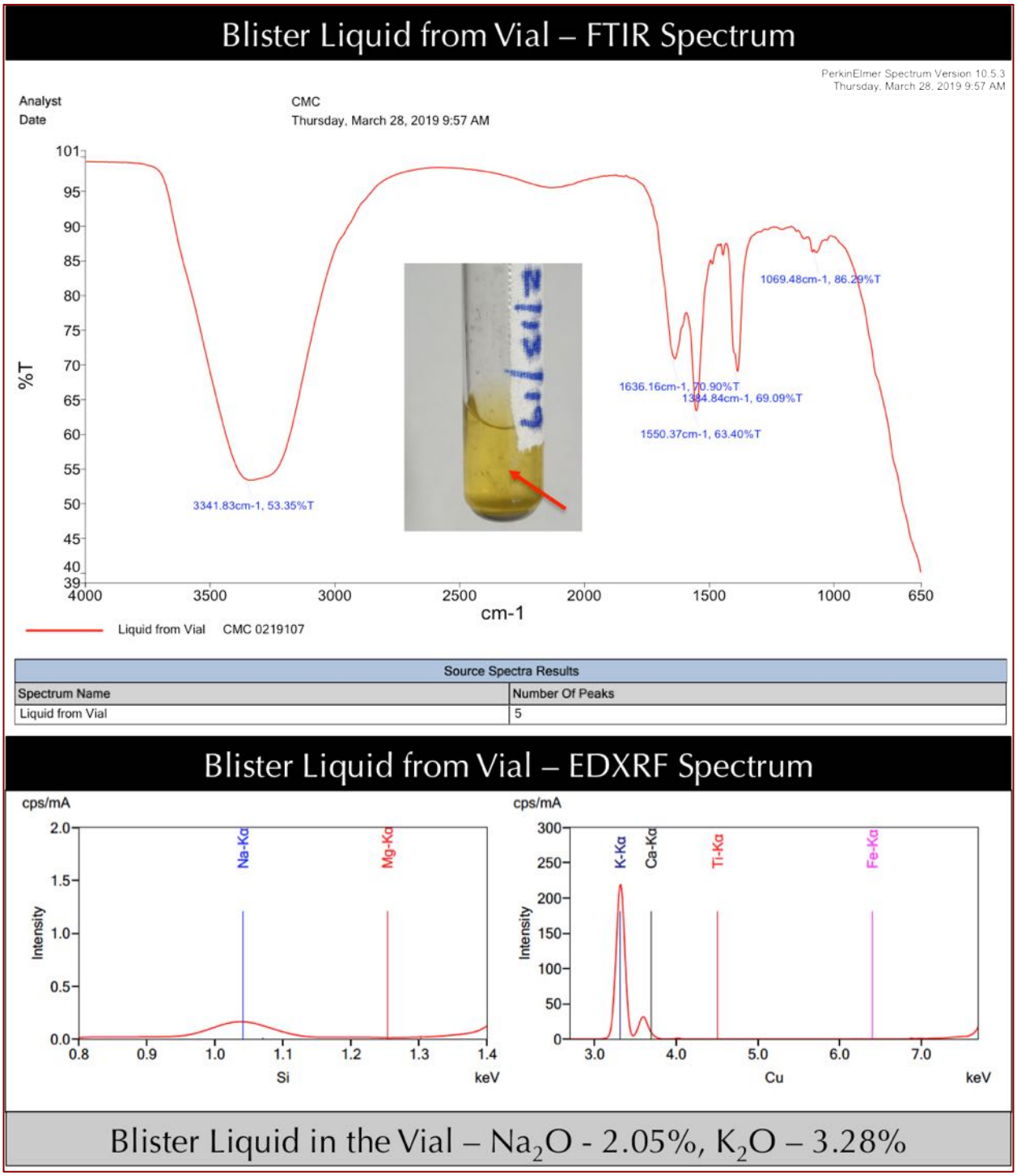

Figure 43: Fourier transform infrared spectroscopy of the yellowish liquid reportedly retrieved from underneath a blister and received in a glass vial shown in the top inset. FTIR spectrum indicates the presence of an organic (possibly of a primer) component in the liquid. Also shown below is elemental spectrum from X-ray fluorescence spectroscopy of the same liquid showing 2.05% sodium and 3.28% potassium oxides in the liquid. Both studies were done after filtering the liquid through two 0.22-micorn filter papers to collect the filtrate. The pH of liquid is tested to be 11.2.

FOURIER TRANSFORM INFRARED SPECTROSCOPY

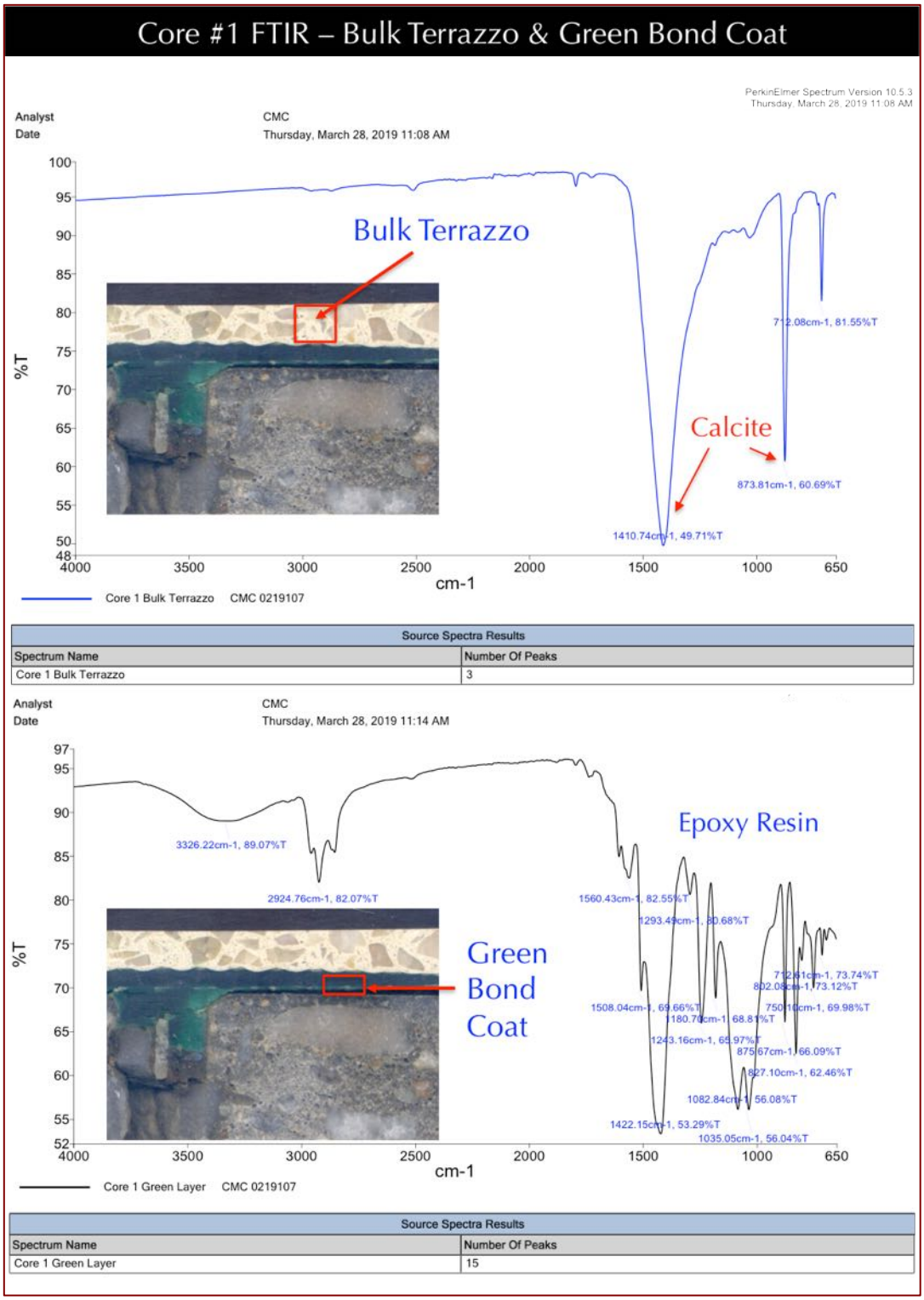

Figure 44: FTIR spectra of bulk terrazzo (top) and green bond coat adhered at the base of terrazzo (bottom) in Core 1. Terrazzo spectra shows dominant peaks for calcite from calcite/limestone/marble chips, whereas underlying green bond coat shows the presence of epoxy resin in the bond coat.

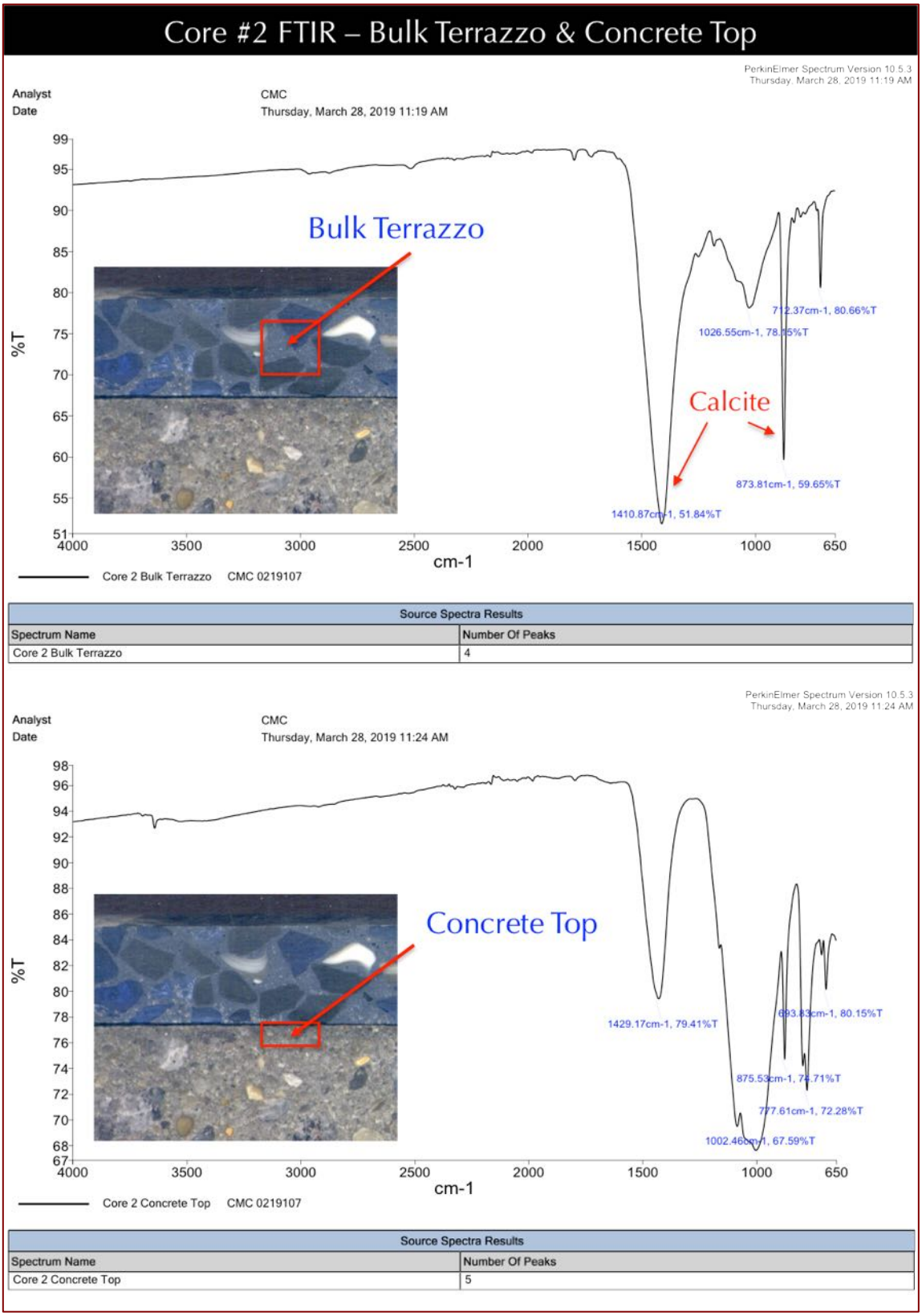

Figure 45: FTIR spectra of bulk terrazzo (top) and surface region of concrete (bottom) in Core 2. Terrazzo spectra shows dominant peaks for calcite from calcite/limestone/marble chips, whereas underlying concrete shows the presence of similar peaks for calcite from carbonated surface of concrete.

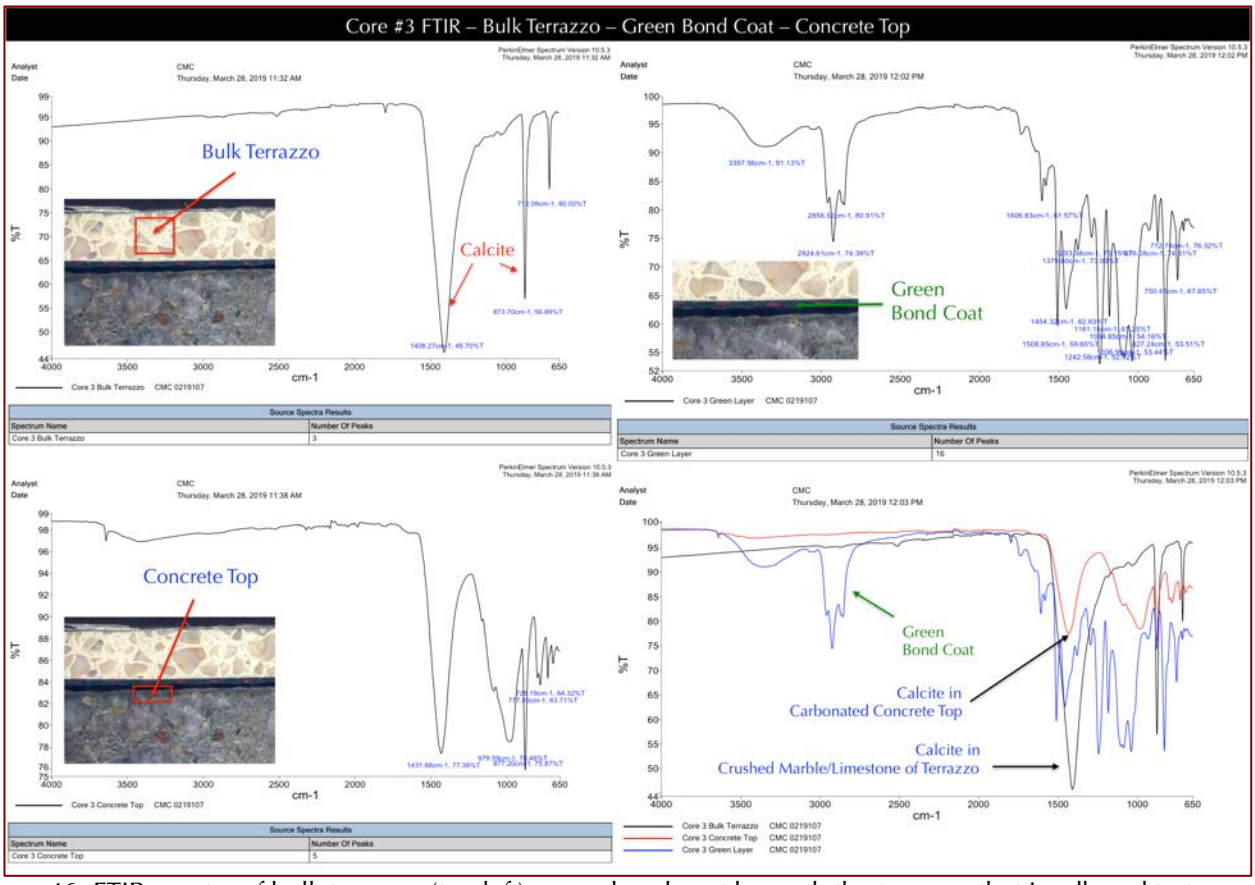

Figure 46: FTIR spectra of bulk terrazzo (top left), green bond coat beneath the terrazzo that is adhered to terrazzo but completely de-bonded from concrete (top right), and surface region of concrete (bottom left) in Core 3, as well as comparison of spectra from all three components in the bottom right photo. Terrazzo spectra shows dominant peaks for calcite from calcite/limestone/marble chips, green bond coat shows the polymeric composition, whereas underlying concrete shows the presence of similar peaks for calcite from carbonated surface of concrete.

Fourier transform infrared spectroscopy of terrazzo flooring, underlying green bond coat, and top surface of concrete showed compositional similarity of white terrazzo consisting of calcite from marble and limestone chips and an epoxy resin binder in Cores 1, 3, and 4. By contrast the blue terrazzo in Core 2 shows a different epoxy resin binder, which is shown in Figure 48 where terrazzo from Cores 1, 3, and 4 are compared. The concrete surface shows compositional similarity in all cores (bottom graph in Figure 45) and calcite from carbonated surface, which is also found in the terrazzo spectra from limestone/marble chips. Spectra of concrete tops indicates application of an organic component found in many primers. The green bond coat found in Cores 1 and 3 are also compositionally similar (compared in the middle photo of Figure 48).

The binder in white terrazzo individually show typical absorbance spectra of epoxy resin having characteristic absorbance peaks at 1606, 1507, 1451, 12451, 1181, and 827 cm^{-1} (Figure 49).

In all plots, bulk samples are finely ground pulverized masses placed on UATR module, whereas individual epoxy binder in Figure 49 was carefully extracted from a lapped cross section with a stereomicroscope. Liquid in vial shown in Figure 50 was directly placed on diamond of UATR module in Spectrum 100 FTIR.

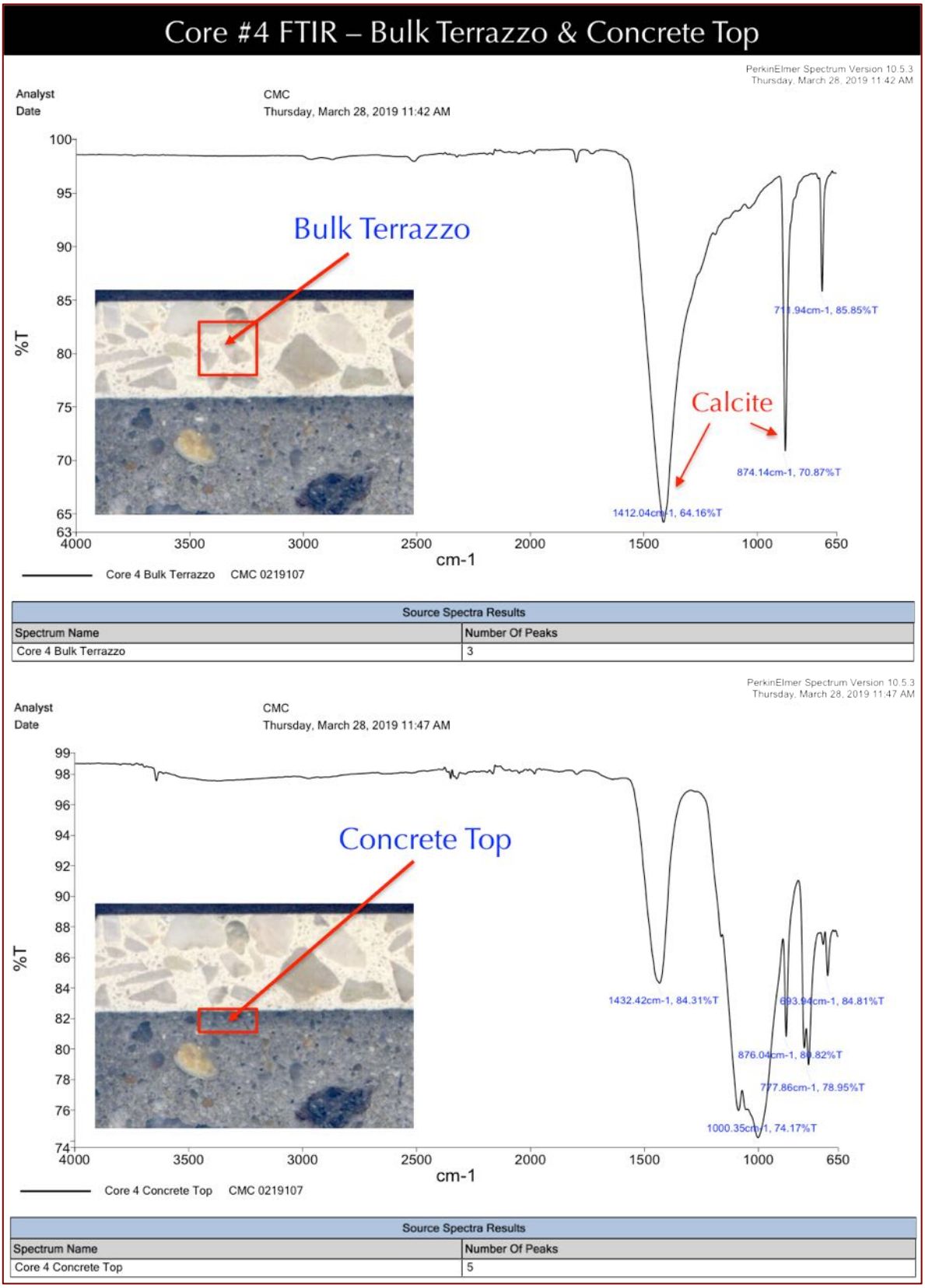

Figure 47: FTIR spectra of bulk terrazzo (top) and surface region of concrete (bottom) in Core 4. Terrazzo spectra shows dominant peaks for calcite from calcite/limestone/marble chips, whereas underlying concrete shows the presence of similar peaks for calcite from carbonated surface of concrete.

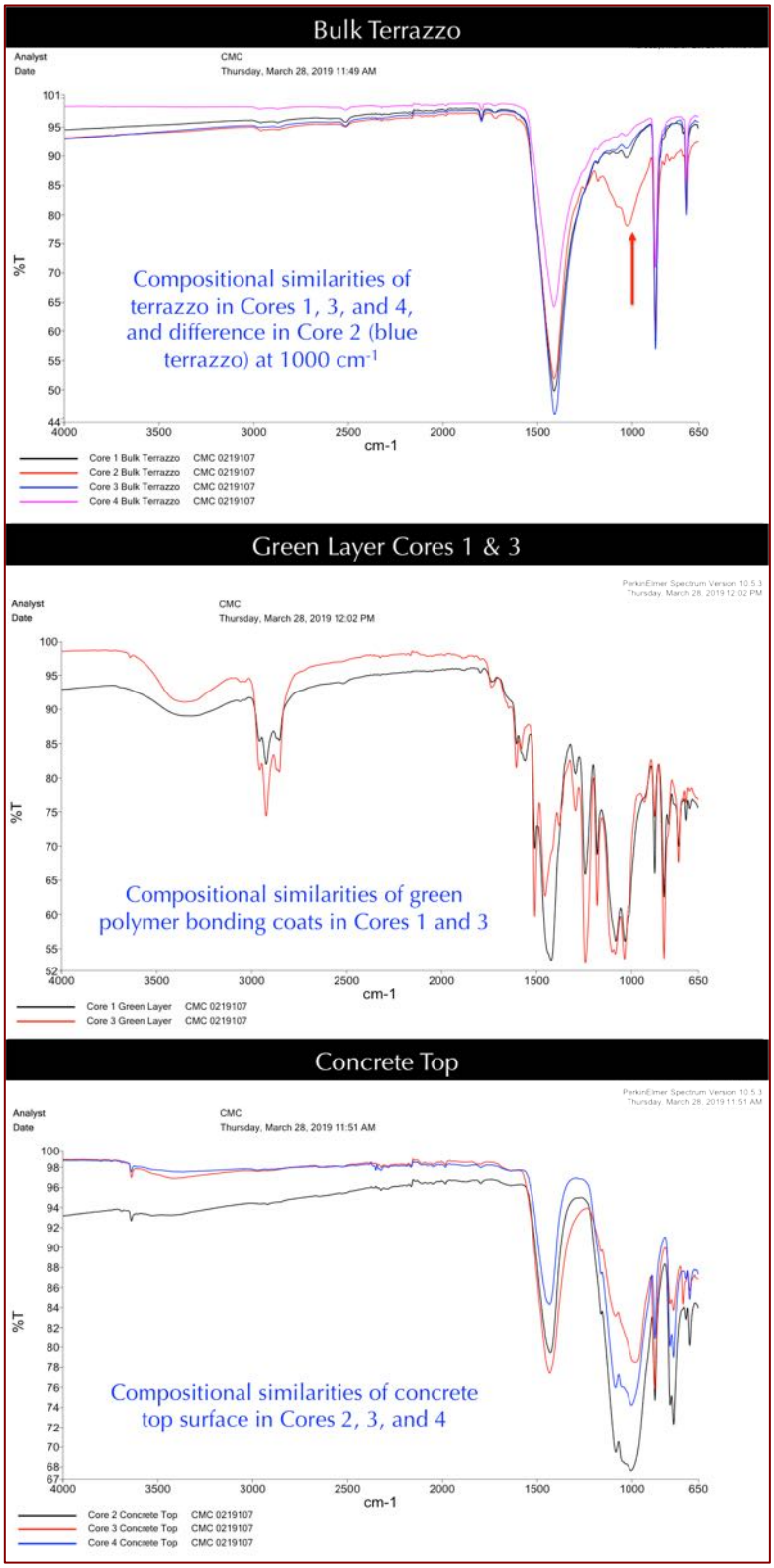

Figure 48: Compositional similarities of white terrazzo in Cores 1, 3, and 4, and difference from dark blue terrazzo in Core 2 with slight variations in absorbance peaks of terrazzo in the top photo. Middle spectra shows compositionally similar green bond coat in Cores 1 and 3 that are well-bonded to their respective terrazzo bases but mostly de-bonded from concrete. Bottom photo shows compositional similarities of carbonated concrete surfaces in Cores 2, 3, and 4.

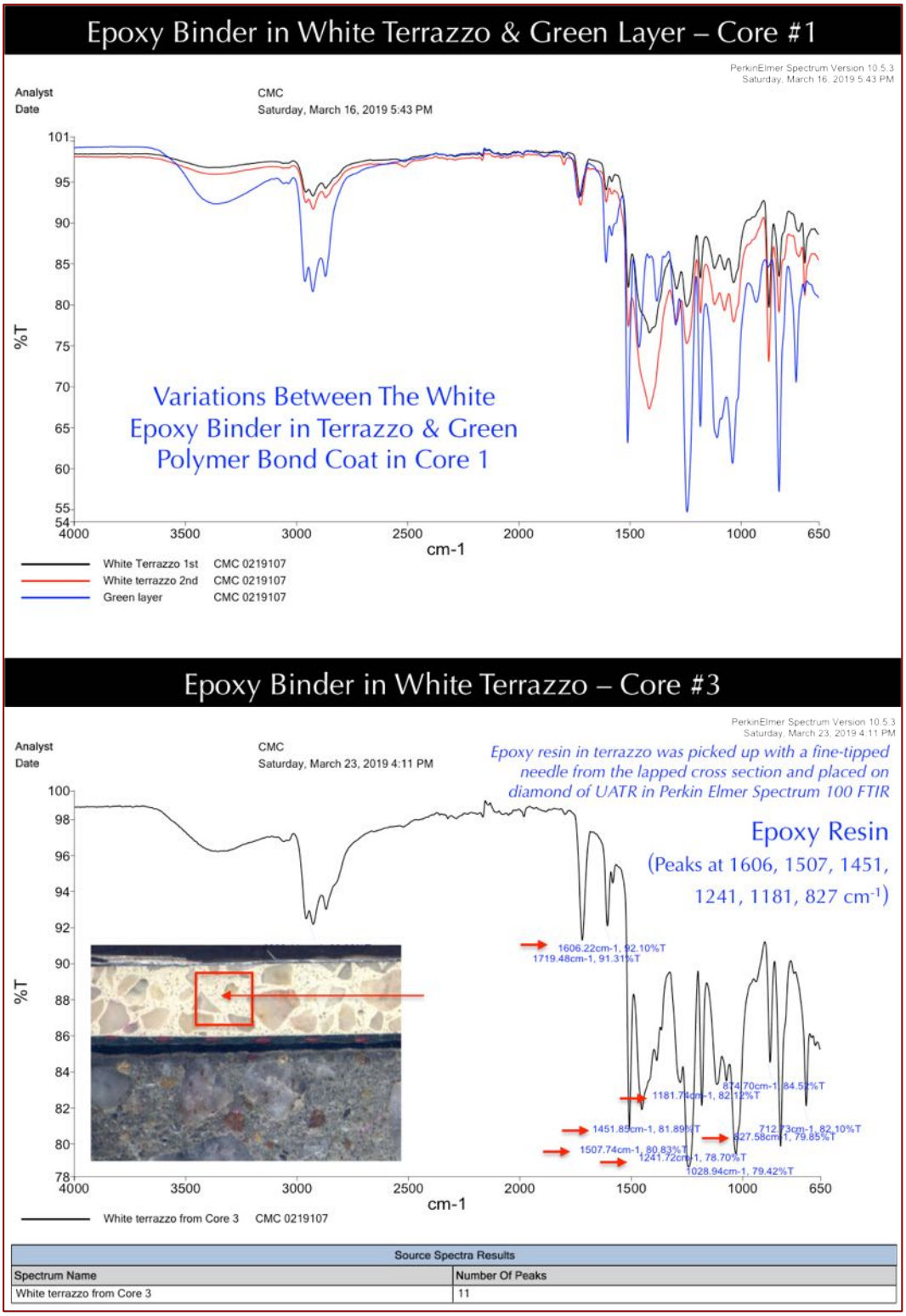

Figure 49: FTIR spectra of the binder phase of white terrazzo (top) carefully removed from lapped cross section of Core 1, as well as the underlying green bond coat showing compositional differences between the white polymer binder of terrazzo and the underlying green bond coat. Bottom spectra shows another white polymer binder of terrazzo from Core 3, which shows compositional similarities to the polymer binder of terrazzo in Core 3, where epoxy resin binder is confirmed from characteristic absorbance peaks at 1606, 1507, 1451, 12451, 1181, and 827 cm^{-1}.

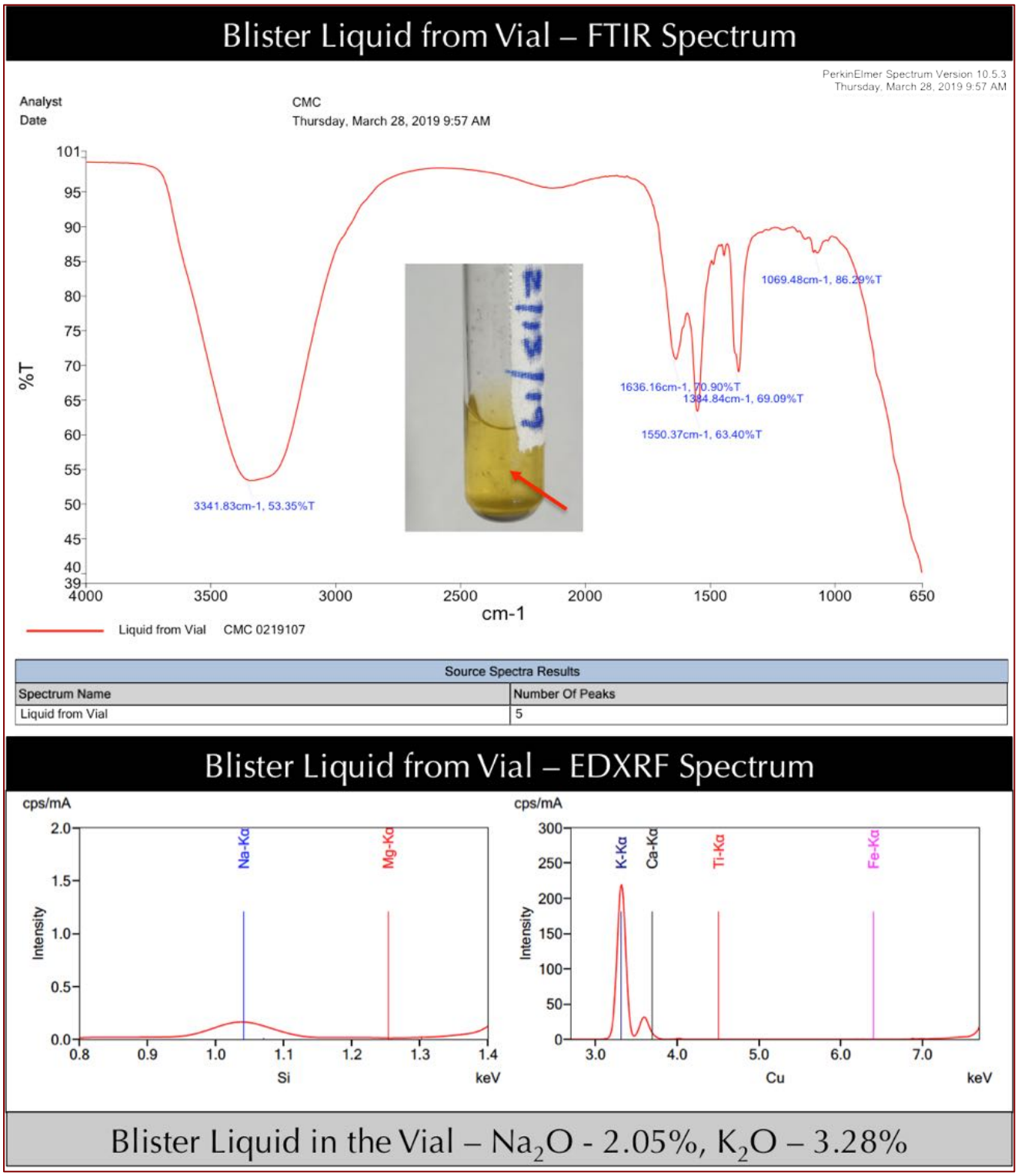

Figure 50: FTIR spectra (top) and X-ray fluorescence elemental spectra (bottom) of yellow liquid in the vial reportedly collected from underneath a blister. FTIR spectra indicates the presence of organic components in the liquid, possibly from a primer component applied to the surface, whereas XRF spectra clearly showed noticeable peaks for sodium and potassium, having 2.05% Na_2O and 3.28% K_2O in the liquid.

CONCLUSIONS

BLUE TERRAZZO BANDS IN WHITE TERRAZZO FLOORING

Two types of polymer terrazzo are present in four cores: (a) a white terrazzo in Cores 1, 3, and 4 consisting of crushed marble and crushed limestone chips mixed with finer sized marble dust and all crystalline components are mixed in a titanium oxide-based pigmented white epoxy resin binder, and (b) a dark blue terrazzo in Core 2 consisting of crushed marble, limestone, crushed glass in a pigmented blue polymer binder (different from the white epoxy resin binder in white terrazzo). These two types correspond to the dark blue color bands of terrazzo on the overwhelming white terrazzo flooring across the core locations. Nominal thicknesses of terrazzo varied from 7 mm, 12 mm, 10 mm, and 10 mm in Cores 1, 2, 3, and 4, respectively. Coarse marble and limestone chips are nominal 2 to 3 mm in white terrazzo and as coarse as 5 mm in blue variety. Except a fine, hairline long visible crack in white terrazzo in Core 3 which has extended through the 10 mm thickness of terrazzo but did not extend beyond, in three other cores terrazzo flooring is present in visually crack-free and sound conditions. There is no evidence of any chemical or physical deterioration of terrazzo or its components are found in the cores examined to indicate its potential for the reported failure.

Invented by the Venetians in the 1500s, cement-based terrazzo is one of the oldest types of decorative flooring systems. The mosaic-like cement-based terrazzo floor topping is conventionally made by embedding small pieces of marble or granite in a cement mortar, followed by polishing the surface. Compared to the traditional cement-based terrazzo, an epoxy-based terrazzo as the one examined here is relatively recent and offers a host of benefits that has threatened to shrink the market for traditional cement-based systems.

Epoxy-based system is a thin-set terrazzo poured-in-place as topping for concrete substrates that goes on at a thickness of only $^{1}/_{4}$ to $^{3}/_{8}$ inch, as opposed to traditional terrazzo that must be applied at thicknesses of 2 to 3 inches. This modern-day epoxy-based terrazzo is excellent for multicolored patterns and designs because the epoxy resin matrix can be pigmented, like paint, to achieve an unlimited spectrum of colors. The present white terrazzo is usually formed by mixing of a titanium-oxide based pigment to impart the characteristic white color tone, whereas the blue tone in blue bands was imparted by mixing a different pigment. Epoxy-based terrazzo can accommodate a wide variety of richly colored aggregates, including chips of marble, granite, limestone, recycled glass, mother of pearl, and various synthetic materials. With the creative use of divider strips to separate areas of contrasting colors, it's possible to produce borders, logos, geometrical designs, and other artistic compositions. Epoxy systems have captured more than 70 percent of today's terrazzo market. They offer outstanding durability and wear, making them tough enough for use in high-traffic commercial and industrial environments. Because the binder is 100% epoxy, the finished floor surface provides greater resiliency, chemical resistance, compressive strengths, and flexibility than cement-based systems.

GREEN BOND COAT

Cores 1 and 3 show the presence of a thin (2.5 to 3 mm thickness) green polymer bond coat well-adhered to the underside of terrazzo but completely de-bonded from the concrete beneath. This bond coat contained a fibermesh reinforcement mostly at the base of the coat which did not provide any benefit to bond the coat to the concrete.

DE-BONDING OF TERRAZZO/BOND COAT FROM CONCRETE

In Cores 2 and 3, terrazzo showed complete de-bonding from concrete irrespective of having a green reinforced bond coat in Core 3 or its complete absence in Core 2. In Cores 1 and 4, terrazzo is bonded to concrete, again irrespective of having a green bond coat in Core 1, or not having it in Core 4 (latter with a thin polymer surface film on the concrete that was probably applied as a primer or a bonding agent). The top concrete surface in all four cores showed a dense, trowel-finished surface with densified paste to a depth of 5 to 6 mm, which is darker gray and free of any air due to trowel-finishing compared to paste in the interior body. A thin film of carbonated concrete is found in all four cores, indicating inadequate removal of carbonated and trowel-densified surface from concrete slab both of which would densify the very top and potentially hinder development of a good bond to a newly placed polymer-based epoxy system.

In cores having debonded flooring from concrete no trace of terrazzo and/or bonding coat is found on the concrete surface (except only a trace in Core 3) and no trace of concrete is found on the underside of terrazzo or bonding coat. This indicates a clear separation of flooring from concrete and application of flooring on a relatively smooth flat surface found to be the dense trowel-finished surface of slab where newly placed flooring components did not penetrate into concrete or developed any good mechanical interlocking for a good bond.

In the absence of any potentially deleterious reactions (e.g., alkali-aggregate reaction) in terrazzo or concrete, especially at the top surface region of concrete, and in the absence of any chemical fingerprint of moisture upwelling through the slab to bring potentially deleterious components (e.g., alkalis) towards the surface to inhibit the bond, the reported deboning of flooring is judged to be due to inadequate preparation of concrete slab surface to make it more receptive to the new flooring, e.g., with better and deeper grinding to remove the carbonated skin and dense trowel-finished surface, thorough cleaning of the prepared surface to remove any dirt or moisture, using appropriate bonding agent to actually bond to the concrete surface rather than only to the terrazzo (as is the case here) for eventual bonding of the new flooring to concrete, etc. Flooring failures driven by moisture upwelling would have caused debonding at the location of Core 4 where concrete slab is significantly thicker than that at the locations of Cores 2 and 3, and does not have a polymer bond coat except a thin film of an organic film (e.g., primer) which may have helped adhere the flooring to concrete (despite the fact that concrete still has a dense trowel-finished carbonated surface that should have been removed for better mechanical bond). This indicates use of proper

bonding agent resistant to moisture and high alkali situations usually encountered in a concrete slab to develop good bond between a polymer terrazzo and cementitious substrate systems.

LIQUID IN BLISTER

High alkalis, alkalinity (pH 11.2), and organic components found in the liquid reportedly collected from a blister can come from multiple sources, both from: (i) interior concrete slab e.g., by moisture upwelling (hydrostatic pressure, osmotic pressure, capillary rise) from concrete's batch water, sub slab vapor from soil substrate, etc., as well as from (ii) exterior sources, e.g., ambient humidity, floor cleaning solutions, curing water, dewpoint, precipitation, etc. Without knowing the source of the liquid, or for that matter examining a so-called 'blister' itself, analyses of liquid in a vial cannot provide clues to the moisture-induced flooring failure. If it is from an external source then it has no direct role on terrazzo failure except perhaps destabilization of bonding agent by its high alkalinity. However, if it is indeed from an internal source, e.g., from concrete's batch water that has risen by moisture upwelling under a relative humidity gradient then moisture build up beneath an impermeable terrazzo floor can create enough pressure to cause blistering or debonding. Terrazzo in four cores examined, however, showed no evidence of 'blistering' as dome-shaped upwelling of terrazzo or possible extrusion by buildup of moisture and/or other ingredients (e.g., alkali-silica gel) that are commonly suspected from blister formation. Terrazzo in all four cores is very dense, hard, and showed complete separation from concrete with a flat smooth separation of its base from concrete, irrespective of presence or absence of an intermediate bond coat. Cores 1 and 3 show the presence of a thin (2.5 to 3 mm thickness) green polymer bond coat well-adhered to the underside of terrazzo but completely debonded from concrete.

THE CONCRETE SLAB

The concrete slab beneath the terrazzo flooring is found to be compositionally similar non-air-entrained Portland cement concrete consisting of crushed marble coarse aggregate having a nominal maximum size of 1 in. (25 mm), natural siliceous (quartz-quartzite-feldspar) sand fine aggregate having a nominal maximum size of $^{3}/_{8}$ in. (9.5 mm), a dense Portland cement paste which is denser, harder, and darker gray at the top 5 to 6 mm due to trowel-finishing operations, having water-cement ratio estimated at the trowel densified surface to be 0.35 to 0.40, and a relatively normal dense paste in the interior body where cement content is estimated to be $6^{1}/_{2}$ to 7 bags per cubic yard and water-cement ratio estimated to be similar throughout the depth of each core and across all four cores, between 0.40 to 0.45. Since the slab was placed over a plastic vapor retarder in all four cores, and was dense trowel-finished, the internal moisture of concrete from mix water was used to well hydrate the cement and create a dense concrete.

Both coarse and fine aggregate particles in concrete are sound and did not contribute to any potentially deleterious reactions such as alkali-aggregate reactions to cause the reported flooring failure. Alkali-silica reaction (ASR) in concrete, often triggered by moisture and alkalis brought to the surface by moisture upwelling is often considered

as the cause of floor covering failure. Present cores do not show any evidence of such a reaction, or reaction products (ASR gel), or reaction microstructures (e.g., microcracking from reactive aggregates to paste) to consider such a process to be the cause.

Profiles of water-soluble anions and alkalis across the depths of cores show no obvious increase of water-soluble ions (chloride, sulfate, sodium, potassium) towards the top of the cores, indicating perhaps moisture upwelling if occurred was not strong enough to leave its chemical fingerprint in terms of elevated alkali, chloride, sulfate levels towards the top.

DISCUSSIONS

CAUSES OF TERRAZZO FLOOR FAILURES

Two common causes of failure of terrazzo flooring from concrete substrate are related to: (a) moisture, and (b) surface preparation of concrete. Moisture-related failure includes (i) osmotic and/or hydrostatic pressures from moisture buildup beneath impermeable, nonbreathable floor covering causing blistering and delamination, (ii) alkali-silica reaction and related distress beneath the flooring causing blistering, cracking, and debonding, (iii) moisture-upwelling-induced increased alkali level at the surface causing destabilization and failure of flooring adhesives, adhesive staining, etc. Surface preparation-related failures include: (i) presence of dust, dirt, or other surface contaminants from improper cleaning and surface preparation, or surface-parallel near-surface microcracks from surface scarification processes, all of which could act as a bond breaker to prevent adhesion of new flooring, (ii) absence of a bonding agent to develop a good 'chemical bond' of flooring to concrete, (iii) inadequate roughening or scarification of concrete surface to prevent development of a good 'mechanical bond' between flooring and concrete, etc.

All these options were considered to investigate possible causes of reported failure of terrazzo flooring. Cores received showed 'clean separation' of terrazzo with or without an underlying green bond coat from lightly scarified concrete surface where the concrete surface still has a thin carbonated skin and a dense trowel-finished surface to a depth of 5 to 6 mm.

Moisture upwelling to cause accumulation beneath terrazzo flooring and blistering can occur under: (a) a relative humidity gradient from a wet slab to dry ambient air above, or (b) by osmotic pressure where moisture travels through a semi-permeable membrane into a solution of higher solute concentration, which is driven by a force that tends to equalize the concentrations of dissolved solute (typically salts) on the two sides of the membrane. Both processes can lead to formation of liquid-filled blisters in floor coatings, typically 5 to 50 mm diameter and from one to several millimeters in height. These blisters are under pressure and water will squirt out from a blister when punctured. Pressures can be quite high, causing blisters to form even under 9.5-mm thick epoxy-terrazzo flooring

(Smith 2001). Floor coverings bonded to concrete with adhesives do experience moisture-related failures for a variety of reasons.

Common quantitative moisture tests done prior to terrazzo installation are according to ASTM F1869, *Standard Test Method for Measuring Moisture Vapor Emission Rate of Concrete Subfloor Using Anhydrous Calcium Chloride* or F2170, *Standard Test Method for Determining Relative Humidity in Concrete Floor Slabs Using in situ Probes*. Qualitative, comparative methods such as a plastic sheet test (ASTM D 4263), mat bond test, or handheld electronic moisture meters for electrical resistance test or electrical impedance test, nuclear moisture gauge, may be useful as survey tools but should not be used to accept a floor prior to terrazzo installation.

REFERENCES

ASTM C 144, "Standard Specification for Aggregate for Masonry Mortar," In Annual Book of ASTM Standards, Section Four Construction, Vol. 04.05 Chemical-Resistant Nonmetallic Materials; Vitrified Clay Pipe; Concrete Pipe; Fiber-Reinforced Cement Products; Mortars and Grouts; Masonry; Precast Concrete; ASTM Committee C12 on Mortars for Unit Masonry, 2007.

ASTM C 1324, "Standard Test Method for Examination and Analysis of Hardened Masonry Mortar," In Annual Book of ASTM Standards, Section Four Construction, Vol. 04.05 Chemical-Resistant Nonmetallic Materials; Vitrified Clay Pipe; Concrete Pipe; Fiber-Reinforced Cement Products; Mortars and Grouts; Masonry; Precast Concrete; ASTM Committee C12 on Mortars for Unit Masonry, 2007.

ASTM C 856, "Standard Practice for Petrographic Examination of Hardened Concrete," In Annual Book of ASTM Standards, Section Four Construction, Vol. 04.02; ASTM Subcommittee C 9.65, 2010.

ASTM C 1723, "Standard Guide for Examination of Hardened Concrete Using Scanning Electron Microscopy," In Annual Book of ASTM Standards, Section Four Construction, Vol. 04.02; ASTM Subcommittee C 9.65, 2010.

Jana, D., "Sample Preparation Techniques in Petrographic Examinations of Construction Materials: A State-of-the-art Review", *Proceedings of the 28th Conference on Cement Microscopy*, International Cement Microscopy Associates, Denver, Colorado, pp. 23-70, 2006.

Smith, L, *An Introduction to Coating Concrete Floors*, Jnl Protective Coatings and Linings, pp 40-43, Dec 2001.

Pfaff, F A and Gelfant F S, *Osmotic Blistering of Epoxy Coatings on Concrete*, Jnl Protective Coatings and Linings, pp52-64, Dec 1997.

Kanare, H., *Terrazzo Flooring* Concrete Slabs and Moisture Issues: Guide Document for *Architects-Engineers,* Prepared for The National Terrazzo & Mosaic Association, Inc., and The International Masonry Institute, 2004.

✪ ✪ ✪ END OF TEXT ✪ ✪ ✪

APPENDIX –

METHODOLOGIES FOR CMC'S LABORATORY TESTING OF TERRAZZO FAILURES FROM CONCRETE SLAB

METHODOLOGIES

Laboratory investigation of terrazzo failures from concrete floor was done by following a variety of investigative methods starting with: (a) optical microscopy (*a la* ASTM C 856), (b) scanning electron microscopy and X-ray microanalysis (*a la* ASTM C 1723), (c) X-ray diffraction, (d) X-ray fluorescence of terrazzo and water-soluble alkali contents in concrete, (e) Fourier transform infrared spectroscopy to determine the organic components in terrazzo and concrete along with interfacial bonding agents, (f) potentiometric titration of chloride contents from various depths of concrete slab for chloride migration (*a la* ASTM C 1218), and (g) ion chromatography of water-soluble ions (e.g., chloride, sulfate) through various depths of slab to investigate moisture upwelling. Additionally, the liquid sample reportedly received from underneath a blister was tested by Fourier transform infrared spectroscopy (by attenuated total reflectance method) and X-ray fluorescence for organic component and water-soluble alkali content, respectively.

Optical Microscopy

Sawcut sections and lapped cross sections of terrazzo-concrete composite cores were prepared by successive grinding the saw-cut sections in various metal and resin-bonded diamond grinding discs for examinations in a Stereozoom microscope at low magnifications. Subsequently, thin sections of terrazzo-concrete composites were prepared for examinations in a petrographic microscope. For thin section preparation, representative portions were placed in a flexible (molded silicone) sample holder, and encapsulated with a colored (blue or fluorescent) dye-mixed low-viscosity epoxy resin under vacuum to impregnate any pore spaces and/or cracks in terrazzo and improve the overall integrity by the cured epoxy. The epoxy-encapsulated cured solid block of sample was then de-molded and processed through coarse to fine grinding/lapping from metal to resin-bonded diamond grinding discs, attachment of the lapped surface to a frosted large-area (50 × 75 mm) glass slide, precision sectioning and precision grinding in a thin-sectioning machine (Microtec Engineering's Microtrim for automated precision sectioning and grinding of four 50 × 75 mm samples, or Buehler's Petrothin for a single sample, Figure A-1), and final polishing steps on a glass slide with 15 micron alumina abrasive followed by polishing on a polishing cloth with submicron diamond abrasive to prepare a final polished thin section of ~30 micron thickness suitable for examinations in a petrographic microscope and subsequently in SEM-EDS. Sample preparation steps are described in detail in Jana 2005, 2006.

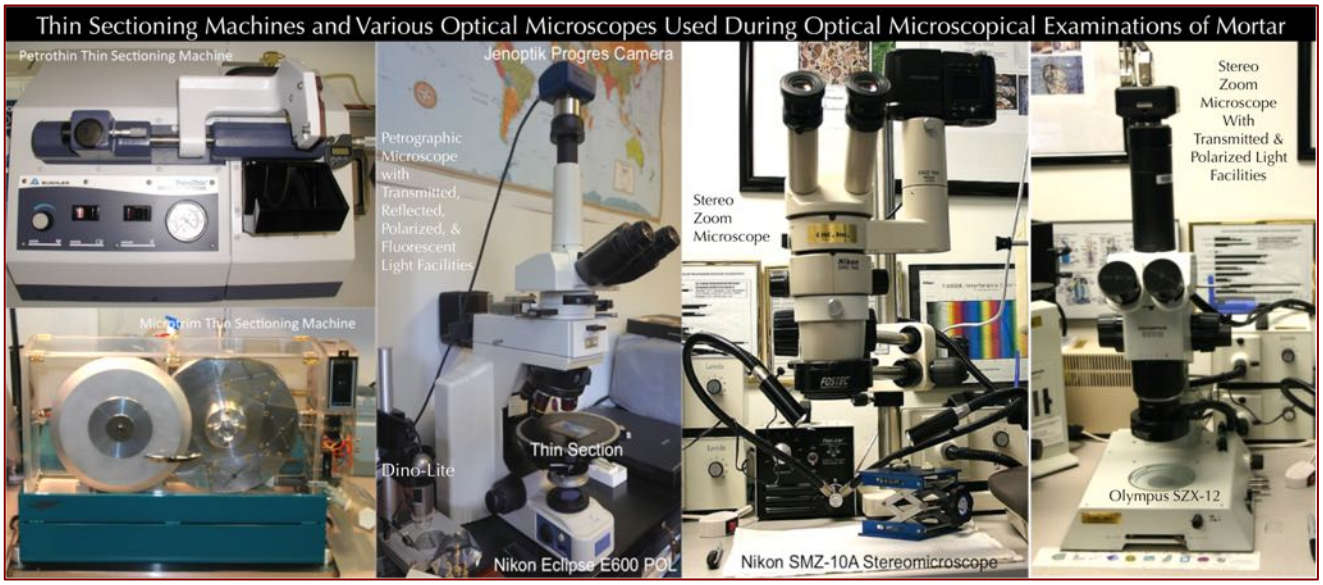

Figure A-1: Buehler (top, left) and Microtrim (bottom left) thin-sectioning machines used for production of less than 30-micron thin sections. Four 50 × 75 mm size thin sections can be simultaneously prepared by the Microtrim unit. Nikon Eclipse E600 POL petrographic microscope with Jenoptik Progres Camera (2nd from left), Nikon SMZ-10A Stereozoom reflected-light microscope with Lumenera Infinity camera (3rd from left), and Olympus SZX-12

Stereozoom microscope with reflected, transmitted, and polarized light facilities and Progres camera (right) used for examinations of terrazzo.

Steps followed during light optical microscopical examinations of terrazzo-concrete composite samples include:

a. Visual examinations of samples, as received, to select areas for detailed optical microscopy; and initial digital and flatbed scanner photography of sample as received;

b. Low-power stereomicroscopic (e.g., by using Nikon Stereozoom microscope shown in Figure A-1) examinations of saw-cut and freshly fractured sections of samples for evaluation of textures, compositions, and appearances;

c. Examinations of oil immersion mounts for special features and materials from the samples in a petrographic microscope (e.g., Nikon Eclipse E600 POL shown in Figure A-1);

d. Examinations of colored (blue or fluorescent) dye-mixed epoxy-impregnated polished thin sections of samples in a transmitted-light Stereozoom microscope (e.g., Olympus SZX-12 microscope shown in Figure A-1) for determination of size, shape, angularity, and distribution of aggregates, as well as abundance and distribution of void and pore spaces that are highlighted by the colored dye-mixed epoxy;

e. Examinations of colored (blue or fluorescent) dye-mixed epoxy-impregnated polished thin sections of samples in a petrographic microscope (Figure A-1) for detailed compositional, mineralogical, textural, and microstructural analyses of aggregates and binders in samples, along with diagnoses of evidence of any deleterious processes. The purpose of using a colored dye-mixed epoxy is to highlight the overall variations in density/porosity of samples as well as highlighting any void spaces and cracks in the samples;

f. Examinations of any physical or chemical deterioration of samples or signs of improper construction practices from microstructural evidences; and,

Scanning Electron Microscopy and Energy-Dispersive X-Ray Spectroscopy (SEM-EDS)

Portions of the thin sections used for optical microscopy are subsequently coated with a thin conductive gold film for detailed SEM-EDS studies. Procedures for SEM examinations are described in ASTM C 1723. Polished and coated thin section (or polished solid encapsulated block) of sample is examined in a CamScan SEM equipped with backscatter detector, secondary electron detector, and x-ray fluorescence spectrometer (Figure A-2) to observe

a) The morphology and microstructure of various phases; and,

b) Determine the chemical compositions of the binders, including the original components of the binders, and the hydration and/or carbonation/alteration products.

c) Investigation of potential deleterious reactions in concrete substrate, e.g., alkali-silica reaction;

d) Determination of pigmenting constituents in terrazzo, etc.

Figure A-2: Cambridge CamScan Series II Scanning Electron Microscope and 4Pi Revolution software, backscatter detector, secondary electron detector, and energy-dispersive X-ray fluorescence spectrometer used for microstructural and microchemical analyses of mortar.

X-ray Diffraction

X-ray diffraction is carried out in a Siemens D5000 Powder diffractometer (Figure A-3) employing a long line focus Cu X-ray tube, divergent and anti-scatter slits fixed at 1 mm, a receiving slit (0.6 mm), diffracted and incident beam Soller slits (0.04 rad), a curved graphite diffracted beam monochromator, and a sealed proportional counter. Generator settings used are 45 kV and 30mA. A dry, finely ground sample pulverized to pass US 325 sieve (44-µm) is placed in a 1-in. diameter circular sample holder and excited with the copper radiation of 1.54 angstroms. Tests are performed at a 2-theta range from 4° to 64° with a step of 0.02° and a dwell time of one second. The resulting diffraction patterns are collected by using DataScan 4 software of Materials Data, Inc. (MDI), analyzed by using Jade 9.0 software of MDI with ICDD PDF-4 (Minerals 2017) diffraction data, and, phase identification, and quantitative analyses were carried out with MDI's Search/Match and Easy Quant modules, respectively.

Figure A-3: Siemens D5000 X-ray diffractometer used for determination of mineralogical composition of terrazzo.

Energy-Dispersive X-Ray Fluorescence Spectroscopy (ED-XRF)

An energy-dispersive bench-top X-ray fluorescence unit from Rigaku Americas Corporation (NEX-CG, Figure A-4) is used for determination of bulk chemical (oxide) composition of terrazzo. The instrument is calibrated by using various certified (CCRL, NIST, GSA, and Brammer) reference standards of cements and rocks. A representative portion of terrazzo (about 8.0 grams) is pulverized down to minus US 325 sieve (finer than 45 microns size) with anhydrous alcohol in a Rocklab pulverizer with a grinding aid/binder (fixed 7.5% binder by weight of sample), and then pelletized (approximately 7.0 grams of sample thus prepared) to a 32-mm diameter pellet with a 25-ton hydraulic press.

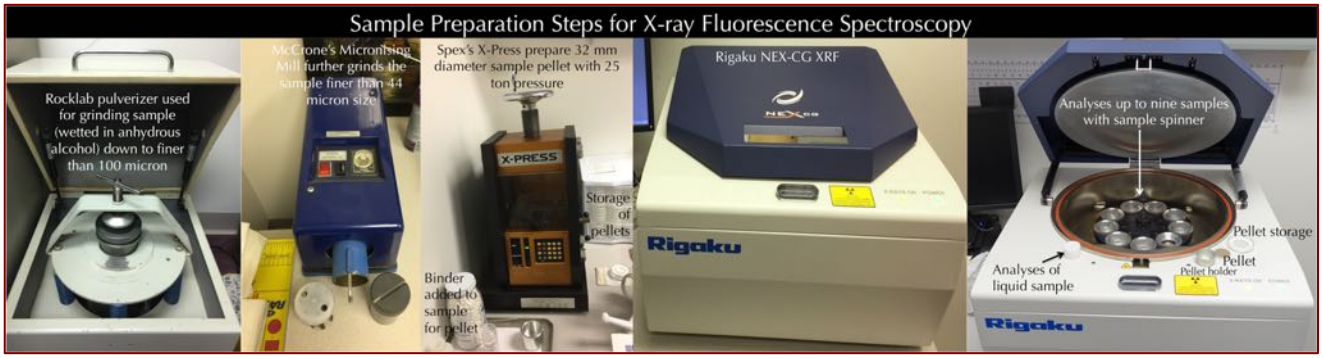

Figure A-4: Rigaku NEX-CG bench-top ED-XRF unit used for bulk chemical composition of terrazzo and water-soluble alkali content in bluster liquid.

Fourier Transform Infrared Spectroscopy (FT-IR)

FT-IR measurements are done in a Perkin Elmer Spectrum 100 FT-IR spectrophotometer (Figure A-5) running with Spectrum 10 software. Samples were measured using attenuated total reflection (ATR) on a single bounce diamond/ZnSe ATR crystal. Sample was measured between a frequency range of 4000 to 650 cm^{-1}. Each run was collected at 4 cm^{-1} resolution with Strong Beer-Norton apodization. Data were collected with a temperature-stabilized deuterated triglycine sulfate (DTGS) detector by placing the sample in contact with the ATR crystal and by applying force from the pressure applicator supplied with the ATR accessory. The application of pressure enabled

the sample to be in intimate contact with the ATR crystal, ensuring a high-quality spectrum was achieved. Additionally, more conventional KBr pellet is also used for samples on as-needed basis.

Figure A-5: Perkin Elmer Spectrum 100 FT-IR unit in CMC with Universal ATR and Liquid Sipper attachments. The FT-IR unit can analyze a sample as-received in the Universal ATR (left), or as a pressed pellet after mixing with KBr powder in a KBr press (middle), or as a liquid either in Universal ATR or in Liquid Sipper unit (right).

Ion Chromatography

Ion chromatography is an established technique for analysis of various anion and cation in salts (e.g., chloride, sulfate, and nitrate anions, and magnesium, calcium, alkali, ammonium cations) to assess magnitude of environmental impacts on terrazzo and concrete, and subsequent effects of such salt ingress or moisture-driven migration of water-soluble ions through concrete. Concrete samples are pulverized, disgusted in deionized water to remove all water-soluble salts, then solid residues are filtered out and the water-digested filtrates are analyzed by an ion chromatograph.

Figure A-6: Ion chromatography of water-soluble ions after digestion of pulverized masonry mortar in deionized water to determine various anions (sulfate, chloride, nitrate, nitride, phosphate, bromide, etc.) extracted from mortar.

Procedures followed in Ion chromatography are described in ASTM D 4327 "Standard Test Method for Anions in Water by Chemically Suppressed Ion Chromatography." Briefly, an aliquot of 1 gram of pulverized sample (passing No. 50 sieve) is digested in 50 ml distilled water for 6 to 8 hours on a magnetic stirrer at a temperature below boiling point of water; then the digested sample is filtered through two 2.5-micron filter papers using vacuum, followed by a second filtration through micro-filter (0.22 micron) paper, then the filtrate was diluted to 200 ml with deionized water, and used for analysis to get ppm-level fluoride, chloride, nitrite, bromide, nitrate, phosphate, and sulfate contents in the water-digested sample in Metrohm 881 Compact IC Pro IC with attached 858 Professional Sample Processor (Figure A-6). The instrument is calibrated against ten different custom-made Metrohm anion standard solutions having all these anions from 1-ppm to 100-ppm levels. To check the accuracy of the instrument, 20-ppm and 80-ppm standard solutions were run first prior to the analyses of samples.

END OF REPORT[1]

[1] The CMC logo is made using a lapped polished section of a 1930's concrete from an underground tunnel in the U.S. Capitol.